# Sedimentary phosphorus dynamics in response to lake trophy and mixing regime changes during the Late-Glacial, Holocene and the Anthropocene: three case studies from deep lakes in Switzerland

Inauguraldissertation

der Philosophisch-naturwissenschaftlichen Fakultät

der Universität Bern

vorgelegt von

**Luyao Tu**

Von Henan Province, China

Leiter der Arbeit:

Prof. Dr. Martin Grosjean

Universität Bern

Von der Philosophisch-naturwissenschaftlichen Fakultät angenommen

Bern, 03.03.2021

Der Dekan:

Prof. Dr. Z. Balogh

# Table of Contents

# List of Figures

# List of Tables

# List of Abbreviations

| | |
|---|---|
| a.s.l. | Above Sea Level |
| Bphe-*a* | Bacteriopheophytin *a* |
| C/N | Carbon to Nitrogen ratio |
| Chl-*a*/-*b* | Chlorophyll-*a*/-*b* |
| CONISS | Constrained Incremental Sums of Squares cluster analysis |
| DI-TP | Diatom-inferred Epilimnetic Total Phosphorus |
| EDTA | Ethylenediamine Tetraacetic Acid |
| ENVI | Environment for Visualizing Images |
| HSI | Hyperspectral Imaging |
| ICP-MS | Inductively Coupled Plasma Mass Spectrometry |
| LOI | Loss On Ignition |
| MAR | Mass Accumulation Rates |
| OM | Organic Matter |
| PCA | Principal Component Analysis |
| RABA | Relative Absorption Band Area |
| RABD | Relative Absorption Band Depth |
| RDA | Redundancy Analysis |
| RGB | Red, Green, Blue |
| SMT | Standards, Measurements and Testing |
| TChl | Total Chlorophylls |
| TIC | Total Inorganic Carbon |
| TOC | Total Organic Carbon |
| TP | Total Phosphorous |
| TN | Total Nitrogen |

| | |
|---|---|
| UV/VIS | Ultraviolet / Visual |
| VNIR | Visual to Near Infrared |
| XRD | X-ray Powder Diffraction |
| XRF | X-Ray Fluorescence |

# Abstract

Phosphorus (P) released from sediments into surface waters, termed internal P loadings, has been widely recognized as a key P source contributing to delayed recovery from human-induced eutrophication in lakes where external P loadings have been reduced. It is critically important to evaluate the availability of sediment-P and its release risks into lake water by studying P fractions in sediment profiles. However, previous studies focused only on well-mixed shallow lakes and did not examine the relationships between sediment records of P fractions and lake trophic status in seasonally stratified, deep lakes. Additionally, records of P fractions spanning longer than a few decades have not been studied. Hypolimnetic waters in temperate eutrophic deep lakes tend to become anoxic during stratification periods, which can lead to high internal P loadings and sustain eutrophication. It is not yet fully understood whether, and how, lake trophic levels and hypolimnetic redox conditions can influence the long-term behavior of sedimentary P fractions and potentials of internal P loadings in deep lakes.

Our research questions were: (i) How have P fractions in sediment profiles and potentials of internal P loadings varied with different lake trophic levels over the past few decades? (ii) What was the role of hypolimnetic anoxia and lake trophic state in affecting P cycling, sediment P fractions stratigraphy, and potentials of internal P loadings in the last century prior to cultural eutrophication? (iii) Is the P cycling under natural or pre-anthropogenic anoxic conditions comparable with the P cycling under anthropogenic eutrophication and anoxia in recent times? In order to address these questions, we selected three deep lakes in Switzerland: the Ponte Tresa basin of Lake Lugano, Lake Burgäschi, and Soppensee. We investigated sediment cores from these lakes to produce records of P fractions in sediments, lake trophy, and anoxia history covering the past few decades, more than one century, and the Late-glacial and Holocene periods, respectively. The Ponte Tresa basin was selected because it is one of several deep lakes in Switzerland that have not yet recovered from human-induced eutrophication after large reductions of external P loadings, and the lake's eutrophication history since the mid-20th century is already well documented. Lake Burgäschi was selected because there were substantial changes in trophic levels and possibly lake mixing regimes during the last century, and the lake has exceptionally long historical and limnological survey data available for most of the last 50 years. We selected Soppensee because it is a deep, eutrophic lake featuring a varved sediment record, its sediments have an exceptionally good chronology, and it has a record of diatom-inferred epilimnetic total P (DI-TP) concentrations available for the entire Holocene.

Hyperspectral imaging (HSI) was applied for high-resolution analysis of sedimentary pigments, combined with geochemical analyses, which allows reconstructions of lake primary production (eutrophication history) and hypolimnetic redox conditions. XRF core scanning was used to determine the elemental composition of sediments and these geochemical variables were related to in-lake and catchment processes (e.g. XRF-Mn and Fe/Mn ratios as redox proxies). In this study, different P forms in sediments were characterized by P-fractionation schemes, mainly by sequential P extraction procedures and the standards, measurements and testing (SMT) protocol. The results of P-fractionation showed that, in each lake, labile P fractions (mainly the redox sensitive Fe-bound P or Fe/Al metal oxides bound P) were the dominant P form in anoxic sediments during most of the periods studied. This phenomenon suggests high potentials of internal P loadings in the three lakes. Hypolimnetic redox conditions appear to control contents of redox-sensitive Fe and Mn in sediments, which in turn influences P retention in sediment profiles of the lakes.

In the Ponte Tresa basin of Lake Lugano, we find that net burial rates of total P and the labile P fraction (mainly redox sensitive Fe-bound P) in sediments showed significant decreasing trends from 1959 to 2017, when the lake underwent higher eutrophic levels and severe anoxia. This finding suggests that, in the Ponte Tresa basin, higher eutrophication conditions increased internal P loadings, thus reducing net burial rates of P in sediments. This case study highlights the concern that eutrophication restoration might be hindered in deep, seasonally stratified lakes by extensive internal P cycling and reduced capacity of P-trapping in surface sediments.

In Lake Burgäschi, the results highlight the importance of hypolimnetic redox conditions in controlling the long-term P cycling and P retention in sediments since the 1900s. We found relatively high total P and labile P fractions in Fe- and Mn enriched layers when the hypolimnion was seasonally oxygenated. The results also imply that hypolimnetic water withdrawal in Lake Burgäschi can effectively reduce P retention in sediments and potentials of internal P loadings.

In Soppensee, we estimated long-term qualitative internal P loadings by comparing the Holocene record of DI-TP concentrations with the labile P fraction (Fe/Al-P) concentrations in sediments under changing trophic, redox, and lake mixing regimes. The results demonstrate that enhanced internal P loadings acted as a positive feedback to promote and maintain natural eutrophication process in Soppensee from ~9000 to 6000 cal BP. However, such a positive feedback was not inferred for other eutrophic phases. For example, ferromagnetic minerals from magnetotactic bacteria preserved in sediments from ~6000 to 2000 cal BP and

Fe-rich layers formed from ~2000 to 200 cal BP appear to have prevented internal P loadings in these two periods, resulting in high labile P fraction in sediments.

In summary, this project provides new insights about the influence of lake primary production and hypolimnetic redox conditions on P cycling and the record of sediment P fractions on short and long timescales in seasonally stratified, deep lakes. We conclude that, in stratified deep lakes, sedimentary total P and P fractions may not reflect lake trophic evolution and the history of external P loadings. However, comparisons of the lake trophic history and the record of sediment P fractions can shed light on in-lake P cycling in the past.

# Chapter 1: Introduction

## 1.1 Research background

### 1.1.1 Lake eutrophication and phosphorus cycling

Eutrophication is originally a natural process of nutrient enrichment as a water ecosystem ages and is gradually filled in with sediments, which might take a very long time (perhaps thousands of years) (Chislock et al., 2013). However, intensified agriculture and rapid industrial development since the late nineteenth century have greatly accelerated the eutrophication process by introducing excessive loadings of nutrients (particularly nitrogen (N) and phosphorus (P)) into aquatic ecosystems. This human-induced eutrophication phenomenon is thus referred to as "cultural eutrophication" (Schindler, 2012). Cultural eutrophication in fresh aquatic ecosystems has become an environmental problem of global concern for several decades (Schindler, 1974; 2006). The detrimental ecosystem imbalances, water oxygen depletion, and cyanobacterial blooms caused by eutrophication have long been recognized to lead to poor water quality, loss of ecosystem services to society, and human health concerns (Paerl and Fulton, 2006). The scientific community has long agreed that excessive P loadings are the main cause of lake eutrophication because P is the limiting nutrient controlling primary production in many freshwater lakes, especially in deep ones (Lewis Jr and Wurtsbaugh, 2008; Qin et al., 2020). The nutrient P enters in freshwater lakes from nonpoint sources, for example, catchment runoffs (agricultural fertilization, non-agricultural or groundwater) and atmospheric deposition (Fig. 1.1), and from point sources such as municipal and industrial sewage and wastewater treatment plants discharges.

Since as early as the 1960s, multiple remediation measures have been adopted worldwide to decrease eutrophication in freshwater lakes and to improve water quality, mostly by reducing external loadings of N and especially P (Carpenter, 2008). For example, nutrient diversions (Edmondson, 1970), implementation of wastewater treatment plants, decreased use of fertilizers, and regulations requiring elimination of P in detergents were applied in most developed countries in Europe and North America (Hering et al., 2012). These strategies have proven to be generally successful in decreasing water-P concentrations and trophic levels in some lakes (Schindler et al., 2016), with the typical examples of Lake Zurich in Switzerland (Hering et al., 2012), Lake Erie in the USA (DePinto et al., 1986), and Lake Bourget in France (Jacquet et al., 2014) etc. Nevertheless, other lakes witnessed a delayed response to such reductions of external P loadings, usually because of recycling of nutrients from bottom sediments into surface waters (Marsden, 1989; Jeppesen et al., 2005). Alternative management practices for eutrophication control include chemical treatments to remove P from the water column (Lürling and van Oosterhout, 2013), biomanipulation (Benndorf, 1990), and artificial mixing (Gibbs and Howard-Williams, 2018) etc. Despite good improvements of

water quality in many freshwater lakes after decades of restoration, lake eutrophication is still a prevalent global problem, especially in developing countries (Smith and Schindler, 2009).
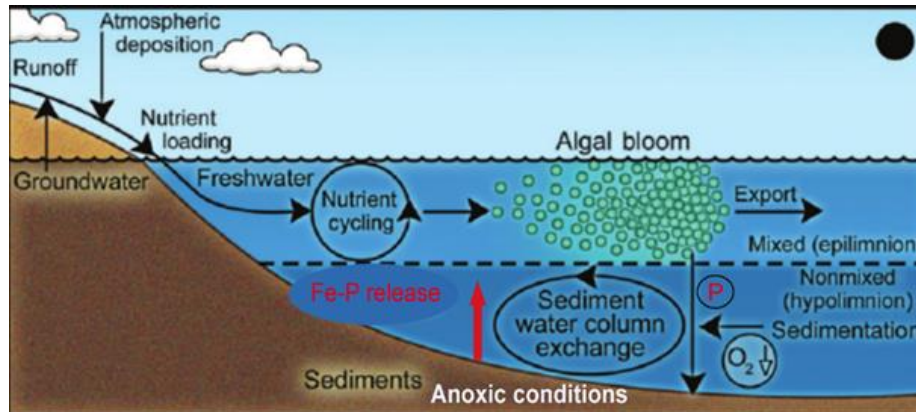


**Figure 1.1**: The overview conceptual scheme of external nutrient (N or P) loadings and internal P loadings. Water over-nourishment (eutrophication) causes algal blooms, $O_2$ depletion or hypoxia in the hypolimnion after decomposition of sedimented organic matter, and, ultimately, internal P loadings (here mainly P release after the reductive dissolution of Fe-bound P from anoxic sediments) under stratified water-column conditions. The figured is modified from Paerl and Justic (2011).

## 1.1.2 Sediment phosphorus release (internal phosphorus loadings) in freshwater lakes

P accumulated in lake sediments exists in various inorganic and organic forms, where it can be either permanently buried or released back into water columns via pore water (commonly referred to as "internal P loadings"). Internal P loadings have been known to keep P concentrations in the lake water high and to delay lake recovery from eutrophication after reductions of external P loadings (Nürnberg, 1991; Wu et al., 2017).
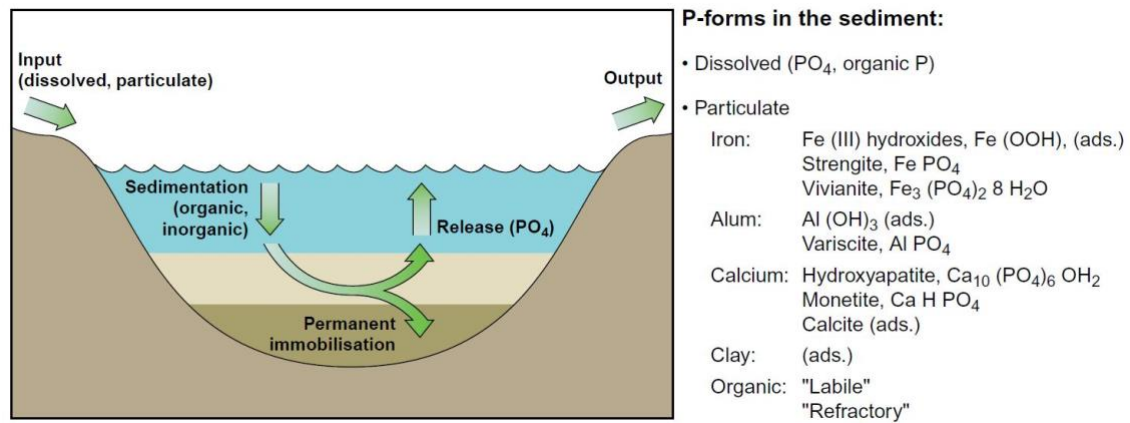
**Figure 1.2**: A conceptual model of the external P input and output in a shallow lake and P forms in sediments. The left-side figure emphasizes the process of gross sedimentation of P, sediment P release, and permanent P immobilization (P retention) in sediments (left side). The right-side text shows the main P fractions and compounds in sediments. Note that ads. represents adsorption. The figure is from Sondergaard et al. (2001).

The classical model from Einsele (1936) and Mortimer (1941) has long been accepted to emphasize that, under anoxic conditions at the sediment–water interface (SWI), the reductive dissolution of Fe (oxyhydr)oxides bound P is the main mechanism responsible for internal P loadings. However, this paradigm has recently been revised based on findings that indicate internal P loadings involve physical and biogeochemical processes that are more complex than anoxia-driven P release from sediments into surface waters (Golterman, 2001; Prairie et al., 2001; Katsev et al., 2006; Hupfer and Lewandowski, 2008). Internal P loadings can also occur under various, even oxic conditions (Marsden, 1989; Caraco et al., 1991). Nowadays, the scientific community has agreed that there are numerous physical, chemical, and biological mechanisms that cause internal P loadings in lakes. Alternative proposed mechanisms include: pH at the SWI that affects the competition between hydroxyl ions and phosphate anions in metal (Fe, Al) (oxyhydr)oxide complexes in aerobic sediments (Christophoridis and Fytianos, 2006), release and uptake of polyphosphate by sediment bacteria (Gächter, 1998; Hupfer et al., 2007), organic matter (OM) decomposition under both aerobic and anaerobic conditions (Hupfer and Lewandowski, 2008; Joshi et al., 2015), and precipitation and dissolution of carbonate-bound P (Ramisch et al., 1999; Jin et al., 2006) etc. Solid-phase P can also be recycled into the water column via resuspension of sediment particles (Orihel et al., 2017).

Sulfate and nitrate concentrations in bottom waters, climate change and temperature, and sediment characteristics have been recognized as potentially important factors in affecting P

availability of surface sediments (Jensen and Andersen, 1992). For example, increases of sulfate concentrations in bottom waters are suggested to increase P availability in sediment porewaters via two main mechanisms: 1) preventing ferrous-P mineral formation (e.g. vivianite) during the scavenging of porewater Fe ions by iron-sulfide mineral formation (Gächter and Müller, 2003), and 2) reductive dissolution of ferric (oxyhydr)oxides bound P by $H_2S$ generated by microbially mediated sulfate reduction (Katsev et al., 2006). By contrast, nitrate has a duel effect on sediment P mobility. High nitrate concentrations in overlaying waters can prevent the release of Fe-bound P from surface sediments by keeping Fe oxidized at the SWI (Caraco et al., 1993). On the other hand, the addition of nitrate has been shown to stimulate Fe-reducing bacteria growth at anoxic SWIs, leading to more sediment P release back into surface waters (Jensen and Andersen, 1992).

The impact of climate changes on lake primary productivity and P cycling has been recognized in temperate lakes. Climatic changes strongly influence phytoplankton growth and lake mixing regimes, particularly in seasonally stratified lakes (North et al., 2014). Under modeling scenarios with higher air temperatures in the 21$^{st}$ century, many lakes worldwide are predicted to experience enhanced surface water temperature and water column stability, and seasonally stratified lakes will mix less frequently (Woolway and Merchant, 2019). A warmer climate, in a direct way, will boost cyanobacterial dominance in freshwater systems (Paerl and Huisman, 2008). Indirectly, with increasing temperatures, OM degradation and microbial respiration are stimulated, which leads to lower redox potentials at SWIs and increased release of Fe/Al-bound P, exacerbating internal P loadings (Jensen and Andersen, 1992). Additionally, in-situ experiments and modeling studies suggest that warmer temperatures are likely to stimulate sediment P release and, as a consequence, intensify eutrophication and harmful algal blooms in shallow lakes (Genkai-Kato and Carpenter, 2005; Kosten et al., 2012). The monitoring data from Loch Leven, Scotland, demonstrated summer water temperature being the positive driver of internal P loadings during 1968-2008 (Spears et al., 2011). North et al. (2014) acknowledged the importance of climate-induced expansion of deep-water hypoxia in driving internal P loadings of the last 40 years in (Lower) Lake Zurich, Switzerland. Given the importance of anoxia-induced sediment P release in deep lakes, rising temperatures may consequently introduce more internal P loadings under stratification/anoxia events, ultimately making restoration more challenging and less successful in eutrophic lakes.

Parameters of surface sediments like bulk density, porewater P-bearing minerals saturation, and metal and clay minerals contents, etc. additionally exert strong influences on P mobility at the SWI (Søndergaard et al., 1996; Katsev et al., 2006), which subsequently influences internal P loadings. The environmental drivers of internal P loadings are complex and vary in space and time within the same freshwater ecosystem. This also makes controlling internal P

loadings in eutrophic lakes a great challenge for long-term lake management. Furthermore, the dominant mechanisms of internal P loadings may differ among different lake systems and environments (e.g. shallow and deep lakes, oligotrophic and eutrophic lakes, and calcareous and non-calcareous lakes) and depend on timescales of interest (e.g. seasonal versus decadal). For example, for deep lakes (> 5 m water depth), particularly with seasonally anoxic hypolimnions, Fe-bound P release accounts for a large portion of internal P loadings during lake stratification (Parsons et al., 2017). Compared with deep lakes, shallow lakes often have fewer anoxia-driven internal P loadings because of generally good mixing and higher $O_2$ concentrations throughout the water column (Sondergaard et al., 2001; Hickey and Gibbs, 2009). The exceptions are some shallow eutrophic lakes where the decomposition of dead algae during algal blooms causes $O_2$ depletion in bottom waters. In shallow lakes, given a high ratio of sediment surface vs water column depth and short-term redox oscillations at the SWI, sediment-water interactions have potentially higher significance in the water P budget (Søndergaard, 2003). Bioturbation, wind resuspension, and high pH conditions at the SWI can contribute to high internal P loadings in shallow lakes (Welch and Cooke, 2005; Jensen et al., 2017).

The widely reported conclusions from short-term (days or months) laboratory and in-situ observations demonstrate that, in seasonally anoxic lakes, higher $O_2$ concentrations in bottom waters potentially restrict seasonal P release from the SWI (Penn et al., 2000; Chen et al., 2018). However, it is proposed that SWI oxygenation might not influence long-term (e.g. decades) internal P loadings and may not be appropriate for universal situations (Gächter, 1998). The general failure of the hypolimnetic oxygenation/aeration restoration in controlling long-term internal P loadings (Müller et al., 2012; Kuha et al., 2016; Tammeorg et al., 2017) supports this notion. In fact, oxygen levels at the SWI only affect internal P loadings over the timescale of the Fe cycle in sediments (i.e. years), and thus should not be the main controlling factor on longer timescales (Katsev and Dittrich, 2013). Reactive-transport model simulations (Katsev et al., 2006; Dittrich et al., 2009; Katsev and Dittrich, 2013) revealed that, on decadal and longer timescales, internal P loadings are predominantly sensitive to the sedimentation flux of degradable OM, followed by dissolved $O_2$ levels at the SWI. All in all, on the long term, the restoration of eutrophic lakes still predominantly relies on reducing external P inputs into lakes.

To minimize internal P loadings and speed-up lake recovery after reductions of external P loadings, lake managers employ a variety of strategies in eutrophic lakes. For well-mixed shallow lakes, sediment dredging and clay capping (e.g. the use of alum and zeolite) are widely applied measures and are observed as highly effective in controlling internal P loadings in multiple cases (Welch and Cooke, 2005). In seasonally stratified or deep lakes, hypolimnetic

oxygenation/aeration is a commonly used tool for preventing anoxia in bottom waters and reducing internal P loadings (Nürnberg, 2007). In some cases, hypolimnetic oxygenation clearly improved bottom-water oxygen conditions, but no desired effects on internal P loadings and water quality were observed, e.g. in Lake Sempach in Switzerland (Gächter, 1998) and in Lake Jyväsjärvi in Finland (Kuha et al., 2016). In recent years, the long-term effectiveness of this restoration measure has been questioned (Gächter, 1987; Liboriussen et al., 2009).

Hypolimnetic water withdrawal is another in-lake restoration treatment normally applied to thermally stratified lakes or reservoirs. It is carried out by pumping the nutrient-rich bottom water to the lake discharge during thermal stratification, whereby P and other nutrients in the hypolimnion are directly removed from the lake. Several studies have reported an overall positive assessment of this restoration technique. For instance, decreased P concentrations in the lake water and possibly lower internal P loadings after the treatment have been reported (Gächter, 1976; Nürnberg et al., 1987; 2007; Premazzi et al., 2005). Nevertheless, the long-lasting effectiveness of this method is still questionable for well-mixed shallow lakes mainly because thermal stratification of the water column is a prerequisite for treatment success. Regardless of all restoration techniques above, the considerable reduction of external nutrient loadings is still the best practice to improve lake water quality and accelerate recovery of eutrophic lakes.

### 1.1.3 Sediment phosphorus fractionation

The down-core distribution of sedimentary P in dated sediment cores can be used to assess historical biogeochemical cycling of P and P inputs in lakes. Theoretically, P retention in sediments is the difference between gross P sedimentation and internal P loadings from sediments into the water column. Specifically, short-term P retention in surficial lake sediments (uppermost ~ 20 cm depths) is the result of the dynamic interplay among gross P sedimentation from water columns, downward P flux into deeper sediment layers, and upward P flux into dissolved P in water columns. These processes often depend on the lake trophic state and environmental drivers, such as redox-potentials and pH changes (Orihel et al., 2017). Long-term stable P retention within sediments represents the P pool which is permanently deposited in sediments, and it is ultimately determined by the P-retaining capacity of deeper sediment layers after early diagenesis.

P in sediments exists as dissolved and particulate forms (Fig. 1.2). Dissolved P represents P in the aqueous phase. Particulate P includes P that is absorbed to clay minerals or to Fe, Al, and Ca compounds, coprecipitated with metal minerals (e.g. apatite, vivianite, and variscite), and organic P etc. (Sondergaard et al., 2001). P speciation in lake sediments has received considerable attention by researchers aiming to precisely estimate the risks of sediment P

release (a.k.a. potentials of internal P loadings) at the SWI and within a sediment profile (Søndergaard et al., 1996; Fytianos and Kotzakioti, 2005; Gao et al., 2005; Shilla et al., 2008). This approach relies on the fact that different P fractions in sediments have different labilities of P release. Moreover, knowing P fractionation patterns in sediment profiles is also critically important to better understand P cycling in whole-lake systems. This information can also inform management decisions on controlling internal P loadings and water-quality improvements in specific cases. A variety of P fractionation schemes has been established to characterize P fractions in sediments, e.g. the sequential extraction (SEDEX) method (Ruttenberg, 1992), the Williams method (Williams et al., 1976; Burrus et al., 1990), the Standards Measurements and Testing (SMT) method (Ruban et al., 2001), and the Jensen method (Jensen and Thamdrup, 1993; Jensen et al., 1998). Among these, the sequential P extraction has been widely used to determine operationally defined P fractions in lake sediments.

The different P forms in sediments commonly include (i) loosely absorbed P in porewater, (ii) redox sensitive Fe and Mn (oxyhydr)oxides bound P, (iii) P bound to hydrated oxides of Al and nonreducible Fe (surface-bound), (iv) Ca-bound P (e.g. apatite-P), and (v) organic P. Loosely absorbed P is water-soluble P and the most bioavailable P form. Redox sensitive Fe-bound P often exists in the ferric Fe (III)-phosphate phase and, under oxic conditions, is strong adsorbed to Fe (oxyhydr)oxides in sediments (Dittrich et al., 2013). However, under anoxic conditions, it undergoes reductive dissolution, which leads to both P and Fe(II) releases into the porewater and, ultimately, into the overlaying water. Core incubation experiments (Sun Loh et al., 2013), in-situ porewater profiles (Ding et al., 2016; Wu and Wang, 2017), and chemical extraction data (Smith et al., 2011) further provide direct evidence that sediment P mobility is mostly coupled with Fe cycling. Although more complex mechanisms rather than the classical concept of Fe-P coupling have been suggested (see Section 1.1.2), the Fe-bound P fraction in lake sediments is typically considered as one of the major potentially labile P sources for internal P loadings (Rydin, 2000; Petticrew and Arocena, 2001).

Ferric and ferrous-P minerals can be spectroscopically or mineralogically identified in lake sediments. For example, several studies have shown that vivianite ($Fe_3(PO_4)_2 \cdot H_2O$) in lake sediments represents a permanent P sink in anoxic sediments (Nembrini et al., 1983; Fagel et al., 2005; Rothe et al., 2014). Al/Fe-bound P can also be released under anoxic conditions or high pH environments via P exchange with soluble $OH^-$ in bases (Dittrich et al., 2009). Ca-P usually results from the co-precipitation of P with calcium carbonate and is relatively stabile under anoxic conditions, but it can be released in low pH environments (pH < 6; Orihel et al., 2017). Organic P in sediments is divided into refractory and labile forms, of which the labile fraction may become a potentially bioavailable P source for lake primary production.

**1.1.4 Hyperspectral imaging of sedimentary pigments**

Contemporary lake monitoring data is commonly used to evaluate lake trophic status and recovery status after lake restoration measures. However, monitoring data in lake waters, in many cases, spans only short periods of time (decades). To better understand lake responses to recent and past environmental changes (e.g. climate changes and human impacts), and to identify pre-disturbance conditions, it is critically necessary to have longer-term perspectives of lake history. Fortunately, paleolimnological evidence from sedimentary records can shed light on lake ecosystem developments on timescales from years to millennia and provide information of the background or reference conditions of the lake (Simpson and Hall, 2012). This information is helpful in guiding management of nutrient-enriched lakes and setting restoration targets for lake recovery.

Well-preserved algal and bacterial pigments in anoxic sediments play a useful role in reconstructing past trophic changes in aquatic systems (Reuss et al., 2005). Recently, novel, non-destructive hyperspectral imaging (HSI) scanning techniques (in the visible and near infrared range, VNIR) have been used to quantify sedimentary chloropigments and bacteriopheophytins at very high (µm-scale) resolution (Butz et al., 2015). Specifically, HSI-inferred green pigment (chlorophyll-*a* and its diagenetic products) concentrations in sediments are used to reconstruct lake primary production (Butz et al., 2016; Schneider et al., 2018). HSI-inferred bacteriopheophytin *a* (Bphe-*a*) serves as a proxy for lake stratification and hypolimnetic anoxia (Butz et al., 2017; Makri et al., 2020; Zander et al., 2021).

**1.2 Research gaps, motivation and questions**

Lake eutrophication, along with increased external P loads into lakes and gross P sedimentation from water columns, has not always increased concentrations and net burial rates of P in surface sediments. The eutrophication process, however, tends to cause anoxic bottom waters and subsequently higher internal P loadings (Jeppesen et al., 2005; Smith et al., 2011). Higher internal P loadings have been reported from eutrophic and hypereutrophic lakes and reservoirs in Canada (Penn et al., 2000; Orihel et al., 2017), Denmark (Andersen and Ring, 1999), and the USA (Carter and Dzialowski, 2012). Understanding the fate and availability of P in lake sediments is essential for evaluating P cycling and its potential impacts on water quality. Nonetheless, most of the relevant research has been conducted in well-mixed shallow lakes and on short-term timescales. There is a lack of studies on investigating the response of sediment P availability to changes in lake trophy and hypolimnetic redox conditions from deep lakes. To our knowledge, few studies have reported the influence of lake eutrophication on potentials of internal P loadings and sediment P availability on longer timescales (from decadal to millennial timescales; prior to human-induced eutrophication).

This project aims at filling the abovementioned research gaps by studying sediments of three eutrophic deep lakes in Switzerland: the Ponte Tresa basin of Lake Lugano, Lake Burgäschi, and Soppensee (Fig. 2.1). The Ponte Tresa basin was selected because it is one of several deep lakes in Switzerland that have not yet recovered from anthropogenic eutrophication after large reductions of external P loadings, and the lake's eutrophication history since the mid-20th century is already well documented. Lake Burgäschi was selected because there were substantial changes in trophic levels and possibly lake mixing regimes documented during the last century, and the lake has exceptionally long historical and limnological survey data available for most of the last 50 years. We selected Soppensee because it is a deep, eutrophic lake featuring a varved sediment record, its sediments have an exceptionally good chronology, and it has a record of diatom-inferred epilimnetic total P (DI-TP) concentrations available for the entire Holocene.

This study addresses the following research questions:

i. How have P fractions in sediment profiles and potentials of internal P loadings varied with different lake trophic levels over the past several decades?

ii. What was the role of hypolimnetic anoxia and lake trophic state in affecting P cycling, sediment P fractions, and potentials of internal P loadings in the last century prior to cultural eutrophication?

iii. Is the P cycling under natural or pre-anthropogenic anoxic conditions comparable with the P cycling under the anthropogenic eutrophication and anoxia in recent times?

To answer these research questions, we investigated P fractions in sediments and their net burial rates in response to aquatic productivity and anoxia through time.

## 1.3 Outline of the thesis

The thesis consists of six chapters. Chapter 1 is the introduction of the topic and the research questions of the study.

Chapter 2 provides a general description of the three studied lakes and the applied methods.

Chapter 3 presents the case study of the Ponte Tresa basin of Lake Lugano. Net burial rates (NBR) of different P fractions and potentially bioavailable organic P in sediments were evaluated in relation to lake trophic history from 1959 to 2017. The aim of the chapter is to answer the first research question addressed in the previous section. This chapter has been published in the journal *Science of the Total Environment* (Tu et al., 2019).

Chapter 4 investigates the main factors controlling the long-term retention of P fractions in sediments of Lake Burgäschi since the 1900s and examines the effects of 40-years of

hypolimnetic water withdrawal on sedimentary P fractions. The main aim of this chapter is to answer the second research question. This chapter has been published in the journal *Biogeosciences* (Tu et al., 2020).

Chapter 5 investigates a 15,000-year record of P fractions in sediments, lake paleoproduction, and anoxia in Lake Soppensee. We estimated long-term qualitative internal P loadings by comparing the Holocene record of diatom-inferred epilimnetic total P (DI-TP) concentrations (Lotter, 2001) with sedimentary labile P fraction data under changing trophic, redox, and lake mixing regimes during the Late-glacial and Holocene periods. The main aim of this chapter is to answer the third research question. We have submitted this chapter to the journal *Earth and Planetary Science Letters* (Tu et al., 2021, submitted).

Chapter 6 highlights the main findings and conclusions of the present study and thesis.

## 1.4 References

Benndorf, J., 1990. Conditions for effective biomanipulation; conclusions derived from whole-lake experiments in Europe, Biomanipulation Tool for Water Management. Springer, Dordrecht, pp.187-203.

Burrus, D., Thomas, R., Dominik, B., Vernet, J.P., Dominik, J., 1990. Characteristics of suspended sediment in the Upper Rhone River, Switzerland, including the particulate forms of phosphorus. Hydrological Processes 4, 85-98.

Butz, C., Grosjean, M., Fischer, D., Wunderle, S., Tylmann, W., Rein, B., 2015. Hyperspectral imaging spectroscopy: a promising method for the biogeochemical analysis of lake sediments. Journal of Applied Remote Sensing 9, 096031.

Butz, C., Grosjean, M., Goslar, T., Tylmann, W., 2017. Hyperspectral imaging of sedimentary bacterial pigments: a 1700-year history of meromixis from varved Lake Jaczno, northeast Poland. Journal of Paleolimnology 58, 57-72.

Butz, C., Grosjean, M., Poraj-Górska, A., Enters, D., Tylmann, W., 2016. Sedimentary Bacteriopheophytin a as an indicator of meromixis in varved lake sediments of Lake Jaczno, north-east Poland, CE 1891–2010. Global and Planetary Change 144, 109-118.

Caraco, N., Cole, J., Likens, G., 1993. Sulfate control of phosphorus availability in lakes. Hydrobiologia 253, 275-280.

Caraco, N.F., Cole, J.J., Likens, G.E., 1991. Phosphorus release from anoxic sediments: lakes that break the rules. Internationale Vereinigung für theoretische und angewandte Limnologie: Verhandlungen 24, 2985-2988.

Carpenter, S.R., 2008. Phosphorus control is critical to mitigating eutrophication. Proceedings of the National Academy of Sciences 105, 11039-11040.

Chen, M., Ding, S., Chen, X., Sun, Q., Fan, X., Lin, J., Ren, M., Yang, L., Zhang, C., 2018. Mechanisms driving phosphorus release during algal blooms based on hourly changes in iron and phosphorus concentrations in sediments. Water Research 133, 153-164.

Chislock, M.F., Doster, E., Zitomer, R.A., Wilson, A., 2013. Eutrophication: causes, consequences, and controls in aquatic ecosystems. Nature Education Knowledge 4, 10.

Christophoridis, C., Fytianos, K., 2006. Conditions affecting the release of phosphorus from surface lake sediments. Journal of Environmental Quality 35, 1181-1192.

DePinto, J., Young, T., McIlroy, L., 1986. Impact of phosphorus control measures on water quality of the Great Lakes. Environmental Science & Technology 20, 752-759.

Ding, S., Wang, Y., Wang, D., Li, Y.Y., Gong, M., Zhang, C., 2016. In situ, high-resolution evidence for iron-coupled mobilization of phosphorus in sediments. Scientific Reports 6, 24341.

Dittrich, M., Chesnyuk, A., Gudimov, A., McCulloch, J., Quazi, S., Young, J., Winter, J., Stainsby, E., Arhonditsis, G., 2013. Phosphorus retention in a mesotrophic lake under transient loading conditions: insights from a sediment phosphorus binding form study. Water Research 47, 1433-1447.

Dittrich, M., Wehrli, B., Reichert, P., 2009. Lake sediments during the transient eutrophication period: Reactive-transport model and identifiability study. Ecological Modelling 220, 2751-2769.

Edmondson, W., 1970. Phosphorus, nitrogen, and algae in Lake Washington after diversion of sewage. Science 169, 690-691.

Einsele, W., 1936. Über die Beziehungen des Eisenkreislaufs zum Phosphatkreislauf im eutrophen See. Archiv für Hydrobiologie 29, 664-686.

Fagel, N., Alleman, L., Granina, L., Hatert, F., Thamo-Bozso, E., Cloots, R., André, L., 2005. Vivianite formation and distribution in Lake Baikal sediments. Global and Planetary Change 46, 315-336.

Fytianos, K., Kotzakioti, A., 2005. Sequential fractionation of phosphorus in lake sediments of Northern Greece. Environmental Monitoring and Assessment 100, 191-200.

Gächter, R., 1998. Ten Years of Artificial Mixing and Oxygenation: No Effect on the Internal Phosphorus Loading of Two Eutrophic Lake. Environmental Science & Technology 32, 3659–3665.

Gächter, R., 1976. Die tiefenwasserableitung, ein Weg zur Sanierung von Seen. Schweizerische Zeitschrift für Hydrologie 38, 1-28.

Gächter, R., 1987. Lake restoration. Why oxygenation and artificial mixing cannot substitute for a decrease in the external phosphorus loading. Swiss Journal of Hydrology 49, 170-185.

Gächter, R., Müller, B., 2003. Why the phosphorus retention of lakes does not necessarily depend on the oxygen supply to their sediment surface. Limnology and Oceanography 48, 929-933.

Gao, L., Zhou, J.M., Yang, H., Chen, J., 2005. Phosphorus fractions in sediment profiles and their potential contributions to eutrophication in Dianchi Lake. Environmental Geology 48, 835-844.

Genkai-Kato, M., Carpenter, S.R., 2005. Eutrophication due to phosphorus recycling in relation to lake morphometry, temperature, and macrophytes. Ecology 86, 210-219.

Gibbs, M.M., Howard-Williams, C., 2018. Physical Processes for In-Lake Restoration: Destratification and Mixing, Lake Restoration Handbook. Springer, Dordrecht, pp. 165-205.

Golterman, H., 2001. Phosphate release from anoxic sediments or What did Mortimer really write?'. Hydrobiologia 450, 99-106.

Hering, J.G., Hoehn, E., Klinke, A., Maurer, M., Peter, A., Reichert, P., Robinson, C., Schirmer, K., Schirmer, M., Stamm, C., 2012. Moving targets, long-lived infrastructure, and increasing needs for integration and adaptation in water management: an illustration from Switzerland. Environmental Science & Technology, 46,112–118.

Hickey, C.W., Gibbs, M.M., 2009. Lake sediment phosphorus release management—decision support and risk assessment framework. New Zealand Journal of Marine and Freshwater Research 43, 819-856.

Hupfer, M., Gloess, S., Grossart, H.-P., 2007. Polyphosphate-accumulating microorganisms in aquatic sediments. Aquatic Microbial Ecology 47, 299-311.

Hupfer, M., Lewandowski, J., 2008. Oxygen Controls the Phosphorus Release from Lake Sediments - a Long-Lasting Paradigm in Limnology. International Review of Hydrobiology 93, 415-432.

Jacquet, S., Kerimoglu, O., Rimet, F., Paolini, G., Anneville, O., 2014. Cyanobacterial bloom termination: the disappearance of Planktothrix rubescens from Lake Bourget (France) after restoration. Freshwater Biology 59, 2472-2487.

Jensen, H.S., Andersen, F.O., 1992. Importance of temperature, nitrate, and pH for phosphate release from aerobic sediments of four shallow, eutrophic lakes. Limnology and Oceanography 37, 577-589.

Jensen, H.S., McGlathery, K.J., Marino, R., Howarth, R.W., 1998. Forms and availability of sediment phosphorus in carbonate sand of Bermuda seagrass beds. Limnology and Oceanography 43, 799-810.

Jensen, H.S., Thamdrup, B., 1993. Iron-bound phosphorus in marine sediments as measured by bicarbonate-dithionite extraction, Proceedings of the Third International Workshop on Phosphorus in Sediments. Springer, Dordrecht, pp. 47-59.

Jensen, M., Liu, Z., Zhang, X., Reitzel, K., Jensen, H.S., 2017. The effect of biomanipulation on phosphorus exchange between sediment and water in shallow, tropical Huizhou West Lake, China. Limnologica - Ecology and Management of Inland Waters 63, 65-73.

Jeppesen, E., Søndergaard, M., Jensen, J.P., Havens, K.E., Anneville, O., Carvalho, L., Coveney, M.F., Deneke, R., Dokulil, M.T., Foy, B., 2005. Lake responses to reduced nutrient loading–an analysis of contemporary long-term data from 35 case studies. Freshwater Biology 50, 1747-1771.

Jin, X., Wang, S., Pang, Y., Wu, F.C., 2006. Phosphorus fractions and the effect of pH on the phosphorus release of the sediments from different trophic areas in Taihu Lake, China. Environmental Pollution 139, 288-295.

Joshi, S.R., Kukkadapu, R.K., Burdige, D.J., Bowden, M.E., Sparks, D.L., Jaisi, D.P., 2015. Organic matter remineralization predominates phosphorus cycling in the mid-bay sediments in the Chesapeake Bay. Environmental Science & Technology 49, 5887-5896.

Katsev, S., Dittrich, M., 2013. Modeling of decadal scale phosphorus retention in lake sediment under varying redox conditions. Ecological Modelling 251, 246-259.

Katsev, S., Tsandev, I., L'Heureux, I., Rancourt, D.G., 2006. Factors controlling long-term phosphorus efflux from lake sediments: Exploratory reactive-transport modeling. Chemical Geology 234, 127-147.

Kosten, S., Huszar, V.L., Bécares, E., Costa, L.S., van Donk, E., Hansson, L.A., Jeppesen, E., Kruk, C., Lacerot, G., Mazzeo, N., 2012. Warmer climates boost cyanobacterial dominance in shallow lakes. Global Change Biology 18, 118-126.

Kuha, J.K., Palomäki, A.H., Keskinen, J.T., Karjalainen, J.S., 2016. Negligible effect of hypolimnetic oxygenation on the trophic state of Lake Jyväsjärvi, Finland. Limnologica 58, 1-6.

Lewis Jr, W.M., Wurtsbaugh, W.A., 2008. Control of lacustrine phytoplankton by nutrients: erosion of the phosphorus paradigm. International Review of Hydrobiology 93, 446-465.

Liboriussen, L., Søndergaard, M., Jeppesen, E., Thorsgaard, I., Grünfeld, S., Jakobsen, T.S., Hansen, K., 2009. Effects of hypolimnetic oxygenation on water quality: results from five Danish lakes. Hydrobiologia 625, 157-172.

Lotter, A.F., 2001. The palaeolimnology of Soppensee (Central Switzerlabnd), as evidenced by diatom, pollen, and fossil-pigment analyses. Journal of Paleolimnology 25, 65-79.

Lukkari, K., Hartikainen, H. and Leivuori, M., 2007. Fractionation of sediment phosphorus revisited. I: Fractionation steps and their biogeochemical basis. Limnology and Oceanography: Methods 5, 433-444.

Lürling, M., van Oosterhout, F., 2013. Controlling eutrophication by combined bloom precipitation and sediment phosphorus inactivation. Water Research 47, 6527-6537.

Makri, S., Rey, F., Gobet, E., Gilli, A., Tinner, W., Grosjean, M., 2020. Early human impact in a 15,000-year high-resolution hyperspectral imaging record of paleoproduction and anoxia from a varved lake in Switzerland. Quaternary Science Reviews 239, 106335.

Marsden, M.W., 1989. Lake restoration by reducing external phosphorus loading: the influence of sediment phosphorus release. Freshwater Biology 21, 139-162.

Mortimer, C.H., 1941. The exchange of dissolved substances between mud and water in lakes. Journal of Ecology 29, 280-329.

Müller, B., Bryant, L.D., Matzinger, A., Wüest, A., 2012. Hypolimnetic oxygen depletion in eutrophic lakes. Environmental Science & Technology 46, 9964-9971.

Nembrini, G., Capobianco, J., Viel, M., Williams, A., 1983. A Mössbauer and chemical study of the formation of vivianite in sediments of Lago Maggiore (Italy). Geochimica et Cosmochimica Acta 47, 1459-1464.

North, R.P., North, R.L., Livingstone, D.M., Köster, O., Kipfer, R., 2014. Long-term changes in hypoxia and soluble reactive phosphorus in the hypolimnion of a large temperate lake: consequences of a climate regime shift. Global Change Biology 20, 811-823.

Nürnberg, G.K., 1991. Phosphorus from internal sources in the Laurentian Great Lakes, and the concept of threshold external load. Journal of Great Lakes Research 17, 132-140.

Nürnberg, G.K., 2007. Lake responses to long-term hypolimnetic withdrawal treatments. Lake and Reservoir Management 23, 388-409.

Nürnberg, G.K., Hartley, R., Davis, E., 1987. Hypolimnetic withdrawal in two North American lakes with anoxic phosphorus release from the sediment. Water Research 21, 923-928.

Orihel, D.M., Baulch, H.M., Casson, N.J., North, R.L., Parsons, C.T., Seckar, D.C., Venkiteswaran, J.J., 2017. Internal phosphorus loading in Canadian fresh waters: a critical review and data analysis. Canadian Journal of Fisheries and Aquatic Sciences 74, 2005-2029.

Paerl, H., Fulton, R., 2006. Ecology of harmful cyanobacteria, Ecology of harmful algae. Springer, Dordrecht, pp. 95-109.

Paerl, H.W., Huisman, J., 2008. Blooms like it hot. Science 320, 57-58.

Paerl, H.W., Justic, D., 2011. 6.03 Primary producers: phytoplankton ecology and trophic dynamics in coastal waters. In: Wolanski, E. and McLusky, D.S. (eds.) Treatise on Estuarine and Coastal Science. Waltham: Academic Press. pp. 23–42.

Parsons, C.T., Rezanezhad, F., O'Connell, D.W., Van Cappellen, P., 2017. Sediment phosphorus speciation and mobility under dynamic redox conditions. Biogeosciences 14, 3585–3602.

Penn, M.R., Auer, M.T., Doerr, S.M., Driscoll, C.T., Brooks, C.M., Effler, S.W., 2000. Seasonality in phosphorus release rates from the sediments of a hypereutrophic lake under a matrix of pH and redox conditions. Canadian Journal of Fisheries and Aquatic Sciences 57, 1033-1041.

Petticrew, E.L., Arocena, J.M., 2001. Evaluation of iron-phosphate as a source of internal lake phosphorus loadings. Science of the Total Environment 266, 87-93.

Prairie, Y.T., de Montigny, C., Del Giorgio, P.A., 2001. Anaerobic phosphorus release from sediments: a paradigm revisited. Internationale Vereinigung für theoretische und angewandte Limnologie: Verhandlungen 27, 4013-4020.

Premazzi, G., Cardoso, A., Rodari, E., Austoni, M., Chiaudani, G., 2005. Hypolimnetic withdrawal coupled with oxygenation as lake restoration measures: the successful case of Lake Varese (Italy). Limnetica 24, 123-131.

Qin, B., Zhou, J., Elser, J.J., Gardner, W.S., Deng, J., Brookes, J.D., 2020. Water Depth Underpins the Relative Roles and Fates of Nitrogen and Phosphorus in Lakes. Environmental Science & Technology 54, 3191-3198.

Ramisch, F., Dittrich, M., Mattenberger, C., Wehrli, B., Wüest, A., 1999. Calcite dissolution in two deep eutrophic lakes. Geochimica et Cosmochimica Acta 63, 3349-3356.

Reuss, N., Conley, D.J., Bianchi, T.S., 2005. Preservation conditions and the use of sediment pigments as a tool for recent ecological reconstruction in four Northern European estuaries. Marine Chemistry 95, 283-302.

Rothe, M., Frederichs, T., Eder, M., Kleeberg, A., Hupfer, M., 2014. Evidence for vivianite formation and its contribution to long-term phosphorus retention in a recent lake sediment: a novel analytical approach. Biogeosciences 11, 5169-5180.

Ruban, V., Lopez-Sanchez, J.F., Pardo, P., Rauret, G., Muntau, H., Quevauviller, P., 2001. Development of a harmonised phosphorus extraction procedure and certification of a sediment reference material. Journal of Environmental Monitoring 3, 121-125.

Ruttenberg, K.C., 1992. Development of a sequential extraction method for different forms of phosphorus in marine sediments. Limnology and Oceanography 37, 1460-1482.

Rydin, E., 2000. Potentially mobile phosphorus in Lake Erken sediment. Water Research 34, 2037-2042.

Schindler, D.W., 1974. Eutrophication and recovery in experimental lakes: implications for lake management. Science 184, 897-899.

Schindler, D.W., 2006. Recent advances in the understanding and management of eutrophication. Limnology and Oceanography 51, 356–363.

Schindler, D.W., 2012. The dilemma of controlling cultural eutrophication of lakes. Proceedings of the Royal Society B: Biological Sciences 279, 4322–4333.

Schindler, D.W., Carpenter, S.R., Chapra, S.C., Hecky, R.E., Orihel, D.M., 2016. Reducing phosphorus to curb lake eutrophication is a success. Environmental Science & Technology 50, 8923–8929

Schneider, T., Rimer, D., Butz, C., Grosjean, M., 2018. A high-resolution pigment and productivity record from the varved Ponte Tresa basin (Lake Lugano, Switzerland) since 1919:

insight from an approach that combines hyperspectral imaging and high-performance liquid chromatography. Journal of Paleolimnology 60, 381–398.

Shilla, D.A., Asaeda, T., Kalibbala, M., 2008. Phosphorus speciation in Myall Lake sediment, NSW, Australia. Wetlands Ecology and Management 17, 85-91.

Simpson, G.L., Hall, R.I., 2012. Human impacts: Applications of numerical methods to evaluate surface-water acidification and eutrophication. In Tracking environmental change using lake sediments. Springer, Dordrecht, pp. 579-614.

Smith, L., Watzin, M.C., Druschel, G., 2011. Relating sediment phosphorus mobility to seasonal and diel redox fluctuations at the sediment–water interface in a eutrophic freshwater lake. Limnology and Oceanography 56, 2251-2264.

Smith, V.H., Schindler, D.W., 2009. Eutrophication science: where do we go from here?. Trends in Ecology & Evolution 24, 201-207.

Søndergaard, M., Jensen, J.P. and Jeppesen, E., 2003. Role of sediment and internal loading of phosphorus in shallow lakes. Hydrobiologia, 506,135-145.

Sondergaard, M., Jensen, P.J., Jeppesen, E., 2001. Retention and internal loading of phosphorus in shallow, eutrophic lakes. Scientific World Journal 1, 427-442.

Søndergaard, M., Windolf, J., Jeppesen, E., 1996. Phosphorus fractions and profiles in the sediment of shallow Danish lakes as related to phosphorus load, sediment composition and lake chemistry. Water Research 30, 992-1002.

Spears, B., Carvalho, L., Perkins, R., Kirika, A., Paterson, D., 2011. Long-term variation and regulation of internal phosphorus loading in Loch Leven, Loch Leven: 40 years of scientific research. Springer, Dordrecht, pp. 23-33.

Sun Loh, P., Molot, L.A., Nowak, E., Nürnberg, G.K., Watson, S.B., Ginn, B., 2013. Evaluating relationships between sediment chemistry and anoxic phosphorus and iron release across three different water bodies. Inland Waters 3, 105-118.

Tammeorg, O., Mols, T., Niemisto, J., Holmroos, H., Horppila, J., 2017. The actual role of oxygen deficit in the linkage of the water quality and benthic phosphorus release: Potential implications for lake restoration. Science of The Total Environment 599-600, 732-738.

Tu, L., Jarosch, K.A., Schneider, T., Grosjean, M., 2019. Phosphorus fractions in sediments and their relevance for historical lake eutrophication in the Ponte Tresa basin (Lake Lugano, Switzerland) since 1959. Science of The Total Environment 685, 806-817.

Tu, L., Zander, P., Szidat, S., Lloren, R., Grosjean, M., 2020. The influences of historic lake trophy and mixing regime changes on long-term phosphorus fraction retention in sediments of deep eutrophic lakes: a case study from Lake Burgäschi, Switzerland. Biogeosciences 17, 2715-2729.

Welch, E.B., Cooke, G.D., 2005. Internal Phosphorus Loading in Shallow Lakes: Importance and Control. Lake and Reservoir Management 21, 209-217.

Williams, J., Jaquet, J., Thomas, R., 1976. Forms of phosphorus in the surficial sediments of Lake Erie. Journal of the Fisheries Board of Canada 33, 413-429.

Woolway, R.I., Merchant, C.J., 2019. Worldwide alteration of lake mixing regimes in response to climate change. Nature Geoscience 12, 271-276.

Wu, Z., Liu, Y., Liang, Z., Wu, S., Guo, H., 2017. Internal cycling, not external loading, decides the nutrient limitation in eutrophic lake: A dynamic model with temporal Bayesian hierarchical inference. Water Research 116, 231-240.

Wu, Z., Wang, S., 2017. Release mechanism and kinetic exchange for phosphorus (P) in lake sediment characterized by diffusive gradients in thin films (DGT). Journal of Hazardous Materials 331, 36-44.

Zander, P.D., Żarczyński, M., Vogel, H., Tylmann, W., Wacnik, A., Sanchini, A., Grosjean, M., 2021. A high-resolution record of Holocene primary productivity and water-column mixing from the varved sediments of Lake Żabińskie, Poland. Science of the Total Environment, 143713.

# Chapter 2: Materials and methods

## 2.1 Site description

The lakes studied in this project are situated in the southern Swiss Alps (the Ponte Tresa basin of Lake Lugano) and the Swiss Plateau (Lake Burgäschi and Soppensee; Fig. 2.1). Detailed information about the three lakes is provided in Table 2.1.
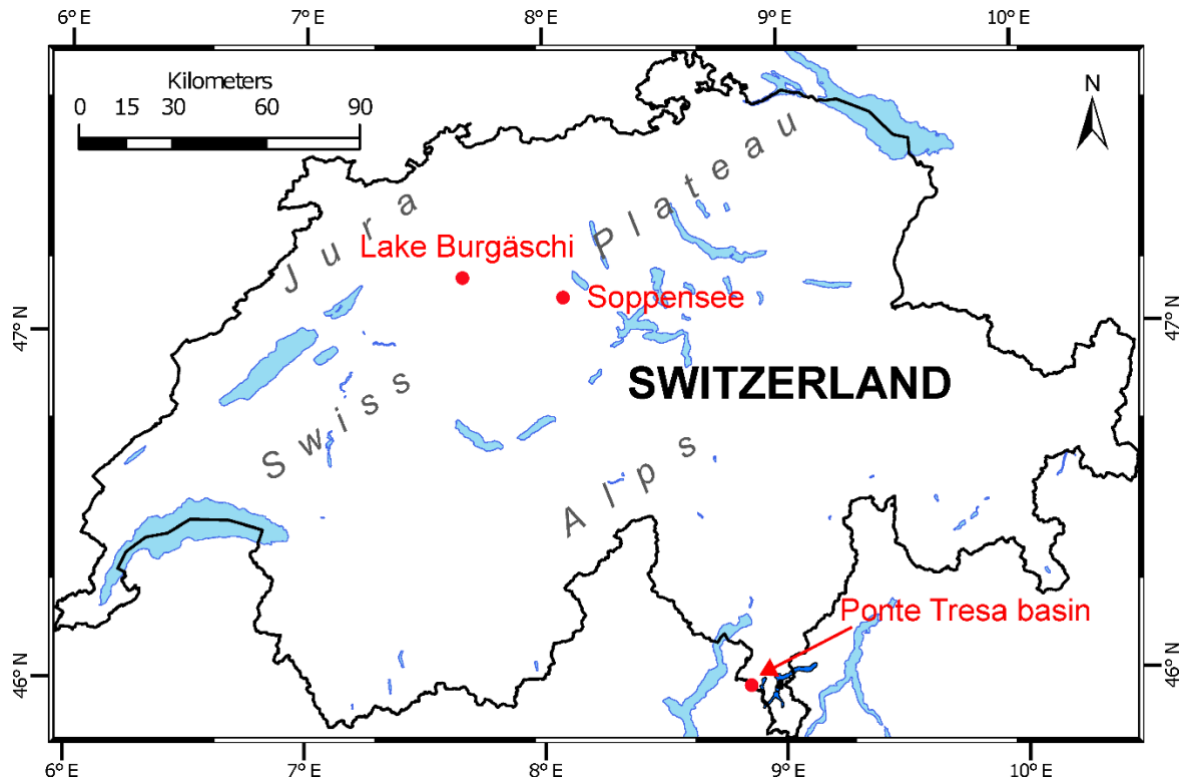


**Figure 2.1**: Map of Switzerland showing the locations of the three lakes investigated in this thesis. Lake Burgäschi, Lake Soppen (Soppensee), and the Ponte Tresa basin of Lake Lugano are indicated by the red dots.

**Table 2.1**: Morphological and hydrological characteristics of the studied lakes.

| | Ponte Tresa basin | Lake Burgäschi | Soppensee |
|---|---|---|---|
| Latitude (N) | 45°58′ | 47°10′ | 47°05′ |
| Longitute (E) | 8°52′ | 7°40′ | 8°05′ |
| Lake elevation (m a.s.l.) | 271 | 465 | 596 |
| Lake surface area (km$^2$) | 1.1 | 0.21 | 0.227 |
| Lake volume (km$^3$) | 0.03 | 0.0028 | 0.0029 |
| Maximun depth (m) | 50 | 31 | 27 |
| Mean depth (m) | 33 | 12.9 | 12.3 |
| Catchment area (km$^2$) | 5.6 | 3.2 | 1.6 |
| Residence time (years) | 0.04 | 1.4 | 3.2 |
| Total phosphorus (µg L$^{-1}$) | 180 | 20-50[a] | 50-116 |
| pH[a] | 7.0–9.1 | 7.3–8.7 | 7.2–8.5 |
| Core name | PTRE 17-2 | Burg17-B | So08-3 |
| | | Burg17-C | |
| Time period covered by the sediment cores (~years) | 60 | 120 | 15,000 |

[a] measured in water depths of 0–20 m

### 2.1.1 The Ponte Tresa basin of Lake Lugano

Lake Lugano (45°59′0″ N, 8°58′0″ E) is a deep lake situated at the border between Switzerland and Italy in the southern Alps (Fig. 2.2). This fluvio-glacial tectonic lake was formed by fluvial erosion during the Tertiary and reshaped during repeated Alpine glaciations in the Pleistocene (Barbieri and Simona, 2001). The watershed of the lake (624 km$^2$) consists of calcareous rocks, gneiss, and porphyry bedrock. The Ponte Tresa basin is the smallest basin of Lake Lugano with only ~50 m of maximum water depth and 1.1 km$^2$ of lake surface area. The details about the morphometric and hydrological characteristics of the three different basins of Lake Lugano are described in Simona et al. (2015). The main outflow of Lake Lugano is in the north-

west of the Ponte Tresa basin (Fig. 2.2). The waters from northern and southern basins are the main nutrient supplier for the Ponte Tresa basin.
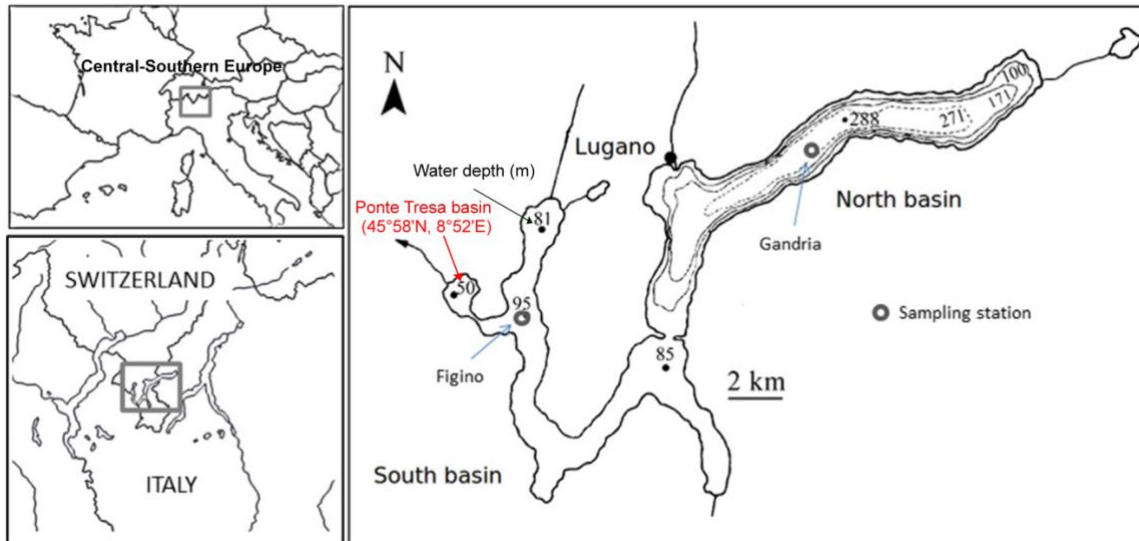


**Figure 2.2:** Location of Lake Lugano and the three basins: the northern basin, the southern basin, and the Ponte Tresa basin. The figure is from Lepori and Roberts (2017).

Lake Lugano became highly eutrophic from the 1960s to the 1970s onwards due to large loads of nutrients (principally P) in sewage from increasing urbanization and industrialization in the watershed. Eutrophication restoration measures, such as the installation of wastewater treatment plants around the lake in 1976 and Switzerland banning phosphate detergents in 1986, have reduced annual external P loadings by 75%. Despite decreased concentrations of water phosphate from the early 1980s until the last decade (2006–2015), the lake is still eutrophic, as shown by phosphate concentrations of 50–60 µg $L^{-1}$ in the northern basin (Barbieri and Simona, 2001). Today, in Lake Lugano sewage and households contribute a large part (85%) of the total external nutrient loadings, followed by industrial and agricultural sources only representing 15% (Barbieri and Simona, 2001). Additionally, internal P loadings in Lake Lugano are an important factor maintaining eutrophication, which is likely favored by the long eutrophication history and the warm monomictic lake mixing regime (Lepori and Roberts, 2017).

This study focusses on the Ponte Tresa basin where varved sediments are formed under highly productive and anoxic bottom-water conditions (Züllig, 1982). The history of human-induced eutrophication in this basin is well-documented by high-resolution sedimentary pigment records (Schneider et al., 2018). It has been shown that eutrophication in the Ponte

Tresa basin started during the 1940–1950s, and then the lake remained highly eutrophic from the 1960s to the present (Sanchini and Grosjean, 2020). Therefore, the Ponte Tresa basin provides an ideal study site for investigating the relationship between net burial rates of sediment P and the lake's eutrophication history in the last few decades. The sediments of the Ponte Tresa basin are presented in Chapter 3.

### 2.1.2 Lake Burgäschi

Lake Burgäschi is a small postglacial lake at 465 m a.s.l. on the Swiss Plateau (Fig. 2.1). The catchment area geologically belongs to the Molasse basin and mostly consists of carbonate-rich sandstone and mudstone (Schmid et al., 2004). The catchment area of this kettle lake is relatively small (~3.2 km$^2$) compared to its maximum water depth of ~31 m (Guthruf et al., 1999). The landscape was originally dominated by mixed beech (*Fagus sylvatica*) forests and peat bogs but was later intensively shaped by agricultural activities. Today, agricultural areas cover ~55% of the total lake catchment (Guthruf et al., 1999).

Lake Burgäschi sediments exhibit annual laminations for most of the last ~6,800 years (Rey et al., 2017). The laminated sediment profile provides an exceptional archive for high-resolution paleolimnology studies. Limnological monitoring data of Lake Burgäschi covers the last 50 years. The lake has been highly productive since the mid-20th century due to intensified agricultural activities around the lake. The high lake primary production leads to strong $O_2$ depletion in deep waters. For example, according to water profile measurements in September 2003, the lake water was completely anoxic at depths greater than 9 m (Guthruf et al., 2013). The restoration technique of hypolimnetic water withdrawal started operating in 1977. However, this treatment has stabilized but not fundamentally improved the lake's trophic state (GSA, 2007; Guthruf et al., 2013). Although hypolimnetic water withdrawal has decreased P concentrations in surface waters, its influence on sediment P fractions has not been examined. Therefore, it is necessary to explore this effect with sediment P data. Importantly, Lake Burgäschi provides a suitable testbed for investigating the response of net burial rates of sedimentary P fractions to changes in lake trophy and hypolimnetic redox conditions since the 20th century, prior to recent eutrophication. Lake Burgäschi sediments were investigated in Chapter 4.

### 2.1.3 Soppensee

Lake Soppensee is a kettle lake in the Swiss Central Plateau (Fig. 2.1). The lake sediments began to accumulate at the end of the last glacial period (~15,000 years; Lotter, 2001). It has a small surface area (0.227 km$^2$) relative to its maximum water depth (27 m). It is mainly fed by groundwater and seasonal surface run-off from a small calcareous sandstone catchment of 1.6 km$^2$ (Lotter, 1989).

In 2008, a field campaign was carried out in Soppensee, and three parallel cores (So08/01–03) were retrieved at the deepest site using an UWITEC piston corer (van Raden, 2012). Sediment cores of So08-01/2 have been studied for XRD mineralogy (van Raden, 2012), terrestrial biomarkers (Gierga et al., 2016), and rock and mineral magnetism (Kind et al., 2012). Soppensee is a naturally nutrient-enriched lake based on trophic reconstructions from diatom assemblages (Lotter, 2001) and chironomids and cladocera (Hofmann, 2001). The diatom-inferred epilimnetic total P (DI-TP) concentrations (20–40 µg L$^{-1}$) suggest mesotrophic to eutrophic conditions for most parts of the Holocene (Lotter, 2001). The long-term sediment record of Soppensee is presented in Chapter 5.

## 2.2 Methods

This section briefly introduces the methods applied during this project. More details about the methods can be found in the corresponding publications (Chapters 3-5).

### 2.2.1 Field methods

In 2008, piston cores (Core So08 3A-C) were recovered from the deepest part of Soppensee (van Raden, 2012) and were transferred to the lab in Geological Institute, ETH Zürich. The cores were tightly sealed and stored in a dark cold room (~4 °C) before opening. In 2017, several short sediment cores (< 1.5 m) were collected from the deepest parts of the Ponte Tresa basin of Lake Lugano and Lake Burgäschi using an UWITEC gravity corer (6 cm PP-tubes). The cores were sealed and transferred into the lab at the Institute of Geography, University of Bern and stored in a dark cold room (~4 °C) before opening.

### 2.2.2 Non-destructive scanning techniques

After the cores were split lengthwise in two halves, A and B, surface sediments of the A-half cores were described following the method in Schnurrenberger et al. (2003). Then, pictures of A-half cores from the Ponte Tresa basin and Lake Burgäschi were taken with a Nikon D80 digital camera. The A-half cores of the three lakes were used for visual correlation and non-destructive scanning techniques including x-ray fluorescence (XRF) and hyperspectral imaging (HSI). The B-half cores were subsampled for destructive geochemical analyses, e.g., P extraction and pigment analysis.

XRF core scanning was applied on fresh sediment cores of Lake Burgäschi and Soppensee for the measurement of the semi-quantitative element composition. For Lake Burgäschi, we used an Avaatech XRF core scanner equipped with a rhodium anode and a 25 µm Be window at the Swiss Federal Institute of Aquatic Science and Technology and applied a 0.5-mm scanning resolution. For Soppensee, we used an ITRAX core scanner equipped with a Chromium anode at the Geological Institute, University of Bern and applied a 5-mm scanning

resolution. Further scanning settings can be found in Chapters 4 and 5. The elements Mg, Si, Al, K, Ti, Rb, P, Fe, Mn, and Ca were selected for the project. The XRF-data are expressed as counts per second (cps) for Lake Burgäschi and total counts per area (cts) for Soppensee.

For sediments of Lake Burgäschi and Soppensee, the HSI scans were made with a Specim Ltd. single core scanner equipped with a hyperspectral linescan camera (Specim PFD-CL-65-V10E) in the visual to near-infrared range (VNIR, 400–1000 nm) following the methodology in Butz et al. (2015). Based on spectral endmembers, relative absorption band depth (RABD) indices were calculated to quantify the absorbance troughs caused by sedimentary chloropigments and bacteriopheophytins in sediments. The spectral index indicative of chloropigments (calculated using the method in Schneider et al., 2018) is used as a proxy for lake primary production of Lake Burgäschi. The $RABD_{845}$ spectral index (calculated following Butz et al., 2015) represents bacteriopheophytins *a* and *b*, a specific biomarker diagnostic for purple sulfur bacteria (PSB) that live at the chemocline of stratified lakes.

### 2.2.3 Pigment extraction and HSI index-calibration

To calibrate RABD indices to absolute concentrations of green pigments (chlorophyll-*a* + pheophytin-*a*) and bacteriopheophytin-*a* (Bphe-*a*) in sediments of Soppensee, we followed a calibration method in Butz et al. (2015). The pigment extraction procedure in Amann et al. (2014) was applied. The pigment concentrations in extracts of selected sediment samples were measured by spectrophotometry (Shimadzu UV-1800). HSI-inferred green pigment concentrations indicate aquatic primary production (Schneider et al., 2018); HSI-inferred Bphe-*a* indicates the presence of chemocline of stratified water columns and serves as a proxy for hypolimnetic anoxia (Butz et al., 2017).

### 2.2.4 Chronologies

At the Ponte Tresa basin, the ages of sediment samples were determined by careful visual stratigraphic correlation (layer by layer) to the dated core in Schneider et al. (2018). At Lake Soppensee, the chronology of the sediment cores was obtained from the correlation of XRF data and sedimentary marker layers to core So08-01/2 dated by Hajdas and Michczyński (2010) and van Raden (2012).

At Lake Burgäschi, the method of ^{210}Pb, [226]Ra, and ^{137}Cs radionuclide dating was applied on freeze-dried and homogeneous sediments. The radionuclide activities were measured with gamma spectrometry at University of Bern. The correction for the total missing inventory of unsupported ^{210}Pb was done according to the protocol in Tylmann et al. (2016). Two [137]Cs- and [241]Am-peaks serve as the time markers of peak fallouts from nuclear weapons testing in 1963 and Chernobyl accident in 1986, respectively. The ^{210}Pb chronology was determined

using the constant rate of supply (CRS) model (Appleby, 2002). We tested two CRS models: one has the chronological marker constraint of ^{137}Cs-peaking in 1963, and the other is without any chronological constrains. The time marker of ^{137}Cs-peaking in 1986 was used to test and validate the two CRS models.

### 2.2.5 Phosphorus fractions extraction and analysis

Different P fractions in fresh anoxic sediments from the Ponte Tresa basin and Lake Burgäschi were determined with a sequential P extraction protocol that was slightly modified from Lukkari et al. (2007). The applied extraction procedures separate P forms mainly into loosely absorbed-P, redox-sensitive Fe-bound P, metal oxides bound P (Al and nonreducible Fe), Ca-bound P (apatite-P), and refractory organic P (Lukkari et al., 2007). At the Ponte Tresa basin, the potential bioavailability of organic P in sediments was evaluated using a phosphatase enzymatic hydrolysis method (Jarosch et al., 2015) after the chemical NaOH-EDTA (0.25 M-0.05 M) extraction on bulk sediments (Bowman and Moir, 1993). The organic P in NaOH-EDTA extracts was further characterized into potentially bioavailable (i.e. enzyme-labile) and potentially non-bioavailable (i.e. enzyme stabile) fractions.

The P fractionation in Soppensee sediments principally followed the harmonized protocol developed by the standards, measurements and testing (SMT) of the European Commission as modified in Ruban et al. (1999) and Ruban et al. (2001) based on Williams et al. (1976). The SMT protocol consists of three independent extraction procedures and defines five P fractions including non-apatite inorganic P, apatite P, inorganic P, organic P, and total P.

Inorganic P concentrations in extracts of samples were analyzed spectrophotometrically with the malachite green method (Ohno and Zibilske, 1991) and the absorbance measured at 610 nm using a UV-VIS spectrophotometer. Total P concentrations in extracts of samples were measured with inductively coupled plasma mass spectroscopy (ICP-MS).

### 2.2.6 Bulk elements analyses

For Lake Burgäschi sediments, total inorganic carbon (TIC) content was determined by loss on ignition ($LOI_{950°C}$) following the method in Heiri et al. (2001). Concentrations of total carbon (TC), total nitrogen (TN), and total sulfur (S) in sediments were determined using an Elementar vario EL cube elemental analyzer. Total organic carbon (TOC) content was calculated using the equation $TOC = TC - TIC$. Water contents (%), dry bulk density ($g \cdot cm^{-3}$), and sediment mass accumulation rates (MAR; $g \cdot cm^{-2} \cdot y^{-1}$) were calculated according to the method in Håkanson and Jansson (2002).

## 2.3 References

Amann, B., Lobsiger, S., Fischer, D., Tylmann, W., Bonk, A., Filipiak, J., Grosjean, M., 2014. Spring temperature variability and eutrophication history inferred from sedimentary pigments in the varved sediments of Lake Żabińskie, north-eastern Poland, AD 1907–2008. Global and Planetary Change 123, 86-96.

Appleby, P.G., 2008. Three decades of dating recent sedi-ments by fallout radionuclides: a review. The Holocene 18, 83–93.

Barbieri, A., Simona, M., 2001. Trophic evolution of Lake Lugano related to external load reduction: Changes in phosphorus and nitrogen as well as oxygen balance and biological parameters. Lakes & Reservoirs: Research & Management 6, 37-47.

Bowman, R., Moir, J., 1993. Basic EDTA as an extractant for soil organic phosphorus. Soil Science Society of America Journal 57, 1516-1518.

Butz, C., Grosjean, M., Fischer, D., Wunderle, S., Tylmann, W., Rein, B., 2015. Hyperspectral imaging spectroscopy: a promising method for the biogeochemical analysis of lake sediments. Journal of Applied Remote Sensing 9, 096031.

Butz, C., Grosjean, M., Goslar, T., Tylmann, W., 2017. Hyperspectral imaging of sedimentary bacterial pigments: a 1700-year history of meromixis from varved Lake Jaczno, northeast Poland. Journal of Paleolimnology 58, 57-72.

Gierga, M., Hajdas, I., van Raden, U.J., Gilli, A., Wacker, L., Sturm, M., Bernasconi, S.M., Smittenberg, R.H., 2016. Long-stored soil carbon released by prehistoric land use: evidence from compound-specific radiocarbon analysis on Soppensee lake sediments. Quaternary Science Reviews 144, 123-131.

GSA: 30 Jahre Tiefenwasser-Ableitung. Wie geht es dem Burgäschisee heute?, Office for Water Protection and Waste Management of the Canton of Bern, Bern, 2007

Guthruf, J., Zeh, M., and Guthruf-Seiler, K.: Kleinseen im Kanton Bern, Water Protection and Waste Management Office of the Canton of Bern, Bern, 1999.

Guthruf, K., Maurer, V., Ryser, R., Zeh, M., and Zweifel, N.: Zustand der Kleinseen, Construction, Transport and Energy Directorate of the Canton of Bern Office for Water and Waste Water and soil protection laboratory, Bern, 2013.

Hajdas, I., Michczyński, A., 2010. Age-depth model of Lake Soppensee (Switzerland) based on the high-resolution 14 C chronology compared with varve chronology. Radiocarbon 52, 1027-1040.

Håkanson, L., Jansson, M., 2002. Principles of Lake Sedimentology. The Blackburn Press, New Jersey.

Heiri, O., Lotter, A.F., Lemcke, G., 2001. Loss on ignition as a method for estimating organic and carbonate content in sediments: Reproducibility and comparability of results. Journal of Paleolimnology 25, 101–110.

Hofmann, W., 2001. Late-Glacial/Holocene succession of the chironomid and cladoceran fauna of the Soppensee (Central Switzerland). Journal of Paleolimnology 25, 411-420.

Jarosch, K.A., Doolette, A.L., Smernik, R.J., Tamburini, F., Frossard, E., Bünemann, E.K., 2015. Characterisation of soil organic phosphorus in NaOH-EDTA extracts: A comparison of $^{31}$P NMR spectroscopy and enzyme addition assays. Soil Biology and Biochemistry 91, 298-309.

Kind, J., Raden, U.J.v., García-Rubio, I., Gehring, A.U., 2012. Rock magnetic techniques complemented by ferromagnetic resonance spectroscopy to analyse a sediment record. Geophysical Journal International 191, 51-63.

Lepori, F., Roberts, J.J., 2017. Effects of internal phosphorus loadings and food-web structure on the recovery of a deep lake from eutrophication. Journal of Great Lakes Research 43, 255-264.

Lotter, A.F., 2001. The palaeolimnology of Soppensee (Central Switzerlabnd), as evidenced by diatom, pollen, and fossil-pigment analyses. Journal of Paleolimnology 25, 65-79.

Lukkari, K., Hartikainen, H., Leivuori, M., 2007. Fractionation of sediment phosphorus revisited. I: Fractionation steps and their biogeochemical basis. Limnology and Oceanography: Methods 5, 433-444.

Ohno, T., Zibilske, L.M., 1991. Determination of low concentrations of phosphorus in soil extracts using malachite green. Soil Science Society of America Journal 55, 892–895.

Rey, F., Gobet, E., van Leeuwen, J.F.N., Gilli, A., van Raden, U.J., Hafner, A., Wey, O., Rhiner, J., Schmocker, D., Zünd, J., Tinner, W., 2017. Vegetational and agricultural dynamics at Burgäschisee (Swiss Plateau) recorded for 18,700 years by multi-proxy evidence from partly varved sediments. Vegetation History and Archaeobotany 26, 571-586.

Sanchini, A., Grosjean, M., 2020. Quantification of chlorophyll a, chlorophyll b and pheopigments a in lake sediments through deconvolution of bulk UV–VIS absorption spectra. Journal of paleolimnology 64, 243-256.

Schmid, S. M., Fügenschuh, B., Kissling, E., Schuster, R., 2004. Tectonic map and overall architecture of the Alpine orogen, Eclogae Geologicae Helvetiae 97, 93–117.

Schnurrenberger, D., Russell, J., Kelts, K., 2003. Classifica-tion of lacustrine sediments based on sedimentary com-ponents. Journal of paleolimnology 29, 141–154.

Simona, M., Lepori, F., Pozzoni, M., 2015. Ricerche sull'evoluzione del Lago di Lugano. Aspetti limnologici. Programma triennale 2013-2015. Campagna 2014.

Tylmann, W., Bonk, A., Goslar, T., Wulf, S., Grosjean, M., 2016. Calibrating 210Pb dating results with varve chro-nology and independent chronostratigraphic markers: Problems and implications. Quaternary Geochronology 32, 1–10.

Van Raden, U.J., 2012. High resolution swiss lake records of climate change. Ph.D. Thesis, ETH, Zürich, pp. 140-141.

Züllig, H., 1982. Untersuchungen über die Stratigraphie von Carotinoiden im geschichteten Sediment von 10 Schwei-zer Seen zur Erkundung früherer Phytoplankton-Entfal-tungen. Schweizerische Zeitschrift für Hydrologie 44, 1–98.

# Chapter 3: Phosphorus fractions in sediments and their relevance for historical lake eutrophication in the Ponte Tresa basin (Lake Lugano, Switzerland) since 1959

## 3.1 Phosphorus fractions in sediments and their relevance for historical lake eutrophication in the Ponte Tresa basin (Lake Lugano, Switzerland) since 1959

Luyao Tu[1, 2, *], Klaus A. Jarosch[2], Tobias Schneider[1, 2], Martin Grosjean[1, 2]

[1]*Oeschger Centre for Climate Change Research, University of Bern, 3012 Bern, Switzerland*

[2]*Institute of Geography, University of Bern, 3012 Bern, Switzerland*

*Correspondence to: Luyao Tu (luyao.tu@giub.unibe.ch)

### *Highlights*

- Redox sensitive Fe-P (NaBD-$P_{tot}$) is the dominant P fraction in the anoxic sediments.
- Phosphorus in the sediment profiles is mainly present as the inorganic form.
- Potentially bioavailable organic P ($P_o$) is high in the surface sediments (top 5 cm).
- Net burial rates of total P and NaBD-$P_{tot}$ in sediments show significantly negative trends with increasing eutrophication levels.

### *Graphic Abstract*
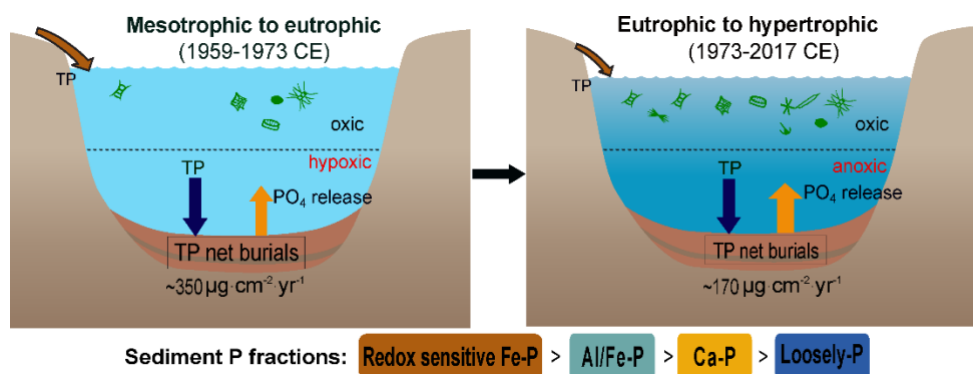
### 3.1.1 Abstract

Lake Lugano is one of several deep lakes in Switzerland that have not yet recovered from eutrophication after large reductions of external phosphorus (P) loadings. Persistent eutrophication has been attributed mainly to internal P loadings from sediments. To achieve the restoration goals, it is critically important to evaluate the sediment P availability and release risk in this lake. In this study, we combined sequential P extraction (four fractions) with enzyme hydrolysis to assess distribution characteristics of P forms and potential bioavailability of organic P in an anoxic sediment profile from the Ponte Tresa basin of Lake Lugano, southern Switzerland. Labile P forms, i.e. mostly redox-sensitive iron bound P and metal oxides bound P (Al/Fe-P), comprised ~70% of total P in the sediment profile (1959-2017 CE), suggesting a high potential for P release from the anoxic sediment. Potentially bioavailable organic P forms (determined by addition of substrate specific enzymes) were considerably higher in the surface sediments (top 5 cm), which is very likely to release P in the near future with early diagenesis. The net burial rates (NBR) of redox sensitive Fe-P fraction and total P in sediments both showed significant decreasing trends from 1959 to 2017 CE, when trophic levels of the lake increased from mesotrophic to hypertrophic status. We suggest that, in the Ponte Tresa basin, higher eutrophication conditions led to enhanced sediment P release (mainly from redox sensitive Fe-P fraction), thus reducing P-NBR in sediments. This study highlights the concern that in deep monomictic lakes, eutrophication restoration might be hindered by extensive internal P cycling and reduced capacity of sediment P-trapping.

### 3.1.2 Introduction

Eutrophication of aquatic ecosystems has been a global environmental concern for decades, especially in freshwater lakes (Cao et al., 2016; Hu et al., 2007; Smith et al., 1999). Excessive phosphorus (P) loading is recognized as one of the main causes of eutrophication as P is the limiting element for primary productivity in many freshwater lakes (Rothe et al., 2014; Worsfold et al., 2016). In many cases, however, management efforts focusing on reducing external P loads have resulted in delayed or even failed lake-system recovery from eutrophication (Søndergaard et al., 2001). The main cause for this was found to be the development of internal P loadings (P release from sediments), which recycles P back to the overlying water, thereby enhancing lake primary productivity and adversely affecting the lake trophic status (Gächter, 1987; Horppila et al., 2017; Tammeorg et al., 2016).

Phosphorus accumulated in lake sediments as a potential source of lake eutrophication has received considerable attention over the last decades. Numerous studies have applied sediment P fractionation to evaluate potential P availability and P release risks into lake water (Cavalcante et al., 2018; Jin et al., 2006; Kaiserli et al., 2002; Kangur et al., 2013; Ruttenberg,

1992). The rational of these fractionation procedures is that different P forms in sediments have different labilities and, thus, potentials to release P back into lake water. For example, apatite-P is considered a relatively stable P fraction contributing to permanent P burial in sediments of most lakes (Zhang et al., 2013), whereas P bound to redox-sensitive Fe and Al/Fe (oxyhydr) oxides can potentially be released under anoxic or varying redox conditions (Burley et al., 2001; Lai and Lam, 2008). While inorganic P ($P_i$) forms in lake sediments were the focus of most previous studies, organic P ($P_o$) speciation has been relatively under-studied (Mitchell, 2005). However, in recent years, $P_o$ has been demonstrated to be a significant component in lake sediments and might play the dominant role in sediment P release in some eutrophic lakes (Ahlgren et al., 2005; Torres et al., 2014; Zhang et al., 2008). To estimate potentially bioavailable $P_o$ in lake sediments, enzymatic hydrolysis has been commonly considered as a useful approach (Zhu et al., 2018; Zhu et al., 2013).

In general, the distribution of P fractions in lake-sediment profiles is affected by various factors, such as external P inputs, sedimentation rates, sediment P release, sediment composition, early diagenetic processes, redox conditions, and other environmental conditions in lakes (Carey and Rydin, 2011; Kaiserli et al., 2002; Søndergaard et al., 1996; Trolle et al., 2010). Sedimentary P species also largely depend on the lake trophic status (Carey and Rydin, 2011; Torres et al., 2014; Torres et al., 2016; Wang et al., 2006). Eutrophication is usually associated with changes in physicochemical conditions such as higher pH in lake water and lower redox potentials in the water-sediment interface, which can prompt P mobility and change P forms in sediments (Cao et al., 2016; Zhang et al., 2009). Heretofore, studies mainly have focused on the relationships between surface sediment P-fraction concentrations and various trophic status in different lakes (Carey and Rydin, 2011; Gonsiorczyk et al., 1998; Huo et al., 2011; Jin et al., 2006; Zhang et al., 2009). To our knowledge, few studies have reported P-fraction net burial rates (NBR) in short sediment cores and their temporal responses to the eutrophication history of the lake. Moreover, most of the sediment P-fractionation studies were conducted in rather shallow polymictic eutrophic lakes (Gao et al., 2005; Søndergaard et al., 2003). By comparison, sedimentary P fractions in deep, eutrophic monomictic or even meromictic lakes remain poorly understood, in particular regarding the time series of P-fraction NBR.

In the present study, we examined a short sediment core from the Ponte Tresa basin (Lake Lugano). We have selected this basin because it is a deep, warm monomictic subalpine lake and its eutrophication history since the mid-last century is well documented. Importantly, Lake Lugano is suffering from a delay of eutrophication recovery despite the reduction of external P loads since the 1980s (Lepori and Roberts, 2017). This delay is mainly reflected by presently still enhanced primary productivity as well as phytoplankton assemblage typically found in

eutrophic waters (Bechtel and Schubert, 2009; Simona, 2003). The recovery from anthropogenic eutrophication in Lake Lugano has been hindered by sediment P release (Lepori and Roberts, 2017) which is further reinforced by some symptoms of eutrophication (e.g. longer stratification and anoxic periods of up to one year) (Lepori et al., 2018). However, little is known about the P composition and availability in the sediment profiles of the lake, and the question how P fractions NBR in sediments changed with different trophic conditions through time.

The aims of this study were to (1) investigate P fractions and potential bioavailability of $P_o$ in sediment profiles of the Ponte Tresa basin, and (2) explore how the P-fraction NBR in sediments have varied with different trophic levels of the lake over the recent past decades. For these purposes, a sequential extraction scheme and enzyme addition assay were employed to characterize different P forms and potentially bioavailable $P_o$ in sediments. The temporal changes of P-fraction NBR were evaluated in relation to the reconstructed trophic history of the lake.

### 3.1.3 Materials and methods

*Study site*

Lake Lugano is a tectonic-glacial lake situated on the border between Switzerland and Italy in the southern Alps (Fig. 3.1a). The lake is fed by a large number of mountain streams and rivers (Cannata et al., 2018), with a total catchment area of 565.6 $km^2$ (Fig. 3.1a). The Ponte Tresa basin (45°58'N, 8°52'E; Fig. 1b) is the smallest (surface area 1.1 $km^2$) and most shallow (maximum water depth at ~51m) basin of Lake Lugano connected to outlet river Tresa (Fig. 3.1a) The direct watershed (land area, 5.6 $km^2$) of this basin is mainly made up of calcareous rocks, gneiss, and porphyry, and mean water residence time is relatively short (ca. 0.04 year; Simona, 2003). A more detailed description on the morphological and hydrological characteristics of the Ponte Tresa basin is reported in Simona (2003).

The climate in the Ponte Tresa catchment is classified as oceanic with warm summers and temperate winters. The basin water remains mostly ice-free during winter season (Franchini et al., 2017). The vegetation in the catchment is composed of oak (*Quercus petraea* and *Q. robur*) and chestnut (*Castanea sativa*) forests (colline belt) with agricultural fields in the lower parts. Residential and industrial buildings dominate on the Holocene alluvial fans to the north and west, and around the lake (Fig. 3.1b). The Ponte Tresa basin has a warm monomictic mixing regime: it is seasonally stratified between early summer and mid-autumn (Premazzi and Marengo, 1982), and experiences typically one mixing event per year, usually in February or March (Lepori and Roberts, 2017).

Lake Lugano has a long history of nutrient pollution starting as early as in the 1930s-1940s (Lehmann et al., 2004). In the Ponte Tresa basin, nutrient enrichments in the lake water started after the 1940s due to increasing urbanization and industrialization in the watershed, and the first massive algal bloom occurred in 1958 (Schneider et al., 2018). The basin was classified as eutrophic according to the measured water phosphate concentrations during 1972-1982 (mostly between 45-160 $\mu g \cdot L^{-1}$ in the late summer months) (Premazzi and Marengo, 1982; Rimer, 2017). From ca. 1970 onwards, the basin has been eutrophic to hypertrophic as indicated by diatom-assemblages data (Lotter, 2001). The eutrophication in the Ponte Tresa basin has led to permanently or temporarily anoxic conditions on the surface of lake sediments (Züllig, 1982). In Lake Lugano, high productivity during summer also tends to cause an increase of pH and calcite preciptation in the surface waters (Bernasconi et al., 1997).

To manage eutrophication in Lake Lugano, several remediation measures were implemented to reduce external P loadingss, such as the installation of wastewater treatment plants in 1976, and a ban on phosphates in detergents in Switzerland in 1986 (Barbieri and Simona, 2001; Span et al., 1994). These lake restoration endeavors have resulted in reductions of external P loads (from 77 to 36 tons per year) and lake-water P concentration during lake mixing (from 113 to 38 $\mu g \cdot L^{-1}$) in the southern basin of the lake from the early 1980s until the last decade (2006-2015) (IST-SUPSI, 2016). Nonetheless, primary productivity in the lake remains at high levels and, in the southern basin of Lake Lugano (connected to Ponte Tresa basin), annual primary production remained as high as > 400 g C$\cdot$ $m^{-2} \cdot y^{-1}$ between 1983 and 2014 (Franchini et al., 2017).
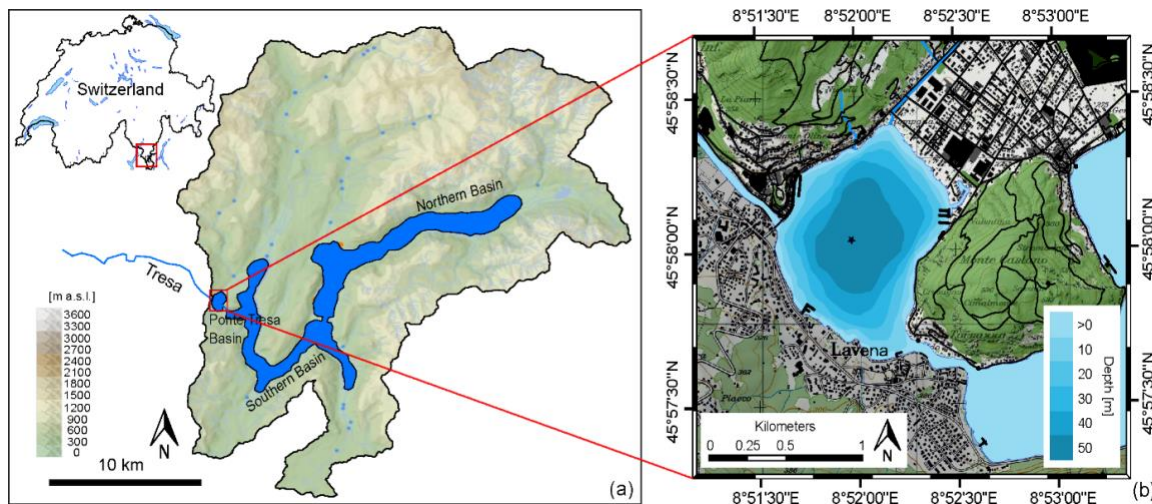
**Figure 3.1**: Study site. (a) An overview of the watershed of Lake Lugano, with the maps of Lake Lugano (in the dark blue color), the Ponte Tresa basin (red rectangle), and Switzerland (left inset). (b) Bathymetric map of the Ponte Tresa basin. The black asterisk indicates the coring site (color figure online); Grey areas around the lake indicate dwellings, and green areas forests. The figure was adapted from Schneider et al. (2018).

### Sediment coring and sampling

In September 2017, several short sediment cores were collected from the depocenter (i.e. the deepest point where the sediment surface is well preserved) of the Ponte Tresa basin using a UWITEC gravity corer (45°58'00.4''N, 8°51'56.5''E, Fig. 3.1b). After the cores were collected, they were tightly sealed, kept in a cooling box, and , within 5 hours , stored in a dark cold room (~4 °C).

The sediment core selected for this study (PTRE 17-2) was 105 cm long. It was stored for two months before opening. After opening and splitting lengthwise, one-half core (PTRE 17-2-A) was transferred immediately into a glove box with an anoxic atmosphere. Sampling in the glove box was done in a nitrogen ($N_2$) atmosphere to protect sediment samples from oxidation and possible changes in P forms (Lukkari et al., 2007a; Lukkari et al., 2007b). The sediments were continuously sampled from top 0 to 37.5 cm in 2.5 cm intervals. The fresh sediments for each sample slice were homogenized. After sampling the sediment for sequential P extraction, the remaining sediment was freeze-dried for water contents measurements and NaOH-EDTA extraction. The other half core (PTRE 17-2-B) was stored in the cold (4°C) conditions. After the sediment surface became oxidized and varves were more visible, core pictures were taken with a Nikon D80 digital camera for visual stratigraphic correlation and chronology.

### Sequential P extraction

The P-fractionation extraction protocol was slightly modified from the method described by

Lukkari et al. (2007a). In our procedure (Fig. 3.2), P in fresh sediments (corresponding to ~0.4 g dry weight) was sequentially extracted by 50 mL extractants into four different fractions (F1 to F4). The first two steps (F1 and F2) were performed in the absence of oxygen ($N_2$ atmosphere). Fraction 1 was extracted with 0.46M sodium cloride (NaCl) (ACS grade, Carl Roth GmbH&Co.), fraction 2 with 0.11 M sodium dithionite ($Na_2S_2O_4$) (assay (iodometric) ≥87 %, Merck KGaA) in 0.11 M sodium bicarbonate ($NaHCO_3$) (ACS grade, Merck KGaA) buffer (pH 7.0) which is referred to later as NaBD, fraction 3 with 0.1 M sodium hydroxide (NaOH) (R.G. grade, Hänseler AG), and fraction 4 with 0.5 M hydrochloric acid (HCl) (ACS grade). Extractant solutions were all prepared using deionized and filtered water (Merck MilliQ-water). All extractions were performed in triplicates for each sediment slice. All extraction steps described in Fig. 3.2 were carried out in Corning® 50 mL centrifuge tubes at room temperature using an orbital shaker table (400 rpm). The extraction time depended on the extractants (from 1 to 18 h, Fig. 3.2), and all rinse steps were 15 min. After each extraction and rinsing step, supernatant was seperated by centrifugation at 4000 rpm for 15 min at room temperature. We made the following adjustments compared to the originally published extraction method (Lukkari et al., 2007a). Firstly, the extraction procedure was ended after the F4 fraction because, in our study, we are not interested in the residuals after F4 fraction, which is mostly refractory organic P accoring to Lukkari et al. (2007a); Secondly, we did not aerate the supernatants of NaBD-extracted samples prior to colorimetric quantification of soluble reactive P, as recommended in the original method. The aeration procedure was skipped because we used the malachite green method (Ohno and Zibilske, 1991) instead of the molybdenum blue method to determine the soluble reactive P concentrations in all extracts (Lukkari et al., 2007a). Tests showed that sample aeration between 0 to 4 hours had no effect on the quantified P concentrations in NaBD extracts (Fig. S3.1a-c in Supplementary data). In the malachite green method, decomposition products of dithionite in aerobic aqueous solutions have no effect on malachite green and the phosphomolybdate complex and thus, no interference with spectrophotometric analysis of soluble reactive P (Barberis et al.,1998). Lastly, P quantification in all obtained extracts (F1 to F4) was perfomed in the unfiltered samples. Pre-tests comparing colorimetrically determined P concentrations in both unfiltered and filtered samples (0.45 µm nitrocellulose membrane) from F1 to F3 fractions showed an average difference of 1.3% (data not shown), suggesting that particulate P (undissolved P) in the extracts was minor. This appears to agree with previous findings in the Ponte Tresa basin that a great part of particulate P is mineralized at the water-sediment interface (Premazzi and Marengo, 1982).

We assigned the four obtained P fraction (F1 to F4) to different P forms, according to the literature. NaCl-$P_{tot}$ (F1) represents loosely adsorbed P on particle surfaces of sediments and

in pore water. This P fraction can easily be released from the interstitial water to overlaying waters, and thus be available for algae growth (Jin et al., 2006; Ribeiro et al., 2008). NaBD-$P_{tot}$ (F2) includes redox-sensitive fractions of P bound to hydrated oxides, mainly those of Fe. It has been confirmed that, under anoxic conditions, this fraction is highly labile and can be released from sediments to the lake water where it is available for algae growth (Ding et al., 2016; Rydin, 2000). NaOH-$P_{tot}$ (F3) is partly inorganic P (NaOH-$P_i$) bound to metal oxides (mainly Al, Fe) and partly organic P compounds (NaOH-$P_o$). NaOH-$P_i$ is potentially labile and may release P under anoxic or high pH environments (Rydin, 2000). NaOH-$P_o$ contains moderately labile $P_o$ in fulvic acids and refractory $P_o$ bound with humic acids (Zhu et al., 2013). The NaOH-$P_o$ fraction could also be bioavailable when labile parts of $P_o$ are released and subjected to enzymatic hydrolysis (Monbet et al., 2007). HCl-$P_{tot}$ (F4) is usually referred to as apatite-P and P bound to carbonates sourced from either co-precipitation with endogenic carbonates or from allochthonous lithogenic material (Gonsiorczyk et al., 1998; Kaiserli et al., 2002). This fraction is mostly considered as non-bioavailable and "permanently" buried P pool in lake sediments but it can dissolve in acidic environments (Wang and Liang, 2015).

We chose the described procedure because it highlights the redox sensitive Fe-bound P and organic P fractions (Lukkari et al., 2007a) which are crucial P pools in deep lakes with seasonally anoxic conditions in the hypolimnion (Gu et al., 2016). Sediments for extraction were shielded from oxygen until the start of step F3 of the procedure (Fig. 3.2) to avoid alterations in P and Fe fractionations due to oxidation artifacts (Lukkari et al., 2007a). However, this method only provides information about total $P_o$ in sediments. It is unclear to what extent the total $P_o$ in sediments is potentially bioavailable. Thus, enzymatic hydrolysis (see Section 3.4.4) was performed to estimate hydrolyzable and, thus, potentially bioavailable $P_o$ in sediment samples.
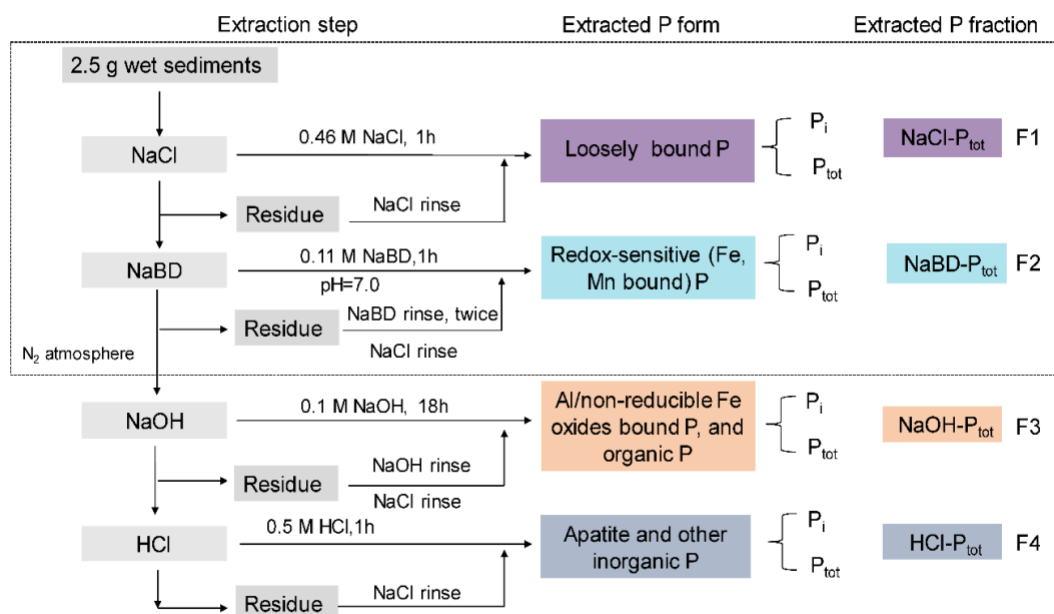
**Figure 3.2**: Sequential P extraction protocol. Sodium dithionite ($Na_2S_2O_4$) dissolved in 0.11 M sodium bicarbonate ($NaHCO_3$) buffer (pH 7.0) henceforth is termed as NaBD. Extraction steps inside the dashed rectangle were carried out in a nitrogen ($N_2$) atmosphere (Color figure online).

### *NaOH-EDTA extraction and enzymatic hydrolysis*

The extraction with 0.25M NaOH and 0.05M ethylenediamine tetraacetic acid (EDTA) was used for total $P_o$ extraction on bulk sediments (Bowman and Moir, 1993; Turner et al., 2005; Zhang et al., 2009). For that, 30 ml NaOH-EDTA (0.25 M-0.05 M) solution was used for total $P_o$ extraction on freeze-dried and homogenized bulk samples (~3 g). Total $P_o$ (NaOH-EDTA $P_o$) was quantified as the difference between total P and inorganic P in NaOH-EDTA extracts.

The $P_o$ in NaOH-EDTA extracts was further characterised into potentially bioavailable (i.e. enzyme-labile) and potentionlly non-bioavailable (i.e. enzyme stabile) $P_o$. In principle, the NaOH-EDTA extract is treated with a combination of different $P_o$ hydrolysing phosphatase enzymes (Jarosch et al., 2015). The increase in $P_i$ in the extract is indicative on the amount of $P_o$ hydrolysed by the substrate specific enzymes. By using a combination of different phosphatases the potential bioavailabilty of $P_o$ can be estimated. Three different enzymes (an acid phosphatase (Sigma P1146), a phosphodiesterase (nuclease, Sigma N8630), and a phytase (Ronozyme ® HiPhos (M)) were used in combination to determine enzyme-labile $P_o$ in the NaOH-EDTA extract. Enyzme dillutions were chosen to ensure full hydrolysis of added model compounds (glycerol phosphoate (Sigma G6501), deoxyribonucleic acid (Sigma

D3159) and phytic acid (Simga P8810)) during incubation at 37°C for 24h. Incubations were performed on 96-well plates with eight analytical replicates per sediment sample under sterile conditions.

### *Extracts and sediment sample analysis*

Phosphorus extracted in each fraction (F1-F4, Fig. 3.2) and NaOH-EDTA extracts was divided into inorganic P ($P_i$) and organic P ($P_o$). The $P_i$ concentrations were measured in the unfiltered samples colorimetrically by the malachite green method (Ohno and Zibilske, 1991) which quantifies the same $P_i$ as the traditional molybdenum blue mothed (Murphy et al., 1962), yet with a higher accuracy at lower $P_i$ concentrations (Uemura et al., 2010). We used 4 mL polystyrene macro-cuvettes with a 10 mm light path, and determined the absorbance at 610 nm using a UV-1800 UV-VIS spectrophotometer (Shimadzu Europe GmbH, Germany). Calibration curves for all colorimetrial analyes were made including the respective extract matrixes. Total P in extract samples was measured by inductively coupled plasma mass spectroscopy (7700x ICP-MS) (Agilent Technologies, Germany) after the dilution with nitric acid ($HNO_3$) to reach a final concentration of 1% v/v $HNO_3$ in Corning® 15 mL centrifuge tubes. The $P_o$ in extracts was determined by the difference between total P and $P_i$. Total P in sediments was obtained from the sum of total P of the four fractions (F1-F4; Fig. 3.2). In the same way, total $P_i$ and total $P_o$ in sediments were calculated by the sum of $P_i$ and $P_o$ of the four fractions, respectively.

Water contents (%), dry bulk density ($g \cdot cm^{-3}$), and sediment mass accumulation rates (MAR; $g \cdot cm^{-2} \cdot y^{-1}$) were determined according to the method of Håkanson and Jansson (1983). The concentrations and net burial rates NBR (fluxes) of P fractions in sediments are expressed as $mg \cdot kg^{-1}$ DW (dry weight) and $\mu g \cdot cm^{-2} \cdot yr^{-1}$, respectively. We calculated NBR of all P fractions by multiplying sediment MAR and P-fraction concentrations in sediments.

### *Sample dating*

The sample ages of Core PTRE 17-2 were based on careful visual stratigraphic correlation (layer by layer) with the chronology of Core PTRE 15-3 (Schneider et al., 2018) which was dated with varve counting and historically documented flood-layer markers. Characteristic marker layers (e.g. flood layers, algae bloom layers, conspicuously thick varves) were identified in Core PTRE 17-2 and used for precise correlation between the two cores (Fig. 3.3). The mean age of each sample was obtained by averaging the ages of the top and bottom depth of the sample.

### Data analysis

Statistical analysis was performed using R statistical computing (R Development Core Team, 2017). Significant trends in time series of NBR of different P fractions and TP in sediments were tested using univariate Mann-Kendall's trend test at the 5% significance level (R-package "Kendall"; McLeod, 2005).

### 3.1.4 Results

### Sample ages

The sediment core of PTRE 17-2 correlated well with the core PTRE 15-3-A from Schneider et al. (2018) but was less compacted (Fig. 3.3). The mean age of each sample with the age uncertainty is shown in the right table of Fig. 3.3. The average resolution of each sample is approximately 4 years and the sediment sample in the lowest part analyzed (35-37.5 cm) dates back to 1959 CE (Common Era).



| Depth (cm) | Mean age (CE) | Uncertainty (-) | Uncertainty (+) |
|---|---|---|---|
| 0-2.5 | 2014 | 2014 | 2015 |
| 2.5-5 | 2009 | 2008 | 2009 |
| 5-7.5 | 2004 | 2004 | 2005 |
| 7.5-10 | 2001 | 2001 | 2001 |
| 10-12.5 | 1998 | 1998 | 1999 |
| 12.5-15 | 1994 | 1994 | 1995 |
| 15-17.5 | 1990 | 1990 | 1991 |
| 17.5-20 | 1987 | 1987 | 1988 |
| 20-22.5 | 1983 | 1983 | 1985 |
| 22.5-25 | 1978 | 1977 | 1981 |
| 25-27.5 | 1973 | 1972 | 1976 |
| 27.5-30 | 1969 | 1968 | 1971 |
| 30-32.5 | 1963 | 1963 | 1965 |
| 32.5-35 | 1960 | 1960 | 1960 |
| 35-37.5 | 1959 | 1959 | 1959 |
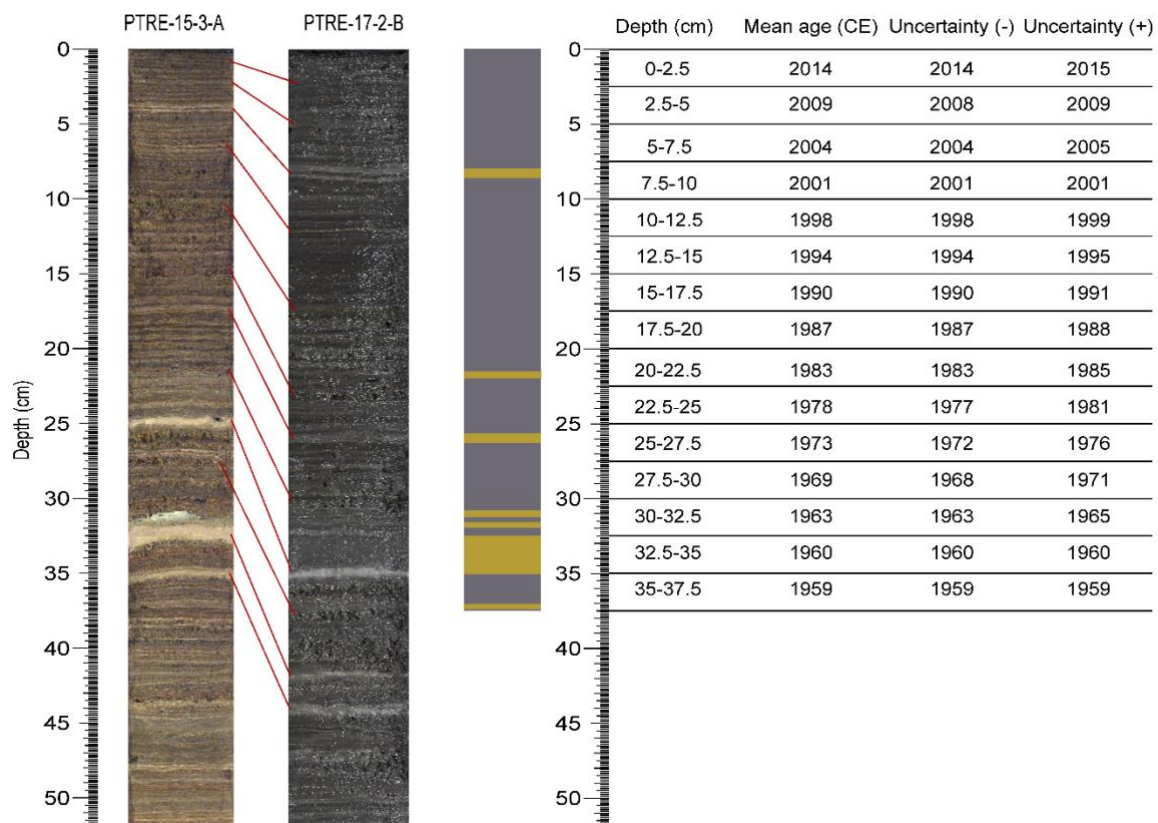
**Figure 3.3**: Core picture and sediment chronology. The left side: RGB (red, green and blue) contrast enhanced sediment core picture of Core PTRE-15-3-A (Schneider et al., 2018), high-resolution true color picture of Core PTRE 17-2 (oxidized sediment surface) and pictograph of the top 0-37.5 cm of Core PTRE 17-2. Red lines between two cores indicate the stratigraphic marker layers; yellow colors highlight the detrital layers from the visual comparison with Core PTRE-15-3-A (Color figure online).

The table on the right side describes the mean age of each sample including the uncertainties (PTRE 17-2), derived from visual stratigraphic correlation (layer by layer) with the chronology of Core PTRE 15-3 (Schneider et al., 2018).

*Sequentially extracted P fractions in sediment profiles*

Total P concentrations of all P fractions (F1-F4), and $P_i$ and $P_o$ concentrations of each fraction in sediment profiles (0-37.5 cm) are shown in Fig. 3.4. Total P (TP) concentration in sediments ranged from 972 to 5143 $mg \cdot kg^{-1}$ (Fig. 3.4a). Sedimentary P was mainly present in the inorganic form (Fig. 3.4b-e), with total $P_i$ concentrations ranging from 739 to 4527 $mg \cdot kg^{-1}$ (average ~79% of TP in sediments). In the $NaBD-P_{tot}$ and $HCl-P_{tot}$ fractions, most of the P was present as $P_i$ (average 83% and 80%, respectively), whereas in the $NaCl-P_{tot}$ and $NaOH-P_{tot}$ fractions, the proportions of $P_i$ were relatively lower (average 70% and 52%, respectively).

The rank order of P fractions in the whole sediment profile was $NaBD-P_{tot}$ (472-2677 $mg \cdot kg^{-1}$, 36-60% of TP in sediments) > $NaOH-P_{tot}$ (325-2000 $mg \cdot kg^{-1}$, 20-39% of TP) > $HCl-P_{tot}$ (134-613 $mg \cdot kg^{-1}$, 7-38% of TP) > $NaCl-P_{tot}$ (34-209 $mg \cdot kg^{-1}$, 2-10% of TP), as seen in Fig. 3.4b-e (relative proportions are given in Fig. S3.2 in Supplementary data).

The vertical variation of TP and P-fraction concentrations in sediment profiles show that TP, $NaBD-P_{tot}$ and $NaOH-P_{tot}$ fractions exhibited a generally similar pattern (Fig. 3.4a, c, and d). The concentrations of TP, $NaBD-P_{tot}$ and $NaOH-P_{tot}$ sharply increased from the bottom (35-37.5 cm, 1959 CE) to a maximum value at 27.5-30 cm (1969 CE). They had a generally decreasing trend towards the topmost sediments, except for a short but distinct peak at a depth of 5-7.5 cm (2004 CE). In contrast, $NaCl-P_{tot}$ and $HCl-P_{tot}$ showed a different structure (Fig. 3.4b and 4e). $NaCl-P_{tot}$ increased from the bottom depth to a peak at 17.5-20 cm (1987 CE), and then declined towards the surface sediments. $HCl-P_{tot}$ decreased from the bottom until a depth of 15-17.5 cm (1990 CE) and then, after a sharp peak at 10-12.5 cm (ca. 1998 CE), declined towards the surface sediments.
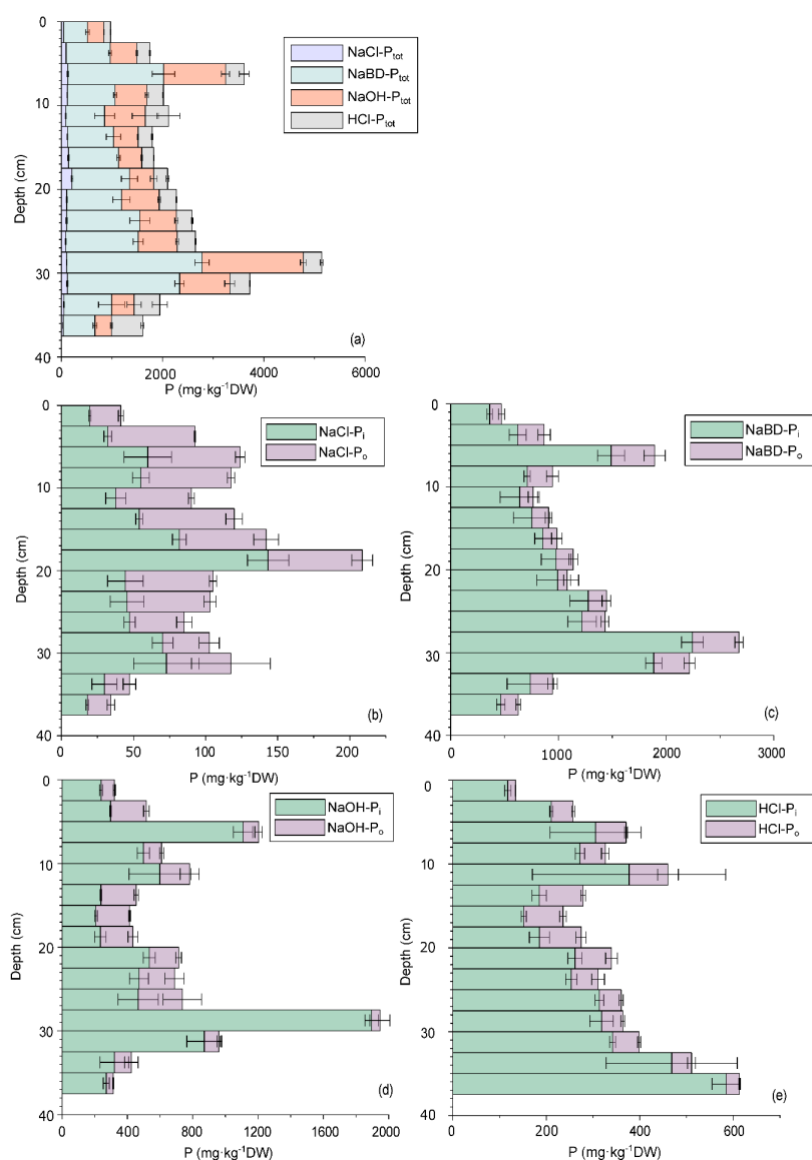
**Figure 3.4**: Vertical profiles of P fractions concentrations. (a) The total phosphorus concentrations with stacked four P fractions. (b-e) The $P_i$ (inorganic P) and $P_o$ (organic P) concentrations of the four P fractions in sediments. Error bars represent one standard deviations of three analysed replicates. The concentration is shown as the mean value of the three replicates in dry weight of sediments (DW); note the different scales for the x-axes (Color figure online).

### Organic P and enzymatic hydrolysis of $P_o$ from NaOH-EDTA extraction on bulk sediments

The average recovery of NaOH-EDTA $P_o$ in all sediment samples was 124%, compared with the sum of $P_o$ from the sequential P extraction (F1-F4, Fig. 3.2; Table S3.1 in Supplementary data), suggesting that a large proportion of sediment $P_o$ was extracted with the NaOH-EDTA procedure. NaOH-EDTA $P_o$ concentrations in sediments ranged from 162 mg·kg$^{-1}$ to 991 mg·kg$^{-1}$, which contributed to 13-57% of NaOH-EDTA TP in sediments (Fig. 3.5a and Fig.

S3.3b in Supplementary data). The vertical variations of NaOH-EDTA $P_o$ in sediments throughout the profile did not follow a discernable pattern (Fig. 3.5a). However, the sediments above the depth of 32.5 cm obviously contained more NaOH-EDTA $P_o$ than those in the bottom layers (32.5-37.5 cm).

Enzyme labile $P_o$ concentrations varied between 56 and 730 mg·kg$^{-1}$, with contributions of 9-91% to NaOH-EDTA $P_o$ (Fig. 3.5b). In the sediment profile (Fig. 3.5a), enzyme labile $P_o$ also displayed higher contents above the depth of 32.5 cm. The concentrations of enzyme labile $P_o$ remained relatively constant in the middle-section sediments (7.5-27.5 cm), but then showed an increasing trend towards the topmost sediments (0-7.5 cm).

### *Phosphorus fractions net burial rates (NBR) in sediments during 1959-2017 CE*

We define four stages in the time series of net burial rates (NBR) of all P fractions and sedimentary TP from 1959 to 2017 CE (Fig. 3.6b), based on the differences of the P data among different stages.

In Stage I (1959-1963 CE; 37.5-32.5 cm), most of the P fractions and TP in sediments had high NBR, except for NaCl-$P_{tot}$, NaOH-$P_o$, and enzyme labile $P_o$ with low NBR values. This stage was marked with multiple flood layers in sediments and considerably high mass accumulation rates (MAR) with values exceeding 0.08 g·cm$^{-2}$·yr$^{-1}$.

In Stage II (1963-1973 CE; 32.5-25 cm), NBR of NaBD-$P_{tot}$, NaOH-$P_i$, enzyme labile $P_o$ and TP of sediments remained high, whereas NaCl-$P_{tot}$, NaOH-$P_o$, and HCl-$P_{tot}$ had generally low NBR values. The MAR values declined from Stage I, remaining at ~ 0.07 g·cm$^{-2}$·yr$^{-1}$.

In Stage III (1973-2004 CE; 25-7.5 cm), compared with Stage II, NBR of labile P fractions, enzyme labile $P_o$ and TP of sediments decreased. At the same time, NaCl-$P_{tot}$ and NaOH-$P_o$ NBR increased. HCl-$P_{tot}$ and enzyme stabile $P_o$ NBR remained mostly at the same levels as in Stage II. After 1994 until 2004 CE, all the P fractions and TP NBR increased, except for enzyme stabile $P_o$ with a decrease at ~ 2000 CE. The MAR in this section was mostly constant except for a sharp increase after 1994 CE.

In Stage IV (2004-2017 CE; 7.5-0 cm), enzyme labile $P_o$ and NaOH-$P_o$ showed enhanced NBR values, whereas NBR of other P fractions and TP of sediments decreased to the lowest levels. The MAR firstly declined but increased again after ~ 2010 CE.

The results from the univariate Mann-Kendall trend test are shown in Table S3.2 (in Supplementary data). From 1959 to 2017 CE, we observe significantly decreasing trends in the NBR of sediment TP and NaBD-$P_{tot}$ fraction (TP: Kendall Score (S) = −37, p-value = 0.04; NaBD-$P_{tot}$: S = −38, p-value = 0.04). For other P fractions, no significant trends in NBR were

found (p-values > 0.05).

### 3.1.5 Discussion

***Phosphorus composition in sediments of the Ponte Tresa basin (1959-2017 CE***)

NaBD-$P_{tot}$ is the overall largest P-fraction in sediments of the Ponte Tresa basin (since 1959 CE). According to Ribeiro et al. (2008) and Ding et al. (2016), this is the most important fraction for sediment P release to lake water under anoxic conditions. Indeed, the recent sediments in the Ponte Tresa basin are anoxic (Schneider et al., 2018; Züllig, 1982), implying that there is still a high potential for sediment NaBD-$P_{tot}$ release back to the lake water supporting continuing eutrophication.

NaOH-$P_{tot}$ is the second largest P form in our sediments. The inorganic part of this fraction (i.e. NaOH-$P_i$) also constitutes a relatively large part of sediment TP (~24%). The anoxic sediment conditions of the Ponte Tresa basin could also prompt P release from NaOH-$P_i$. However, P release from NaOH-$P_o$ is more related to organic matter degradation in sediments (Huo et al., 2011; Zhu et al., 2013). When the mineralization process of organic matter in sediments of Ponte Tresa increases due to a higher trophic level of Lake Lugano (Barbieri and Mosello, 1992), NaOH-$P_o$ might be released from sediments.

HCl-$P_{tot}$ is the third largest P form with generally constant contributions to sedimentary TP (Fig. 3.4a and Fig. S3.2 in Supplementary data), which are within the range of HCl-$P_{tot}$ proportions of TP for calcareous lake sediments (Gonsiorczyk et al., 1998; Jin et al., 2006; Kaiserli et al., 2002; Zhang et al., 2013). The calcareous rocks in the watershed (Harloff, 1926; Salmaso et al., 2007) and endogenic Ca-P formation during $CaCO_3$ precipitation in the lake are possibly responsible for the high contents of sediment HCl-$P_{tot}$ in this basin. Nevertheless, this fraction is minor and relatively stable in sediments compared with NaBD-$P_{tot}$ and NaOH-$P_{tot}$. HCl-$P_{tot}$ is thought to be released only in low pH environments (pH < 6) (Jin et al., 2006). In Lake Lugano, pH in the surface waters was observed to vary from 7 to 9 during the annual cycle (Bernasconi et al., 1997). The pH in the hypolimnion was measured between 6 and 7 during summer stratification of the Ponte Tresa basin (Rimer, 2017), which is unlikely to favor sediment Ca-P release at the water-sediment interface.

NaCl-$P_{tot}$ is the smallest P fraction in the sediments under investigation. NaCl-$P_{tot}$, NaBD-$P_{tot}$, and NaOH-$P_i$ fractions are generally considered as potentially reactive or labile P forms in lake sediments and, therefore, critically important P sources for internal P loadings (Cavalcante et al., 2018). As the concentrations of NaCl-$P_{tot}$ were very low (Fig. 3.4a), NaBD-$P_{tot}$ and NaOH-$P_i$ represent the major labile-P fractions in the present study. Therefore, our results imply that under anoxic conditions, there is still a large proportion of labile P present in the sediments

(~70% of TP, 1959-2017 CE) which might, potentially, be released as internal P loads to the overlying water.

### *Distribution and potential bioavailability of $P_o$ in sediment profiles*

Organic P ($P_o$) production within Lake Lugano is predominantly derived from autochthonous organic matter (Bechtel and Schubert, 2009; Bernasconi et al., 1997) and increases, in principle, with higher primary productivity. However, $P_o$ preserved in sediment profiles is, instead, the net balance of $P_o$ sedimentation, which is the result of $P_o$ deposition to the sediment-water interface and $P_o$ recycling back to lake water or diffusion into deeper layers after early diagenesis and $P_o$ degradation over time (Matisoff et al., 2016; Zhu et al., 2018). Microbial phosphatase enzymes have been found in sediments of numerous reported lakes and may play an important role in the P release from anoxic breakdown of sedimentary $P_o$ (Torres et al., 2016; Zhang et al., 2007; Zhu et al., 2018). Additionally, the decomposition of organic matters can alter the pH-redox conditions within the sediments facilitating the P release to pore water (Yuan, 2017).

Because of the natural degradation of $P_o$ during diagenesis (Ahlgren et al., 2006; Zhang et al., 2013), declines of $P_o$ with increasing sediment depth have been widely observed in mesotrophic-eutrophic lakes, such as Lake Erken (Ahlgren et al., 2005; Reitzel et al., 2007), Lake Taihu (Ding et al., 2013), Lake Dianchi (Zhu et al., 2018), and also in the Baltic Sea (Ahlgren et al., 2006). In the Ponte Tresa basin, we observed no clear declines in concentrations of NaOH-EDTA $P_o$ with greater sediment depth (Fig. 3.5a) and total $P_o$ of sediments from sequential P extraction (Fig. S3.4 in Supplementary data). This may suggest that no intense diagenetic changes occurred over time or the mineralization of $P_o$ was coincidently balanced by its sedimentation. Nevertheless, considerably higher $P_o$ concentrations in the top 0 to 32.5 cm sediments can be likely attributed to increased $P_o$- and OM-sedimentation with eutrophication.

In the Ponte Tresa basin, enzyme labile $P_o$ (i.e. potentially bioavailable $P_o$) concentrations showed a strong decrease from the surface sediments to a depth of 5 cm (Fig. 3.5a), which might be associated with the early degradation of fresh organic matters. According to Torres et al. (2016) and Wobus et al. (2003), microbial phosphatase activity in surface sediments was higher than in deeper layers from many reported lakes in the USA and Europe. Therefore, it appears likely that the recently-sedimented labile $P_o$ in sediments of the Ponte Tresa basin would be degraded by microbes and, eventually, diffuse back to the lake water. The relatively constant enzyme labile $P_o$ in the middle-section sediments (7.5-27.5 cm) is closely related to similarly stable NaOH-EDTA $P_o$ contents (Fig. 3.5a). This could be explained by the fact that at greater depth, microbial phosphatase activities and corresponding enzyme hydrolysis of $P_o$

have been stabilized in sediments (Reitzel et al., 2007). Interestingly, the maximum contents of enzyme labile $P_o$ existed at greater depths (27.5-32.5 cm). Several studies have suggested that Al/Fe (oxyhydr) oxide minerals in sediments can absorb and stabilize $P_o$ in-situ and, thus, protect $P_o$ from extracellular enzymes hydrolysis (Ruttenberg and Sulak, 2011; Zhu et al., 2018). The high amounts of NaBD-$P_{tot}$ and NaOH-$P_i$ fractions in these layers (27.5-32.5 cm) (Fig. 3.4c and d) indicated high sedimentary Al/Fe contents, which might help stabilize and preserve labile $P_o$ in sediments. The high Al/Fe contents can possibly explain the high contents of enzyme labile $P_o$ in these deeper layers.

### *Relationship between P-fraction NBR in sediments and lake trophic state since 1959 CE*

In the Ponte Tresa basin, the eutrophication history since the 1920s is very well documented by sedimentary green pigments data (Chl-*a* and Pheophytin-*a*) at almost annual resolution (Fig. 3.6a) (Schneider et al., 2018). In our study, the time-series of P-fraction NBR only focused on the period when lake mesotrophic conditions changed to eutrophic or even hypertrophic conditions around 1960 CE. Based on our results, during the last 50-60 years, we observed marked differences in the NBR of different P forms and TP in sediments among Stages I-IV (Fig. 3.6b), which generally coincided with different lake trophic conditions since 1959 CE.
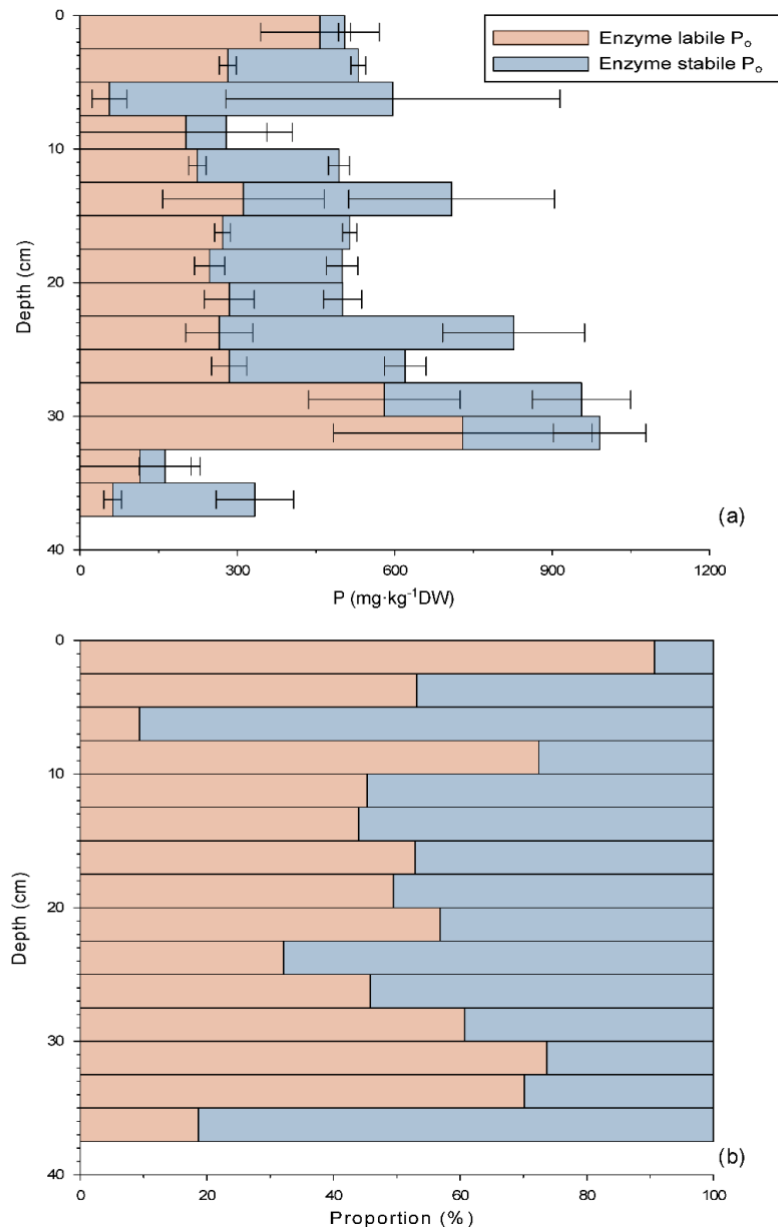
**Figure 3.5**: Vertical profiles of organic P ($P_o$) concentrations. (a) Enzyme labile $P_o$ and enzyme stabile $P_o$ concentrations and (b) their average proportions in NaOH-EDTA extracted total $P_o$ in sediments (Color figure online). Error bars show one standard deviation of eight analytical replicates.

In Stage I and Stage II (1959-1973 CE), overall increasing green pigments concentrations and fluxes (Fig. 3.6a) indicate that the lake was transitioning from mesotrophic to eutrophic conditions (i.e., the trophic level was lower than today but increasing). This is also supported by the study from Salmaso and Mosello (2010). During this period, NBR of TP in sediments and labile P fractions (here $NaBD-P_{tot}$, $NaOH-P_i$ and enzyme labile $P_o$) were clearly higher. This might result from high external P loads and relatively less sediment P release. During this time period (1959-1973 CE), large external P-loadings were reported from Lake Lugano

(Lehmann et al., 2004), which could have resulted in enhanced P sedimentation to surface sediments. Meanwhile, the Ponte Tresa basin had shorter summer stratification/anoxic periods (compared to Stage III) and oxic conditions in the hypolimnion persisted during winter (Züllig, 1982). This should, in principle, have caused less P release from sediments to lake water, and resulted in less dissolved P accumulation in the hypolimnion. Consequently, more NaBD-$P_{tot}$ and NaOH-$P_i$ were preserved in sediments. Moreover, the high NBR of potentially bioavailable $P_o$ was likely related to Al, Fe oxides/minerals as discussed above. However, during Stage I (1959-1960 CE), high NBR of green pigments and some P fractions (e.g. NaBD-$P_{tot}$, NaOH-$P_i$) might be biased through the presence of flood layers and related sediment focusing (including erosion of littoral sediments), both giving rise to very high sediment mass accumulation rates (MAR). High values of MAR, in turn, would result in high NBR of sediment P and green pigments, although the concentrations of both were relatively low (Fig. 3.4 and Fig. 3.6a).

In Stage III (1973-2004 AD), the Ponte Tresa basin was in highly eutrophic to hypertrophic conditions, which is reflected by high levels of green pigments fluxes and several algal blooms (the peaks of green pigment fluxes; Fig. 3.6a). Similar conclusions were reported from studies of Lotter (2001) and Bechtel and Schubert (2009). It is noteworthy that, under severely eutrophic conditions, NBR of NaBD-$P_{tot}$, NaOH-$P_i$ and TP in sediments were generally lower than before (Stage II). This result may be explained by a combined effect of enhanced P release from sediments due to ongoing eutrophication and progressing hypolimnetic anoxia. In seasonally anoxic lakes (e.g. the Ponte Tresa basin and the southern basin of Lake Lugano), and when lake productivity remains sufficiently high, it is very likely to engender prolonged stratification (up to one year) with more severe anoxia at the water-sediment interface (Lepori et al., 2018). Anoxic conditions favor sediment P release from NaBD-$P_{tot}$ and NaOH-$P_i$ fractions and, as a result, the NBR of these two fractions in sediments declined compared with Stage II. Moreover, Al/Fe oxyhydroxides would have decreased in the sediments of this section compared with Stage II, given the low amounts of Al/Fe bound P fractions (i.e. NaBD-$P_{tot}$ and NaOH-$P_i$). Therefore, extracellular phosphatase activity in sediments has been possibly less affected by the protection of $P_o$ by Al/Fe oxyhydroxides. Consequentially, $P_o$ hydrolysis in the sediment layers of Stage III (maximum eutrophication) was likely enhanced. This might be the main reason for lower amounts of enzyme labile $P_o$ preserved in sediments during Stage III. The enhanced NBR of TP and most of the P fractions during the upper part of Stage III (1994 to 2000 CE, 7.5-15 cm depth) is also noteworthy, but it seems to be influenced by increased MAR (possibly not all related with flood layers) whereas the concentrations of P fractions and TP in sediments changed with little variation (Fig. 3.4).

In Stage IV (2004-2017 CE), lake productivity slightly decreased until 2006 CE (see green

pigment fluxes, Fig. 3.6a), but the basin became again more eutrophic up to the present. In the 1980s until the last decade, external P loadings in the entire Lake Lugano have been reduced by ~ 50% (Barbieri and Simona, 2001; Lepori and Roberts, 2017). In the Ponte Tresa basin, the contrast between higher eutrophic status and low P NBR in sediments would suggest a substantial contribution of internal P loads from sediments under high eutrophic levels, which in turn sustained or augmented on-going eutrophication. This process was possibly further favored by complete mixing events after a long stratification period 2006-2009 CE (Schneider et al., 2018; Veronesi et al., 2002) when P from the hypolimnion was brought up to the photic zone. Such high internal P loads were also observed in the southern basin of Lake Lugano, where they were estimated to contribute about 40% to the turnover TP in the lake water during the last decade (Lepori and Roberts, 2017).

Overall, we found significantly decreasing trends in NBR of sediment TP and NaBD-$P_{tot}$ from 1959 to 2017 CE, the time with increasing eutrophic levels in the Ponte Tresa basin. Our results might indicate that, in such a deep seasonally-stratified lake as the Ponte Tresa basin, higher eutrophication levels would be associated with enhanced sediment P release (mainly from the Fe-P fraction). This can serve as a plausible explanation for the reduced sediment TP and NaBD-$P_{tot}$ NBR in the past few decades. On the other hand, our study suggests an importance of sediment P release (internal P loadingss) for the delayed recovery of eutrophication in Lake Lugano, similarly to the conclusions in Lepori and Roberts (2017). Furthermore, during the last few decades climate warming has influenced Lake Lugano's restoration by affecting the surface water temperature and mixing regime of the lake (Lepori and Roberts, 2015). One implication of this study is that the warming scenario would very likely enhance stratification in the Ponte Tresa basin and more internal P loadings might be expected.
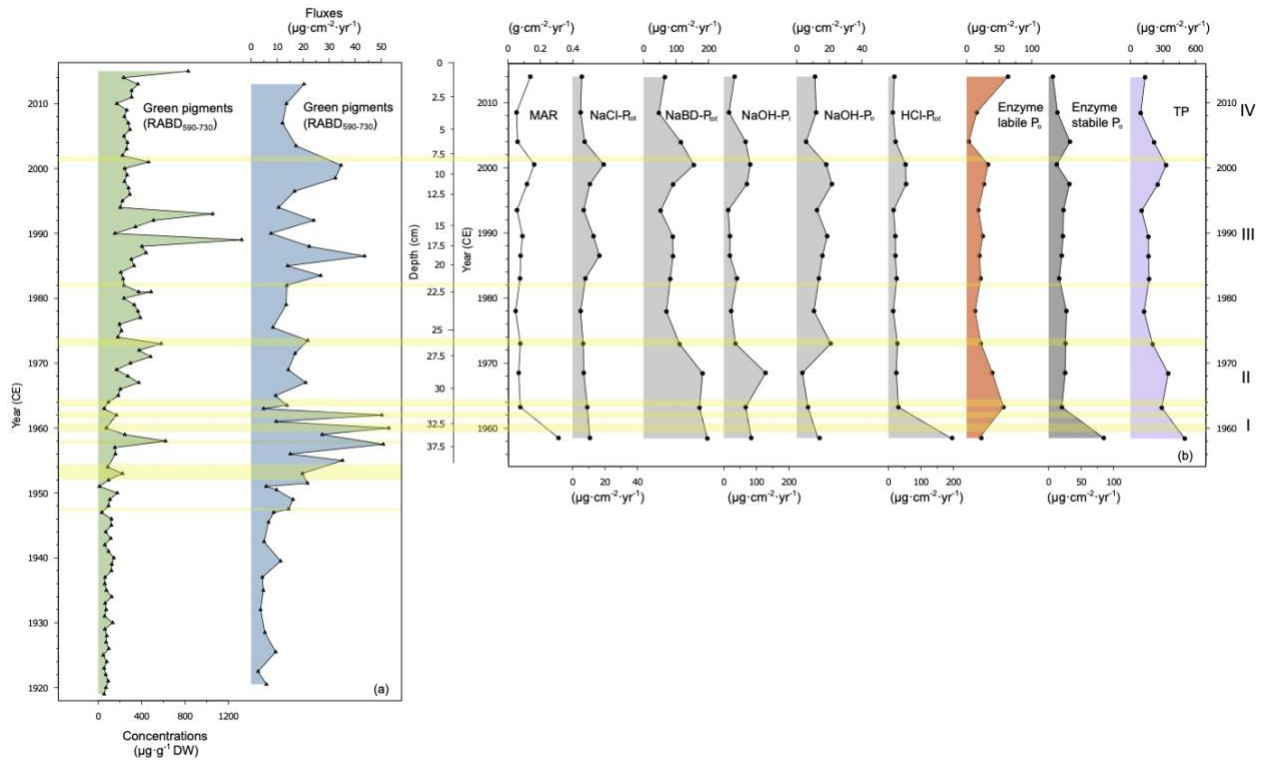
**Figure 3.6**: Time series of P fractions net burial rates in sediments of the Ponte Tresa basin. (a) Green pigments (Chl-*a* + Phe-*a*) concentrations (green color) and fluxes (blue color) recorded in sediments of the Ponte Tresa basin from 1920 to 2015 CE (Schneider et al., 2018); $RABD_{590-730}$ represents the hyperspectral scanning image (HSI) inferred green pigments. (b) The sediment mass accumulation rates (MAR) and net burial rates (NBR) of all P fractions and total P (TP) in sediments of the Ponte Tresa basin between 1959 and 2017 CE. All of the P fractions NBR data except the year of 1960 (flood layer at 32.5-35 cm depth) were used. The light yellow shading highlights flood layers in the Core PTRE 17-2. Green horizontal lines separate the four stages (Stage I to IV) (Color figure online).

### 3.1.6 Conclusions

The P-fractionation results show that labile P fractions (mainly NaBD-$P_{tot}$ and NaOH-$P_i$) were the dominant forms (~70% of TP) in sediments of the Ponte Tresa basin (1959-2017 CE). The anoxic sediment environment highlights high potentials for P-release from the labile P fractions sustaining continuing eutrophication of the lake. The potentially bioavailable $P_o$ in deeper layers seems to be stabilized, but high concentrations of enzyme labile $P_o$ in the top-most sediments (0-5 cm) are very likely to degrade and release P in the future. To the best of our knowledge, this study is the first to investigate the relationship between P-fraction NBR in sediments and historical lake eutrophication of the last few decades in a deep, eutrophic lake. It is interesting to observe that NBR of sediment TP and the NaBD-$P_{tot}$ fraction showed significantly decreasing trends under more eutrophic conditions since the 1960s. We further suggest that, in seasonally stratified deep lakes with hypolimnetic anoxia, of which the Ponte

Tresa basin is an example, higher eutrophication levels could lead to enhanced sediment P release and, thus, reduce P NBR in sediments. This study calls for the concern that, under such conditions, the recovery from anthropogenic eutrophication might be slow and difficult because of extensive internal P cycling and reduced capacity of sediment P-trapping. This study reveals the importance to adopt effective measures to minimize internal P-fertilization in lake restoration programs. The labile-phosphorus data presented by this study supports the geochemical approaches to reduce P release from sediments by applying aluminum and iron as "capping" materials.

### 3.1.7 Acknowledgements

### 3.1.8 References

Ahlgren, J., Tranvik, L., Gogoll, A., Waldebäck, M., Markides, K., and Rydin, E., 2005. Sediment depth attenuation of biogenic phosphorus compounds measured by $^{31}$P NMR. Environmental Science & Technology. 39, 867-872. http://dx.doi.org/10.1021/es049590h

Ahlgren, J., Reitzel, K., Tranvik, L., Gogoll, A., and Rydin, E., 2006. Degradation of organic phosphorus compounds in anoxic Baltic Sea sediments: a $^{31}$P nuclear magnetic resonance study. Limnology and Oceanography. 51, 2341-2348. https://doi.org/10.4319/lo.2006.51.5.2341

Barberis, E., Ajmone-Marsan, F. and Arduino, E., 1998. Determination of phosphate in solution at different ionic composition using malachite green. Communications in Soil Science and Plant Analysis. 29, 1167-1175. https://doi.org/10.1080/00103629809370017

Barbieri, A., and Mosello, R., 1992. Chemistry and trophic evolution of Lake Lugano in relation to nutrient budget. Aquatic Sciences. 54, 219-237. https://doi.org/10.1007/BF00878138

Barbieri, A., and Simona, M., 2001. Trophic evolution of Lake Lugano related to external load reduction: Changes in phosphorus and nitrogen as well as oxygen balance and biological parameters. Lakes & Reservoirs: Research & Management. 6, 37-47. https://doi.org/10.1046/j.1440-1770.2001.00120.x

Bechtel, A., and Schubert, C. J., 2009. A biogeochemical study of sediments from the eutrophic Lake Lugano and the oligotrophic Lake Brienz, Switzerland. Organic Geochemistry. 40, 1100-1114. https://doi.org/10.1016/j.orggeochem.2009.06.009

Bernasconi, S. M., Barbieri, A., and Simona, M., 1997. Carbon and nitrogen isotope variations in sedimenting organic matter in Lake Lugano. Limnology and Oceanography. 42, 1755-1765. https://doi.org/10.4319/lo.1997.42.8.1755

Bowman, R., and Moir, J., 1993. Basic EDTA as an extractant for soil organic phosphorus. Soil Science Society of America Journal. 57, 1516-1518. doi:10.2136/sssaj1993.03615995005700060020x

Burley, K. L., Prepas, E. E., and Chambers, P. A., 2001. Phosphorus release from sediments in hardwater eutrophic lakes: the effects of redox-sensitive and-insensitive chemical treatments. Freshwater Biology. 46, 1061-1074. https://doi.org/10.1046/j.1365-2427.2001.00789.x

Cannata, M., Neumann, J. and Rossetto, R., 2018. Open source GIS platform for water resource modelling: FREEWAT approach in the Lugano Lake. Spatial Information Research. 26, 241-251. https://doi.org/10.1007/s41324-017-0140-4

Cao, X., Wang, Y., He, J., Luo, X., and Zheng, Z., 2016. Phosphorus mobility among sediments, water and cyanobacteria enhanced by cyanobacteria blooms in eutrophic Lake Dianchi. Environmental Pollution. 219, 580-587. https://doi.org/10.1016/j.envpol.2016.06.017

Carey, C. C., and Rydin, E., 2011. Lake trophic status can be determined by the depth distribution of sediment phosphorus. Limnology and Oceanography. 56, 2051-2063. https://doi.org/10.4319/lo.2011.56.6.2051

Cavalcante, H., Araujo, F., Noyma, N. P., and Becker, V., 2018. Phosphorus fractionation in sediments of tropical semiarid reservoirs. Science of Total Environment. 619-620, 1022-1029. https://doi.org/10.1016/j.scitotenv.2017.11.204

Ding, S., Xu, D., Bai, X., Yao, S., Fan, C., and Zhang, C., 2013. Speciation of organic phosphorus in a sediment profile of Lake Taihu II. Molecular species and their depth attenuation. Journal of Environmental Sciences. 25, 925-932. https://doi.org/10.1016/S1001-0742(12)60137-5

Ding, S., Wang, Y., Wang, D., Li, Y. Y., Gong, M., and Zhang, C., 2016. In situ, high-resolution evidence for iron-coupled mobilization of phosphorus in sediments. Scientific Reports. 6, 24341. https://doi.org/10.1038/srep24341

Franchini, F., Lepori, F., and Bruder, A., 2017. Improving estimates of primary production in lakes: a test and a case study from a peri-alpine lake (Lake Lugano). Inland Waters. 7, 77-87. https://doi.org/10.1080/20442041.2017.1294351

Gächter, R., 1987. Lake restoration. Why oxygenation and artificial mixing cannot substitute for a decrease in the external phosphorus loading. Aquatic Sciences-Research Across Boundaries. 49, 170-185.

Gao, L., Zhou, J. M., Yang, H., and Chen, J., 2005. Phosphorus fractions in sediment profiles and their potential contributions to eutrophication in Dianchi Lake. Environmental Geology. 48, 835-844. https://doi.org/10.1007/s00254-005-0005-3

Gonsiorczyk, T., Casper, P., and Koschel, R., 1998. Phosphorus-binding forms in the sediment of an oligotrophic and an eutrophic hardwater lake of the Baltic Lake District (Germany). Water Science and Technology. 37, 51-58. https://doi.org/10.1016/S0273-1223(98)00055-9

Gu, S., Qian, Y., Jiao, Y., Li, Q., Pinay, G., and Gruau, G., 2016. An innovative approach for sequential extraction of phosphorus in sediments: Ferrous iron P as an independent P fraction. Water Research. 103, 352-361. 10.1016/j.watres.2016.07.058

Håkanson, L., and Jansson, M., 1983. Principles of lake sedimentology. Springer-Verlag, Berlin.

Harloff, C., 1926. The geology of the porphyry district of Lugano between Ponte Tresa and Luino. Leidse Geologische Mededelingen. 2, 115-222.

Horppila, J., Holmroos, H., Niemistö, J., Massa, I., Nygrén, N., Schönach, P., Tapio, P., and Tammeorg, O., 2017. Variations of internal phosphorus loading and water quality in a hypertrophic lake during 40 years of different management efforts. Ecological Engineering. 103, 264-274. https://doi.org/10.1016/j.ecoleng.2017.04.018

Hu, J., Shen, Q., Liu, Y., and Liu, J., 2007. Mobility of different phosphorus pools in the sediment of Lake Dianchi during cyanobacterial blooms. Environmental Monitoring and Assessment. 132, 141-153. https://doi.org/10.1007/s10661-006-9509-x

Huo, S., Zan, F., Xi, B., Li, Q., and Zhang, J., 2011. Phosphorus fractionation in different trophic sediments of lakes from different regions, China. Journal of Environmental Monitoring. 13, 1088-1095. http://dx.doi.org/10.1039/c0em00696c

IST-SUPSI Istituto scienze della Terra, 2016. Ricerche sull'evoluzione del Lago di Lugano. Aspetti limnologici. Programma triennale 2013-2015. Campagna 2015 e sintesi pluriennale (in

Italian). [Research on the status of Lake Lugano. Limnological aspects. Triennial program. Campaign 2015 and multi-year summary]. Commissione Internazionale per la Protezione delle Acque Italo-Svizzere (Eds.), pp. 93.

Jarosch, K. A., Doolette, A. L., Smernik, R. J., Tamburini, F., Frossard, E., and Bünemann, E. K., 2015. Characterisation of soil organic phosphorus in NaOH-EDTA extracts: A comparison of $^{31}$P NMR spectroscopy and enzyme addition assays. Soil Biology and Biochemistry. 91, 298-309. https://doi.org/10.1016/j.soilbio.2015.09.010

Jin, X., Wang, S., Pang, Y., and Chang Wu, F., 2006. Phosphorus fractions and the effect of pH on the phosphorus release of the sediments from different trophic areas in Taihu Lake, China. Environmental Pollution. 139, 288-295. https://doi.org/10.1016/j.envpol.2005.05.010

Kaiserli, A., Voutsa, D., and Samara, C., 2002. Phosphorus fractionation in lake sediments– Lakes Volvi and Koronia, N. Greece. Chemosphere. 46, 1147-1155. https://doi.org/10.1016/S0045-6535(01)00242-9

Kangur, K., Haldna, M., Buhvestova, O., Puusepp, L., and Kangur, M., 2013. Spatio-temporal variability of surface sediment phosphorus fractions and water phosphorus concentration in Lake Peipsi (Estonia/Russia). Estonian Journal of Earth Sciences. 62, 171-181. https://doi.org/10.3176/earth.2013.14

Lai, D. Y., and Lam, K. C., 2008. Phosphorus retention and release by sediments in the eutrophic Mai Po Marshes, Hong Kong. Marine Pollution Bulletin. 57, 349-356. https://doi.org/10.1016/j.marpolbul.2008.01.038

Lehmann, M. F., Bernasconi, S. M., Barbieri, A., Simona, M., and McKenzie, J. A., 2004. Interannual variation of the isotopic composition of sedimenting organic carbon and nitrogen in Lake Lugano: A long-term sediment trap study. Limnology and Oceanography. 49, 839-849. https://doi.org/10.4319/lo.2004.49.3.0839

Lepori, F. and Roberts, J.J., 2015. Past and future warming of a deep European lake (Lake Lugano): What are the climatic drivers?. Journal of Great Lakes Research. 41, 973-981. https://doi.org/10.1016/j.jglr.2015.08.004

Lepori, F., and Roberts, J. J., 2017. Effects of internal phosphorus loadings and food-web structure on the recovery of a deep lake from eutrophication. Journal of Great Lakes Research. 43, 255-264. https://doi.org/10.1016/j.jglr.2017.01.008

Lepori, F., Bartosiewicz, M., Simona, M., and Veronesi, M., 2018. Effects of winter weather and mixing regime on the restoration of a deep perialpine lake (Lake Lugano, Switzerland and Italy). Hydrobiologia. 824, 229–242. https://doi.org/10.1007/s10750-018-3575-2

Lotter, A., 2001. The effect of eutrophication on diatom diversity: examples from six Swiss lakes, in: K. J. Jahn R, Witkowski A, Compe`re P (Eds.). Lange-Bertalot-Festschrift. Ruggel, Gantner, pp. 417-432.

Lukkari, K., Hartikainen, H., and Leivuori, M., 2007a. Fractionation of sediment phosphorus revisited. I: Fractionation steps and their biogeochemical basis. Limnology and Oceanography: Methods. 5, 433-444. https://doi.org/10.4319/lom.2007.5.433

Lukkari, K., Leivuori, M., and Hartikainen, H., 2007b. Fractionation of sediment phosphorus revisited: II. Changes in phosphorus fractions during sampling and storing in the presence or absence of oxygen. Limnology and Oceanography: Methods. 5, 445-456. https://doi.org/10.4319/lom.2007.5.445

Matisoff, G., Kaltenberg, E.M., Steely, R.L., Hummel, S.K., Seo, J., Gibbons, K.J., Bridgeman, T.B., Seo, Y., Behbahani, M., James, W.F. and Johnson, L.T., Doan, P., Dittrich, M., Evans, M.A., Chaffin, J.D., 2016. Internal loading of phosphorus in western Lake Erie. Journal of Great Lakes Research. 42, 775-788. https://doi.org/10.1016/j.jglr.2016.04.004

McLeod, A. I., 2005. Kendall rank correlation and Mann-Kendall trend test. R Package Kendall.

Mitchell, A. B., DS, 2005. Organic phosphorus in the environment, Organic phosphorus in the aquatic environment: speciation, transformations and interactions with nutrient cycles Wallingford, UK, CAB International, 309–324.

Monbet, P., McKelvie, I. D., Saefumillah, A., and Worsfold, P. J., 2007. A protocol to assess the enzymatic release of dissolved organic phosphorus species in waters under environmentally relevant conditions. Environmental Science & Technology. 41, 7479-7485. https://doi.org/10.1021/es070573c

Murphy, J.A.M.E.S. and Riley, J.P., 1962. A modified single solution method for the determination of phosphate in natural waters. Analytica Chimica Acta. 27,31-36. https://doi.org/10.1016/S0003-2670(00)88444-5

Ohno, T., and Zibilske, L. M., 1991. Determination of low concentrations of phosphorus in soil extracts using malachite green. Soil Science Society of America Journal. 55, 892-895. https://doi.org/10.2136/sssaj1991.03615995005500030046x

Premazzi, G., and Marengo, G., 1982. Sedimentation rates in a Swiss-Italian lake measured with sediment traps. Hydrobiologia. 91, 603-610.

R Development Core Team, 2017. R: A language and environment for statistical computing. R Foundation for Statistical Computing, Vienna, Austria.

Reitzel, K., Ahlgren, J., DeBrabandere, H., Waldebäck, M., Gogoll, A., Tranvik, L., and Rydin, E., 2007. Degradation rates of organic phosphorus in lake sediment. Biogeochemistry. 82, 15-28. https://doi.org/10.1007/s10533-006-9049-z

Ribeiro, D., Martins, G., Nogueira, R., Cruz, J. V., and Brito, A., 2008. Phosphorus fractionation in volcanic lake sediments (Azores–Portugal). Chemosphere. 70, 1256-1263. https://doi.org/10.1016/j.chemosphere.2007.07.064

Rimer, D., 2017, 20th Century Eutrophication and Flood History Inferred from Lake Sediments of the Ponte Tresa Basin, Lake Lugano, Southern Switzerland: Master's thesis, University of Bern, Bern, Switzerland, pp.46-47.

Rothe, M., Frederichs, T., Eder, M., Kleeberg, A., and Hupfer, M., 2014. Evidence for vivianite formation and its contribution to long-term phosphorus retention in a recent lake sediment: a novel analytical approach. Biogeosciences. 11, 5169-5180. https://doi.org/10.5194/bg-11-5169-2014

Ruttenberg, K. C., 1992. Development of a sequential extraction method for different forms of phosphorus in marine sediments. Limnology and Oceanography. 37, 1460-1482. https://doi.org/10.4319/lo.1992.37.7.1460

Ruttenberg, K., and Sulak, D., 2011. Sorption and desorption of dissolved organic phosphorus onto iron (oxyhydr) oxides in seawater. Geochimica et Cosmochimica Acta. 75, 4095-4112. https://doi.org/10.1016/j.gca.2010.10.033

Rydin, E., 2000. Potentially mobile phosphorus in Lake Erken sediment. Water Research. 34, 2037-2042. https://doi.org/10.1016/S0043-1354(99)00375-9

Salmaso, N., Morabito, G., Garibaldi, L., and Mosello, R., 2007. Trophic development of the deep lakes south of the Alps: a comparative analysis. Fundamental and Applied Limnology / Archiv für Hydrobiologie. 170, 177-196. https://doi.org/10.1127/1863-9135/2007/0170-0177

Salmaso, N., and Mosello, R., 2010. Limnological research in the deep southern subalpine lakes: synthesis, directions and perspectives. Advances in Oceanography and Limnology. 1, 29-66. 10.1080/19475721003735773

Schneider, T., Rimer, D., Butz, C., and Grosjean, M., 2018. A high-resolution pigment and productivity record from the varved Ponte Tresa basin (Lake Lugano, Switzerland) since 1919: insight from an approach that combines hyperspectral imaging and high-performance liquid chromatography. Journal of Paleolimnology. 60, 381–398. https://doi.org/10.1007/s10933-018-0028-x

Simona, M., 2003. Winter and spring mixing depths affect the trophic status and composition of phytoplankton in the northern meromictic basin of Lake Lugano. Journal of Limnology. 62, 190-206. https://doi.org/10.4081/jlimnol.2003.190

Smith, V. H., Tilman, G. D., and Nekola, J. C., 1999. Eutrophication: impacts of excess nutrient inputs on freshwater, marine, and terrestrial ecosystems. Environmental Pollution. 100, 179-196. https://doi.org/10.1016/S0269-7491(99)00091-3

Søndergaard, M., Windolf, J., and Jeppesen, E., 1996. Phosphorus fractions and profiles in the sediment of shallow Danish lakes as related to phosphorus load, sediment composition and lake chemistry. Water Research. 30, 992-1002. https://doi.org/10.1016/0043-1354(95)00251-0

Søndergaard, M., Jensen, P. J., and Jeppesen, E., 2001. Retention and internal loading of phosphorus in shallow, eutrophic lakes. The Scientific World Journal. 1, 427-442. http://dx.doi.org/10.1100/tsw.2001.72

Søndergaard, M., Jensen, J. P., and Jeppesen, E., 2003. Role of sediment and internal loading of phosphorus in shallow lakes. Hydrobiologia. 506, 135-145. https://doi.org/10.1023/B:HYDR.0000008611.12704.d

Span, D. G., Dominik, J., Loizeau, J.-L., Arpagaus, P., and Vernet, J.-P., 1994. Phosphorus evolution in three sub-alpine lakes: Annecy, Geneva and Lugano: influence of lake restoration managements. Eclogae Geologicae Helvetiae. 87, 369-383. http://doi.org/10.5169/seals-167457

Tammeorg, O., Horppila, J., Tammeorg, P., Haldna, M., and Niemisto, J., 2016. Internal phosphorus loading across a cascade of three eutrophic basins: A synthesis of short- and long-term studies. Science of the Total Environment. 572, 943-954. https://doi.org/10.1016/j.scitotenv.2016.07.224

Torres, I. C., Turner, B. L., and Ramesh Reddy, K., 2014. The Chemical Nature of Phosphorus in Subtropical Lake Sediments. Aquatic Geochemistry. 20, 437-457. https://doi.org/10.1007/s10498-014-9228-9

Torres, I. C., Turner, B. L., and Reddy, K. R., 2016. Phosphatase activities in sediments of subtropical lakes with different trophic states. Hydrobiologia. 788, 305-318. https://doi.org/10.1007/s10750-016-3009-y

Trolle, D., Hamilton, D. P., and Pilditch, C. A., 2010. Evaluating the influence of lake morphology, trophic status and diagenesis on geochemical profiles in lake sediments. Applied Geochemistry. 25, 621-632. https://doi.org/10.1016/j.apgeochem.2010.01.003

Turner, B. L., Cade-Menun, B. J., Condron, L. M., and Newman, S., 2005. Extraction of soil organic phosphorus. Talanta. 66, 294-306. https://doi.org/10.1016/j.talanta.2004.11.012

Uemura, T., T. Ogusu, M. Takeuchi, and H. Tanaka, 2010, Spectrophotometric determination of trace phosphate ions by amplitude-modulated flow analysis coupled with malachite green method. Analytical Sciences. 26, 797-801. https://doi.org/10.2116/analsci.26.797

Veronesi, M. L., Barbieri, A., and Hanselmann, K. W., 2002. Phosphorus, carbon and nitrogen enrichment during sedimentation in a seasonally anoxic lake (Lake Lugano, Switzerland). Journal of Limnology. 61, 215-223. https://doi.org/10.4081/jlimnol.2002.215

Wang, S., Jin, X., Zhao, H., and Wu, F., 2006. Phosphorus fractions and its release in the sediments from the shallow lakes in the middle and lower reaches of Yangtze River area in China. Colloids and Surfaces A: Physicochemical and Engineering Aspects. 273, 109-116. https://doi.org/10.1016/j.colsurfa.2005.08.015

Wang, L., and Liang, T., 2015. Distribution characteristics of phosphorus in the sediments and overlying water of Poyang lake. PLoS One. 10, e0125859. https://doi.org/10.1371/journal.pone.0125859

Wobus, A., Bleul, C., Maassen, S., Scheerer, C., Schuppler, M., Jacobs, E., and Röske, I., 2003. Microbial diversity and functional characterization of sediments from reservoirs of different trophic state. FEMS Microbiology Ecology. 46, 331-347. https://doi.org/10.1016/S0168-6496(03)00249-6

Worsfold, P., McKelvie, I., and Monbet, P., 2016. Determination of phosphorus in natural waters: a historical review. Analytica Chimica Acta. 918, 8-20. https://doi.org/10.1016/j.aca.2016.02.047

Yuan, F., 2017. A multi-element sediment record of hydrological and environmental changes from Lake Erie since 1800. Journal of paleolimnology. 58, 23-42. https://doi.org/10.1007/s10933-017-9953-3

Zhang, T., Wang, X., and Jin, X., 2007. Variations of alkaline phosphatase activity and P fractions in sediments of a shallow Chinese eutrophic lake (Lake Taihu). Environmental Pollution. 150, 288-294. https://doi.org/10.1016/j.envpol.2007.01.007

Zhang, R., Wu, F., Liu, C., Fu, P., Li, W., Wang, L., Liao, H., and Guo, J., 2008. Characteristics of organic phosphorus fractions in different trophic sediments of lakes from the middle and lower reaches of Yangtze River region and Southwestern Plateau, China. Environmental Pollution. 152, 366-372. https://doi.org/10.1016/j.envpol.2007.06.024

Zhang, R., Wu, F., He, Z., Zheng, J., Song, B., and Jin, L., 2009. Phosphorus composition in sediments from seven different trophic lakes, China: a phosphorus-31 NMR study. Journal of Environmental Quality. 38, 353-359. https://doi.org/10.2134/jeq2007.0616

Zhang, R., Wang, L., Wu, F., and Song, B., 2013. Phosphorus speciation in the sediment profile of Lake Erhai, southwestern China: Fractionation and $^{31}$P NMR. Journal of Environmental Sciences. 25, 1124-1130. https://doi.org/10.1016/S1001-0742(12)60163-6

Zhu, Y., Wu, F., He, Z., Guo, J., Qu, X., Xie, F., Giesy, J. P., Liao, H., and Guo, F., 2013. Characterization of organic phosphorus in lake sediments by sequential fractionation and enzymatic hydrolysis. Environmental Science Technology. 47, 7679-7687. https://doi.org/10.1021/es305277g

Zhu, Y., Feng, W., Liu, S., He, Z., Zhao, X., Liu, Y., Guo, J., Giesy, J. P., and Wu, F., 2018. Bioavailability and preservation of organic phosphorus in lake sediments: Insights from enzymatic hydrolysis and $^{31}$P nuclear magnetic resonance. Chemosphere. 211, 50-61. https://doi.org/10.1016/j.chemosphere.2018.07.134

Züllig, H., 1982. Untersuchungen über die Stratigraphie von Carotinoiden im geschichteten Sediment von 10 Schweizer Seen zur Erkundung früherer Phytoplankton-entfaltungen (in German). [Investigations on the stratigraphy of carotenoids in the stratified sediment of 10 Swiss lakes to explore earlier phytoplankton developments]. Schweizerische Zeitschrift für Hydrologie. 44, 1-98. https://doi.org/10.1007/BF02502191

## 3.2 Supplementary materials
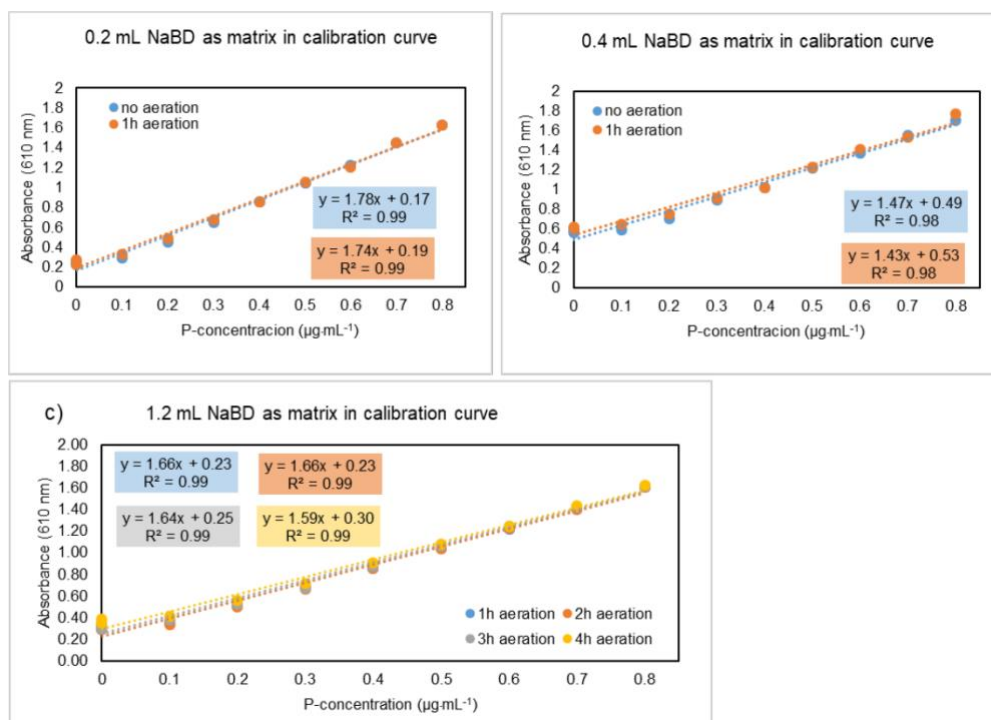


**Figure S3.1**: Pre-test for the effect of aeration on the calibration curve for colorimetric soluble reactive P quantification using NaBD extractant (fraction F2) as matrix. The NaBD extractant was either non-aerated or aerated for 1 hour and either 0.2 mL (Fig. S3.1a) or 0.4 mL (Fig. S3.1b) NaBD were added to the cuvettes with a final volume of 2 mL per colorimetric cuvette. Note that aeration had no effect on slope and intercept of the calibration curve. NaBD extractants may hold minor P impurities as indicated by a slightly higher intercept in Fig. S3.1b. However, when preparing the calibration curve for colorimetric soluble reactive P quantification, the same amount of NaBD matrix was added to the calibration curve as was used for quantification in the cuvettes. Thus, these minor impurities are accounted for. Fig. S3.1c shows the effect of different aeration times of the fraction F2 extractant NaBD (1 to 4 hours) on the calibration curve for colorimetric soluble reactive P quantification. A 1.2 mL matrix aliquot was used in each cuvette with a final volume of 2 mL for colorimetric quantification. Note the constant slopes and intercepts of the calibration curves irrespective of aeration time.
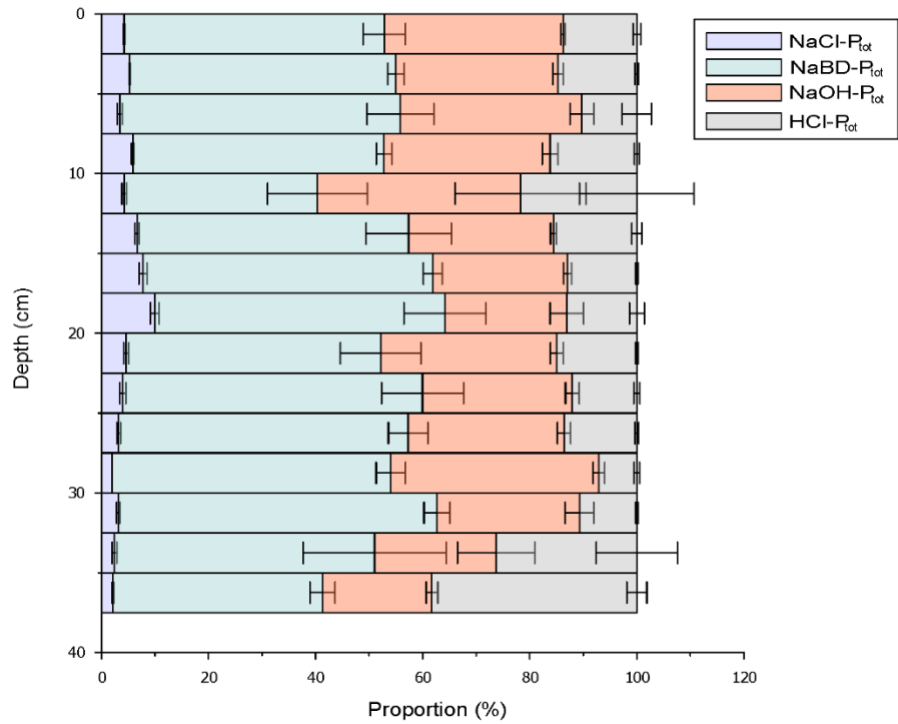
**Figure S3.2**: Vertical profiles of the four different P fractions (F1-F4) expressed as relative proportions. Error bars represent one standard deviation of the three replicates.
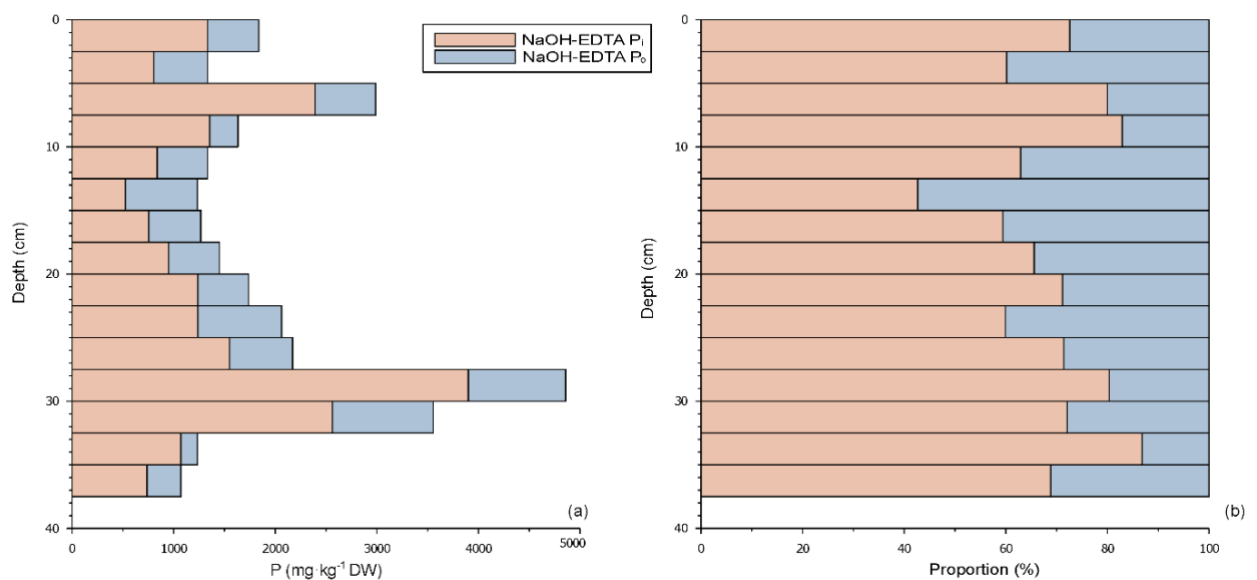


**Figure S3.3**: Vertical profiles of (a) NaOH-EDTA $P_i$ (orange) and NaOH-EDTA $P_o$ (blue) concentrations and (b) their average proportions of total P from NaOH-EDTA extraction on bulk sediments. The concentrations refer to dry weight of sediments (DW).
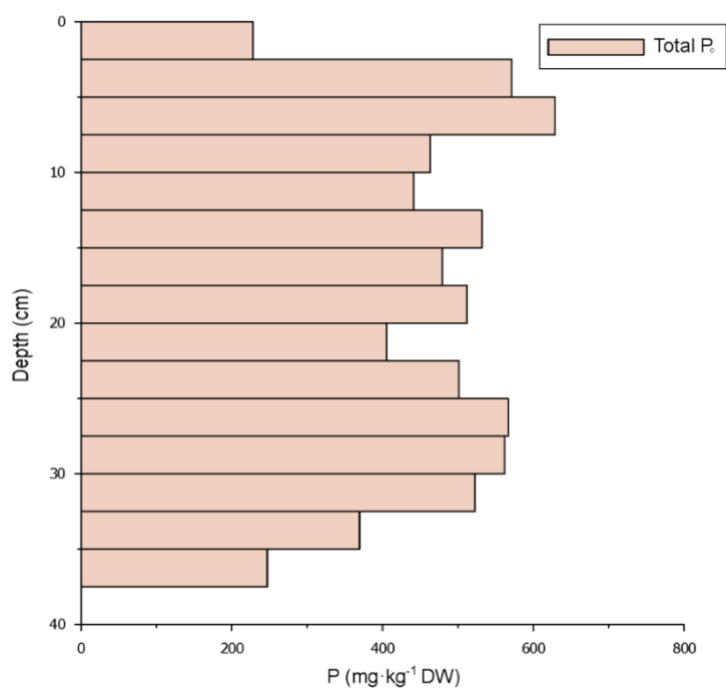
**Figure S3.4**: Vertical profiles of average total $P_o$ as the sum of $P_o$ of the four fractions (F1-F4) from the sequential extraction protocol.

**Table S3.1.** Recovery percentages (%) of $P_o$, $P_i$ and total P extracted by NaOH-EDTA on bulk dry sediment samples, compared with those from the sequential extraction protocol (F1 to F4 fractions).

| Sediment Depth (cm) | NaOH-EDTA $P_o$ /total $P_{o\ (\sum F1\ to\ F4)}$ | NaOH-EDTA $P_i$ /total $P_{i\ (\sum F1\ to\ F4)}$ | NaOH-EDTA TP /TP $_{(\sum F1\ to\ F4)}$ |
|---|---|---|---|
| 0-2.5 | 221 | 181 | 189 |
| 2.5-5 | 93 | 69 | 76 |
| 5-7.5 | 95 | 81 | 83 |
| 7.5-10 | 60 | 88 | 81 |
| 10-12.5 | 112 | 51 | 63 |
| 12.5-15 | 133 | 43 | 69 |
| 15-17.5 | 107 | 58 | 70 |
| 17.5-20 | 98 | 62 | 69 |
| 20-22.5 | 123 | 67 | 76 |
| 22.5-25 | 165 | 61 | 80 |
| 25-27.5 | 109 | 76 | 82 |
| 27.5-30 | 170 | 86 | 94 |
| 30-32.5 | 190 | 81 | 95 |
| 32.5-35 | 44 | 69 | 63 |
| 35-37.5 | 135 | 55 | 67 |
| Average recoveries | 124 | 68[a] | 76[a] |

[a] Values are calculated excluding the first sample (0-2.5 cm depth) as this is detected as an outlier by the boxplot method.

**Table S3.2.** Results from the non-parametric Mann-Kendall trend tests on the time series of NBR of different P fractions and total P in the sediment of lake Ponte Tresa between 1959 to 2017 CE. All of the P fractions and total P NBR data except the year of 1960 (flood layer at 32.5-35 cm depth) were used. (Positive and negative Kendall Score values indicate positive and negative trends, respectively).

| P fractions | Kendall Score (S) | Kendall's tau | Var(Score) [a] | Denominator[b] | p-value[c] |
|---|---|---|---|---|---|
| NaCl-$P_{tot}$ | -10 | -0.11 | 332.7 | 90.5 | 0.62 |
| NaBD-$P_{tot}$ | -38 | -0.42 | 332.7 | 90.5 | 0.04* |
| NaOH-$P_i$ | -28 | -0.31 | 332.7 | 90.5 | 0.14 |
| NaOH-$P_o$ | 5 | 0.06 | 331.7 | 90.0 | 0.82 |
| HCl-$P_{tot}$ | -34 | -0.38 | 330.0 | 89.5 | 0.07 |
| enzyme labile $P_o$ | -4 | -0.04 | 332.7 | 90.5 | 0.87 |
| enzyme stabile $P_o$ | -24 | -0.27 | 332.7 | 90.5 | 0.21 |
| Total P | -37 | -0.41 | 333.7 | 91.0 | 0.04* |

[a] Variance of Kendall Score.

[b] denominator (D), such that Kendall's tau=S/D.

[c] Two-sided p-value; *= p-value < 0.05 indicating statistically significant (monotonic) trends at the 95% confidence level.

**Table S3.3.** The results for the effect of aeration (0 and 1h) on quantified soluble reactive P concentrations. They are shown for extracts of three selected sediment samples (see Table below). Calibration curves used to determine soluble reactive P concentrations were exposed to the same treatment (no aeration and 1h aeration) as the respective samples and are shown in Fig. S3.1a, b.

| Depth (cm) | Treatment | P ($\mu g \cdot mL^{-1}$) |
|---|---|---|
| 2.5-5.0 | no aeration | 2.64 |
| | 1h aeration | 3.06 |
| 12.5-15.0 | no aeration | 0.24 |
| | 1h aeration | 0.22 |
| 32.5 -35.0 | no aeration | 2.35 |
| | 1h aeration | 2.44 |

# Chapter 4: The influences of historic lake trophy and mixing regime changes on long-term phosphorus fraction retention in sediments of deep eutrophic lakes: a case study from Lake Burgäschi, Switzerland

## 4.1 The influences of historic lake trophy and mixing regime changes on long-term phosphorus fractions retention in sediments of deep, eutrophic lakes: a case study from Lake Burgäschi, Switzerland

Luyao Tu[1*], Paul Zander[1], Sönke Szidat[2], Ronald Lloren[3,4], Martin Grosjean[1]

[1]*Oeschger Centre for Climate Change Research and Institute of Geography, University of Bern, Switzerland*

[2]*Oeschger Centre for Climate Change Research and Department of Chemistry and Biochemistry, University of Bern, Switzerland*

[3] *Department of Earth Science, ETH Zürich, Switzerland*

[4] *Eawag, Swiss Federal Institute of Aquatic Science and Technology, Switzerland*

*Correspondence to: Luyao Tu (luyao.tu@giub.unibe.ch)

### 4.1.1 Abstract

Hypolimnetic anoxia in eutrophic lakes can delay lake recovery to lower trophic states via the release of sediment phosphorus (P) to surface waters on short time scales in shallow lakes. However, the long-term effects of hypolimnetic redox conditions and trophic state on sedimentary P-fraction retention in deep lakes are not clear yet. Hypolimnetic withdrawal of P-rich water is predicted to diminish sedimentary P and seasonal P recycling from the lake hypolimnion. Nevertheless, there is a lack of evidence from well-dated sediment cores, in particular, from deep lakes, about the long-term impact of hypolimnetic withdrawal on sedimentary P retention. In this study, long-term sedimentary P-fraction data since the early 1900s from Lake Burgäschi provides information on the benthic P retention under the influence of increasing lake primary productivity (sedimentary green-pigments proxy), variable hypolimnion oxygenation regimes (Fe/Mn ratio proxy), and hypolimnetic withdrawal since 1977. Results show that, before hypolimnetic withdrawal (during the early 1900s to 1977), redox-sensitive Fe/Mn-P fraction comprised ~50% of total P in the sediment profile. Meanwhile, long-term retention of total P and labile P-fractions in sediments was predominantly affected by past hypolimnetic redox conditions, and P retention increased in sedimentary Fe- and Mn enriched layers when the sediment overlaying water was seasonally

oxic. However, from 1977-2017, eutrophication-induced persistent anoxic conditions in the hypolimnion and due to hypolimnetic water withdrawal increasing the P export out of the lake, net burial rates of total and labile P fractions decreased considerably in surface sediments. By contrast, refractory Ca-P fraction retention was primarily related to lake primary production. Due to the lake restoration since 1977, Ca-P fraction became the primary P fraction in sediments (representing ~39% of total P), indicating a lower P bioavailability of surface sediments. Our study implies that in seasonally-stratified eutrophic deep lakes (like Lake Burgäschi), hypolimnetic withdrawal can effectively reduce P retention in sediments and potentials of sediment P release (internal P loads). However, more than 40 years of hypolimnetic syphoning have not improved the lake trophic state or decreased lake productivity. Also, this restoration has not enhanced water-column mixing and oxygenation in hypolimnetic waters. The findings of this study are relevant regarding management of deep eutrophic lakes with mixing regimes typical for temperate zones.

### 4.1.2 Introduction

Phosphorus (P) eutrophication in freshwater lakes is a global problem and has been a matter of concern to the public for several decades. In lakes where the external P loadings has been reduced, internal P loadings (sediment P release to surface waters) is widely recognized as the key factor affecting lake trophic status and delaying lake recovery from eutrophication (Burley et al., 2001; Trolle et al., 2010). Considerable work has been done on sediment-P speciation to evaluate sediment P release potentials and implications for lake restoration management (Gonsiorczyk et al., 1998; Ribeiro et al., 2008).

The paradigm that oxygen levels control the sediment P release via reductive dissolution of Fe-P fraction in surface sediments has been accepted as the classical model for a long time (Einsele, 1936, 1938; Moosmann et al., 2006). Under anoxic conditions, P bound to redox-sensitive Fe and Al/Fe (oxyhydr)oxides can be potentially released from surface sediments into lake water (Burley et al., 2001), which was supported by numerous short-term (days or seasonal) laboratory or in-situ studies (Chen et al., 2018). Based on this paradigm, it was assumed that an oxic sediment–water interface might limit the release of Fe-P from sediments and, therefore, improve P retention in lake sediments. However, the restoration measures with artificial hypolimnetic oxygenation/aeration applied in eutrophic lakes proved to have only short-lasting effects but no direct effects on internal P loadings and redox-dependent sediment-P retention on longer terms (Gächter, 1987; Gächter and Wehrli, 1998; Moosmann et al., 2006; Hupfer and Lewandowski, 2008). Gächter and Müller (2003) and Moosmann et al. (2006) further argued that, on multi-decadal or longer time scales, P retention in lake sediments might eventually primarily depend on the P-binding capacity of anoxic sediments

and sediment composition (e.g. Fe, Mn, Al, and Ca contents). Nevertheless, until now, there is a lack of evidence from well-dated sediment cores, and there is still a need to know which processes may have a dominant influence on sediment P-fraction retention on longer time scales (e.g., decades or more). This information is crucial for predicting and, ultimately, managing sediment P release, especially in deep lakes, because hypolimnetic anoxia in deep lakes can lead to large loads of sediment P release. In contrast to the well-established studies about sediment-P speciation in shallow polymictic lakes (e.g. Kaiserli et al., 2001; Søndergaard et al., 2001; Cavalcante et al., 2008), there are only a few studies available from seasonally-stratified deep lakes. Furthermore, eutrophication has been demonstrated to affect sediment P release via controlling hypolimnetic anoxia and lake mixing regime in seasonally stratified deep lakes (Tu et al., 2019). It is not yet fully understood whether and how lake trophic levels and hypolimnetic anoxia can influence the long-term behavior of sedimentary P-fraction retention in deep lakes.

The restoration technique of hypolimnetic withdrawal has been frequently applied in seasonally stratified lakes in Europe (Kucklentz and Hamm, 1988; Nürnberg, 2007), whereby P-enriched water from the hypolimnion is discharged directly into the lake outflow. This restoration technique has been shown to efficiently reduce P concentrations in lake waters (Nürnberg, 2007). Hypolimnetic withdrawal was also expected to reduce P retention in sediments and seasonal P recycling from the lake hypolimnion to the upper waters, for example, in Lake Mauen, a shallow, eutrophic lake (maximum depth 6.8 m; Gächter, 1976). However, there is lack of empirical evidence from sedimentary P-fraction data, which provides valuable information on possible sediment P release characteristics and potentials of internal P loadingss. Furthermore, for deep lakes, the long-term influence of this restoration on sedimentary P release potentials is unclear.

The objectives of this study were to (1) explore the main factors controlling long-term changes of P-fraction retention in sediments of deep lakes, (2) investigate how sediment P-fraction retention responds to changes in lake eutrophication and hypolimnetic anoxia of the past prior to anthropogenic eutrophication, (3) examine the long-term effects of lake hypolimnetic withdrawal restoration on sedimentary P-fraction retention in seasonally-stratified deep lakes, and (4) evaluate with sediment-P data the predictions from Gächter (1976) that hypolimnetic withdrawal should result in reduced total P contents in sediments and sediment P release to lake water. To achieve these objectives, we investigated short sediment cores from Lake Burgäschi, a deep and eutrophic lake on the Swiss Plateau. Sedimentary green-pigments (chlorophylls and diagenetic products) inferred from hyperspectral imaging (HSI) scanning and XRF-inferred Fe/Mn ratios primarily reflect lake trophic state evolution (aquatic primary productivity) and hypolimnetic oxygenation, respectively. A sequential P-extraction with five P

fractions was performed to uncover P fractionation in sediment profiles. We combined all data to identify the dominant factors responsible for temporal changes in P-fraction retention.

Lake Burgäschi is an excellent study site because there were substantial changes in lake trophic levels and possibly lake-mixing regimes since the last century (Guthruf et al., 1999; Van Raden, 2012), and exceptionally long historical and limnological survey data are available for most of the last 50 years. Hypolimnetic withdrawal restoration is in operation since 1977.

### 4.1.3 Study site

Lake Burgäschi (47°10′8.5″N, 7°40′5.9″E) is a small lake located on the Swiss Plateau (Fig. 4.1a). It has a very restricted catchment (3.2 $km^2$). The catchment area geologically belongs to the Molasse Basin, and mostly consists of carbonate-rich sandstones and mudstones (Schmid et al., 2004). The kettle hole lake was formed after the retreat of the Rhone glacier (ca. 19 k yr. BP; Rey et al., 2017). Currently the maximum water depth is ~31 m, which is quite deep in contrast to the small surface area of 0.21 $km^2$ (Guthruf et al., 1999). The mean retention time of the lake water is ~1.4 year (Nürnberg, 1987). The lake has several small inflows in the southwest (Rey et al., 2017) and one outflow in the north (Fig. 4.1c).

Since the 19th century, the lake's water level was lowered several times to create farmland, with the most recent lowering (up to 2 m) during 1943-1945 (Guthruf et al., 1999). Agricultural area currently covers ~55% of the lake catchment, followed by ~29% area of forests. The lake region experiences a warm humid continental climate (Dfb; Köppen-Geiger classification). The mean annual air temperature is 9 °C and the warmest month is July (mean temperature 19 °C).
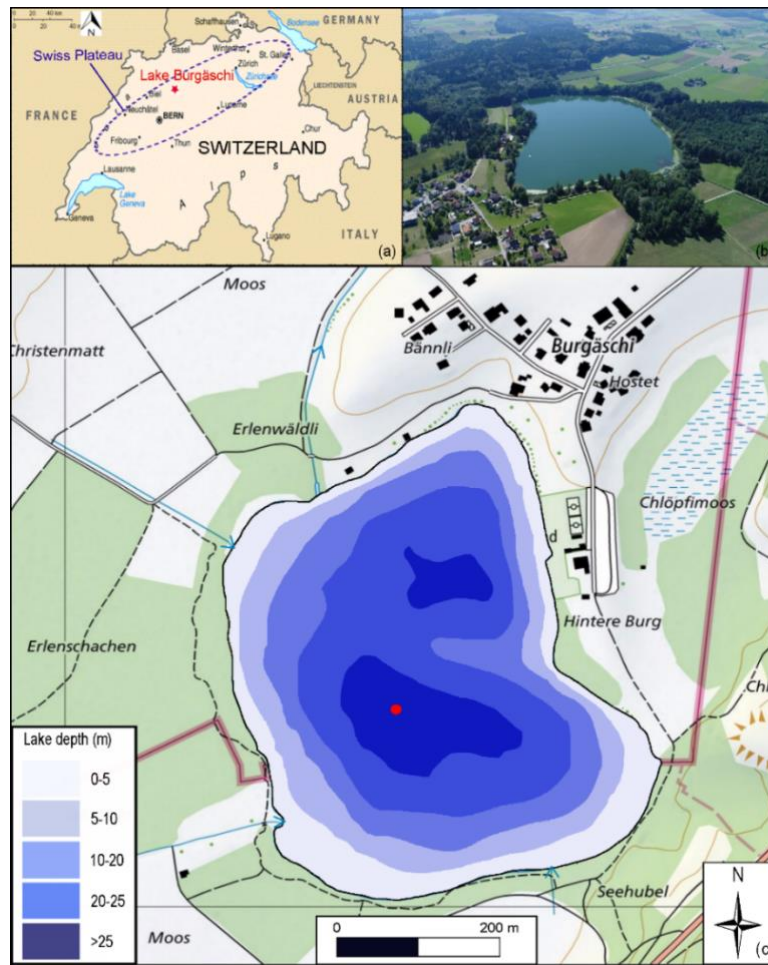
**Figure 4.1**: Study site. (a) Overview map of Switzerland and the Swiss Plateau. Lake Burgäschi is indicated as the red asterisk. (b) Photo of Lake Burgäschi and catchment (© 2018 Google Maps). (c) Bathymetric map of Lake Burgäschi adapted from Guthruf et al. (1999). The red dot indicates the coring site (color figure online). Green areas around the lake indicate forests, white areas agricultural lands. Inflow and outflow to the lake are indicated by blue arrow lines (topographic maps: © swisstopo).

Lake Burgäschi has been highly productive (eutrophic to highly eutrophic state) since the 1970s with high algal-biomass production and anoxic conditions in the hypolimnion (Guthruf et al., 1999, 2013). The eutrophication in Lake Burgäschi has been linked to increased agricultural P inputs via drainage into the lake in the second half of the 20th century (Guthruf et al., 1999). To mitigate the eutrophication, hypolimnetic withdrawal restoration has been applied in Lake Burgäschi since 1977, and the lake water has been monitored twice a year for more than 30 years for various parameters, such as pH, oxygen content, phosphorus concentrations, phytoplankton biomass, etc. Despite a sharp decline in hypolimnetic phosphorus concentrations due to the restoration, a high production of algal biomass continues today (GSA, 2007). Additionally, hypolimnetic oxic/anoxic conditions and the lake trophic state have been stabilized but not fundamentally improved (GBL, 1995; Guthruf et al.,

2013).

### 4.1.4 Materials and methods

*Core collection and sampling*

In September 2017, two 75-cm-long sediment cores (Burg17-B and Burg17-C) were retrieved from the deepest point of Lake Burgäschi (water depth ~31 m) (47°10'8.6"N, 07°40'5.3"E; coring site in Fig. 4.1c) using a UWITEC gravity corer. After the collection, the cores were stored in a dark cold room (~4 °C). After opening and splitting lengthwise, core-half A of Burg17-B was continuously subsampled at 2-cm resolution from 0 to 60 cm for $^{210}$Pb and $^{137}$Cs dating. The oxidized surface of core-half B (Burg17-B) was visually described (Schnurrenberger et al., 2003) before non-destructive XRF core and HSI scanning. After the opening, one-half of core Burg17-C was transferred immediately into a glove box with an anoxic atmosphere where it was continuously subsampled at 2-cm resolution from 0 to 72 cm. The fresh sediments from each sample slice were homogenized and used for sequential P extraction. After sampling for P extraction, the remaining sediment of the 2-cm slice was freeze-dried and homogenized for bulk element analyses.

*Chronology*

The chronology of the core Burg17-B is based on $^{210}$Pb and $^{137}$Cs activity profiles. The freeze-dried and homogeneous samples were stored dry and dark until analysis. The $^{210}$Pb, $^{137}$Cs and $^{226}$Ra radiometric activities were measured by gamma spectrometry at the University of Bern Department of Chemistry and Biochemistry. 1.3-5.1 g of the freeze-dried samples were encapsulated into polystyrene petri dishes (68 mm O.D., 11 mm height; Semadeni, Ostermundigen, Switzerland) together with a polystyrene disk to fill in the headspace above the sample material, and the petri dishes were vacuum-sealed into a gas-tight aluminum foil for equilibration. $^{210}$Pb (46.5 keV), $^{241}$Am (59.5 keV), $^{226}$Ra progenies $^{214}$Pb and $^{214}$Bi (295.2, 351.9 and 609.3 keV), as well as $^{137}$Cs (661.7 keV) were measured using a Broad Energy Germanium (BEGe) detector (Canberra GmbH, Rüsselsheim, Germany). This system is composed of a high-purity germanium crystal of 50 cm$^2$ area and 30 mm thickness with a 0.6 mm thick carbon epoxy window, which shows high absolute full-energy peak efficiencies for close on-top geometries of >20% and ~5% for $^{210}$Pb and $^{137}$Cs, respectively. Low integrated background count rates of 0.20 s$^{-1}$ (energy range of 30-1800 keV) were achieved by application of low-background materials, installation in third underground floor (~10 m of water-equivalent overburden), passive shielding (outside to inside: 10 cm low-background lead, 3 mm ancient lead with negligible $^{210}$Pb content, 2 mm cadmium), flushing of the shield interior with nitrogen gas and an active anti-cosmic shield (plastic scintillator panels of totally 1 m$^2$ area mounted directly above the passive shielding). Supported $^{210}$Pb in each sample was

assumed to be in equilibrium with the in-situ $^{226}$Ra (equilibration time 4 weeks). Unsupported $^{210}$Pb activity was calculated by subtracting $^{226}$Ra activity from total $^{210}$Pb activity level-by-level. The correction for the total unsupported $^{210}$Pb missing inventory followed Tylmann et al. (2016).

The $^{210}$Pb chronology of core Burg17-B was determined using the Constant Rate of Supply (CRS) model (Appleby, 2002), which accounts for variation in sediment accumulation rates. We tested two CRS models: CRS-1 model was unconstrained (i.e. without reference points from the $^{137}$Cs activity). The CRS-2 model was constrained with the chronologic marker of peak fallout from nuclear weapons testing in 1963 ($^{137}$Cs and $^{241}$Am). Both models were then tested and validated with independent time-markers at the onset of nuclear weapons testing in 1953/54 and the Chernobyl accident in 1986/87 (onset of $^{137}$Cs and peak of $^{137}$Cs and $^{241}$Am, respectively).

The two sediment cores (Burg 17-B and Burg 17-C) are visually very similar but show a length-offset due to coring compaction of approximately 2-6 cm (Fig. S4.1 in Supplementary data). The age-depth stratigraphy of Burg17-C core was inferred from the dated core Burg17-B by visual stratigraphic correlation from high-resolution core pictures.

### *Non-destructive geochemical methods*

Non-destructive X-ray fluorescence (XRF) core scanning was done using an Avaatech XRF Core Scanner (Richter et al., 2006) for semi-quantitative element composition measurements at 0.5 mm resolution to capture relative elemental concentrations of the laminae. The core surface was smoothed and covered with a 4-μm-thick Ultralene foil prior to the analysis. Elements were measured using a Rhodium anode and a 25 μm Be window. The lighter elements (e.g. Al, Si, P etc.) were measured for 15 seconds count time at 10 kV with 1500 A, no filter; while the heavier elements (e.g. Mn, Fe, Br etc.) were exposed for 40 seconds at 30 kV with 2000 A, Pd-thin filter. Element intensities (semi-quantitative concentrations) of the selected elements (Mg, Si, Al, K, Ti, Rb, P, Fe, Mn, Ca) are expressed as count rates (counts per second, cps).

Following the methodology in Butz et al. (2015), hyperspectral imaging (HSI) scanning was performed using a Specim Ltd. Single Core Scanner equipped with a visual to near infrared range (VNIR, 400–1000 nm) hyperspectral linescan camera (Specim PFD-CL-65-V10E). Parameters were set for a spatial resolution of ~70 μm/pixel and a spectral sampling of 1.57 nm (binning of 2). Spectral endmembers were determined using the "Spectral Hourglass Wizard" of the ENVI 5.5 software package (Exelisvis ENVI, Boulder, Colorado). The relative absorption band depth (RABD) index calculation was performed following the method in Schneider et al. (2018). However, based on the spectral end members (Fig. S4.2), we used

the absorption feature between the wavelengths R590 and R765 (590-765 nm), i.e. RABD$_{590-765}$. Butz et al. (2017) and Schneider et al. (2018) revealed that this index is well calibrated to absolute green-pigments (chlorophyll *a* + pheophytin a) concentrations in sediments. The sediments in Lake Burgäschi are mostly laminated and organic-rich (Van Raden, 2012), which indicates that the sediments are anoxic, bioturbation is absent, and sedimentary pigments are well-preserved (Reuss et al., 2005). Therefore, in our study, the relative concentrations of green-pigments inferred from RABD$_{590-765}$ index values provide a semi-quantitative reconstruction of lake primary productivity (total algal abundance) at sub-annual resolution, and are suggested to reflect the trophic state evolution of Lake Burgäschi.

***Phosphorus fractionation scheme and bulk elements analyses***

The P-fractionation extraction protocol (Fig. S4.3) principally follows the four-step extraction protocol in Tu et al., (2019). In addition, we added the last extraction step from Lukkari et al. (2007) to determine refractory organic P (F5). This P fraction (F5) is practically biologically unavailable and subject to permanent P burial. The first four fractions are NaCl-TP (F1: loosely bound P), NaBD-TP (F2: redox-sensitive Fe- and Mn-bound P), NaOH-TP (F3: Al- and Fe-bound P), and HCl-TP (F4: Ca-bound P) (Tu et al., 2019), whereby NaCl-TP, NaBD-TP and NaOH-TP fractions together are considered as relatively labile P fractions because they may release P back to the water column under anoxic or high pH environments (Rydin, 2000). The HCl-TP and refractory organic P (Ref.-P$_o$) fractions are classified as relatively stable or refractory P fractions. Total P in sediments was obtained from the sum of the five P fractions. The P in extract samples was measured by inductively coupled plasma mass spectroscopy (7700$\times$ ICP-MS) (Agilent Technologies, Germany) after the dilution with nitric acid (HNO$_3$) to reach a final concentration of 1% v/v HNO$_3$.

Concentrations of total carbon (TC), total nitrogen (TN), and total sulfur (S) in sediment samples were determined using an Elementar vario EL Cube elemental analyzer. Total inorganic carbon (TIC) content was calculated by multiplying loss on ignition at 950 °C (LOI$_{950}$, following the method proposed by Heiri et al. (2001)) by 0.273, i.e. the ratio of the molecular weight of C and CO$_2$. Total organic carbon (TOC) content was calculated using the equation TOC =TC-TIC. Sediment dry bulk density and water content were determined using wet mass (g), dry mass (g) and wet volume (cm$^3$) following the method in Håkanson and Jansson (2002).

### 4.1.5 Data analyses

Multivariate statistical analyses were performed with R version 3.4.2 (R Development Core Team, 2017). Prior to data analyses, RABD$_{590-765}$ index values (resolution 70 μm) were aggregated to a spatial resolution of 0.5 mm (the spatial resolution of XRF data). Stratigraphically constrained incremental sum of squares clustering (CONISS; Grimm, 1987)

was then performed on semi-quantitative proxies (i.e. RADB$_{590-765}$ index and XRF-element data) with R-package "rioja" (Juggins, 2017). The number of significant clusters was determined with a broken-stick test (Bennett, 1996). A principal components analysis (PCA) was performed on the centered and standardized data of semi-quantitative proxies, using the "Vegan" package (Oksanen et al., 2013). XRF-element and RABD$_{590-765}$ index values were averaged within the depth range of each sample taken from core Burg17-C for P fractions. In order to identify the primary factors influencing the variations in sedimentary P fractions, a redundancy analysis (RDA) was performed on the centered and standardized dataset of P fractions (response variables) and other sediment geochemical parameters (explanatory variables) with the "vegan" package. In the RDA computation, the correlation matrix option was selected and the scaling was conducted on a correlation biplot.

### 4.1.6 Results

#### *$^{137}$Cs and $^{210}$Pb chronology*

The two distinctive peaks of $^{137}$Cs in sediment profiles are detected at 31 cm and 15 cm depths (Fig. 4.2b), corresponding to the 1963 and 1986 major fallout events, respectively (Appleby, 2002). Furthermore, $^{241}$Am activity peaks at the same depths (Fig. 4.2b) confirm that the 1963 and 1986 $^{137}$Cs peaks were due to atmospheric fallouts (Michel et al., 2001). The first traces of $^{137}$Cs occur at 37 cm depth, indicating the first widely detectable fallout from atmospheric nuclear testing in 1953/1954 (Pennington et al., 1973).

The $^{210}$Pb activity in core Burg17-B shows a relatively monotonic decrease down to a sediment depth of 17 cm. Further down, larger variations are found (Fig. 4.2a). The $^{210}$Pb and $^{226}$Ra activities do not reach equilibrium; unsupported $^{210}$Pb activity in the oldest sample (59 cm) is still above the limit of detection (14.0±6.8 Bq·kg$^{-1}$). The observed cumulative inventory of unsupported $^{210}$Pb is 2941 Bq·m$^{-2}$. We corrected this value (missing inventory correction; Tylmann et al., 2016) by applying an exponential equation using the lowermost values of cumulative dry mass and unsupported $^{210}$Pb activity between 8 and 60 cm depths. As a result, a correction value of 125.2 Bq·m$^{-2}$ (missing inventory) is added to the final total unsupported $^{210}$Pb inventory (3066 Bq·m$^{-2}$).

The CRS-2 model (constrained through 1963) shows a better agreement with the independent $^{137}$Cs markers at 1953/54 and 1986/87 than the CRS-1 model (Fig. 4.2c). Therefore, CRS-2 model results were chosen for determining the age-depth profile and sediment mass accumulation rates (MAR) of core Burg17-B. The mean age at 59 cm sediment depth dates back to ~1930. The extrapolated mean age at 61 cm depth is ~1926 calculated using the mean sediment accumulation rate between 54-60 cm (2 yr·cm$^{-1}$).
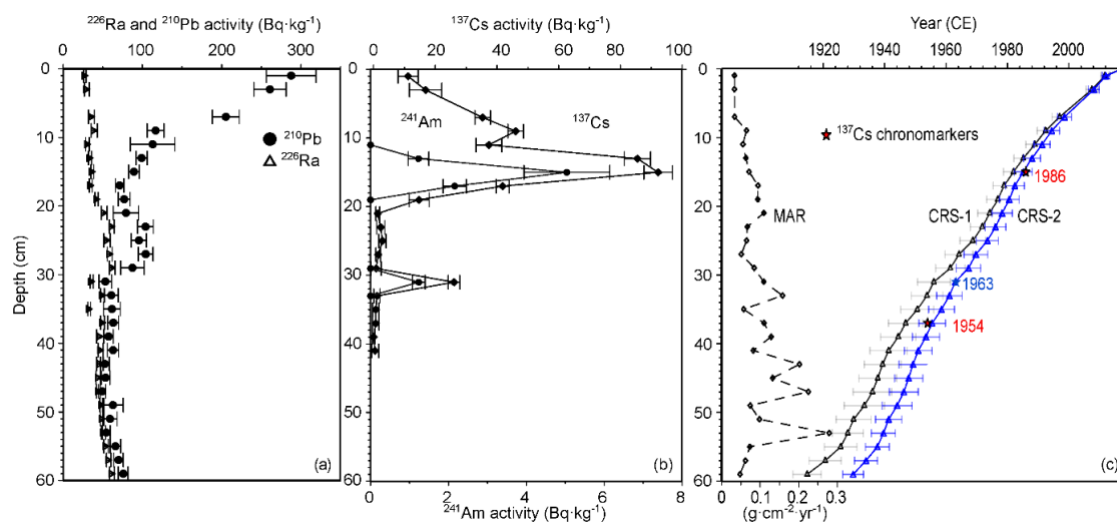
**Figure 4.2**: Sediment chronology. (a) Total $^{210}$Pb, $^{226}$Ra, and (b) $^{137}$Cs and $^{241}$Am activity concentration profiles in sediment core Burg17-B from Lake Burgäschi; (c) The comparison of different $^{210}$Pb CRS models: unconstrained CRS-1 model and constrained CRS-2 model at 1963; the mass accumulation rates (MAR) are obtained from the CRS-2 model.

### Sediment lithology, green-pigments (RABD590-765 index) and XRF-element records

Four sediment facies (I to IV, Fig. 4.3 and 4.4a) are identified based on visual classification and the CONISS-analysis results of XRF-element intensities.
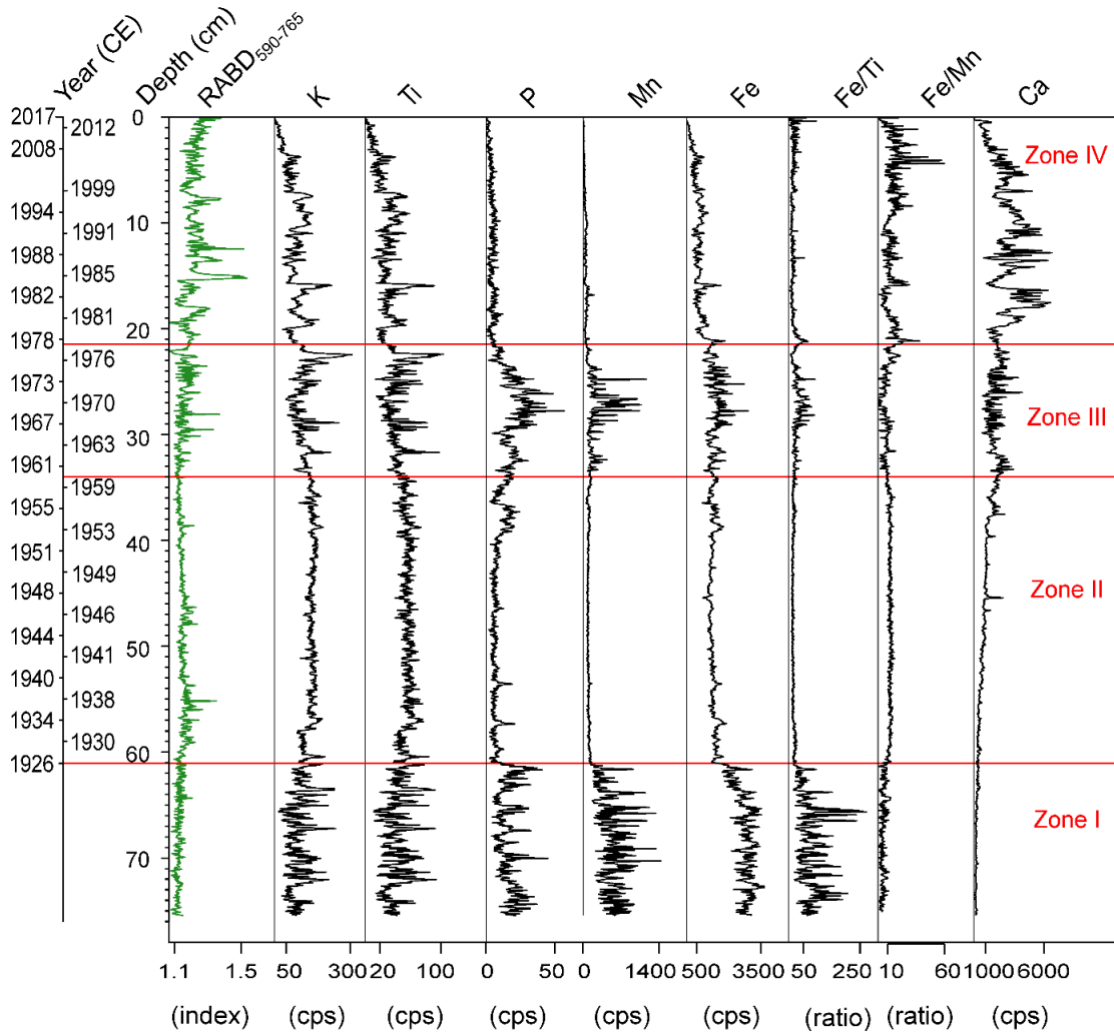
**Figure 4.3:** Stratigraphic records of HSI-inferred green-pigments (RABD$_{590-765}$) and XRF-data in sediments of core Burg17-B. Elemental counts are represented in cps (counts per second). The red horizontal lines separate the four significant clusters retrieved by the CONISS analysis (color figure online).
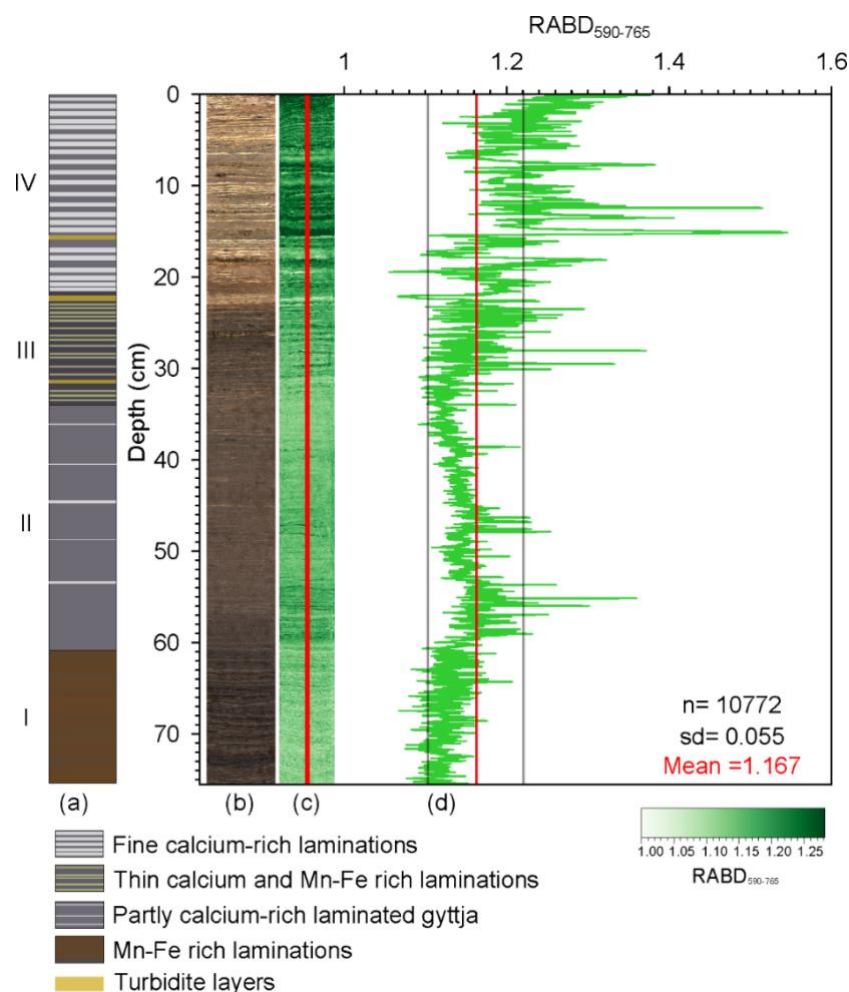
**Figure 4.4**: Core lithology and spectral index. (a) Lithological description of Burg17-B sediment core. The intensities of Ca, Fe and Mn in each unit were inferred from XRF-element counts in Fig. 4.3; Yellow colors highlight the turbidite layers identified from the XRF peaks of siliciclastic elements e.g. K, Ti, and Rb. (b) RGB contrast enhanced sediment core picture. (c) The map of the spectral index $RABD_{590-765}$ (i.e. green-pigments) distribution, and (d) the graphic output of $RABD_{590-765}$ spectral index within the boundary of the red lines (c) which shows the 2-mm wide sampling range. The red line in (d) indicates the mean index value and the grey lines represent the one-standard deviations (sd). The colorbar represents the index values of the distribution map (color figure online). n is the number of rows of the $RABD_{590-765}$ index map.

In Zone I (75.4-61cm, pre ~1926), the sediments consist of visible thin brown-to-reddish laminae (Mn- and Fe rich). Green-pigment concentrations inferred from $RABD_{590-765}$ index values show a homogenous distribution with the lowest values within the sediment profile (Fig. 4.4d). Fe/Mn ratios vary within very low values (mostly below 10). The Mn, Fe, P and Fe/Ti values show high levels with large variability. Extremely low Ca amounts are noted in this zone.

In Zone II (61-34cm, ~1926-1960), the sediments are dark gyttja, partly laminated with light Ca-rich layers. Green-pigment concentrations slightly increase yet still show little variability. A sharp increase of green-pigments concentrations occurs at 60 cm, and the first two local peaks near 55 cm (~1938) and 48 cm (1945) are notable. Fe/Mn ratios remain at slightly higher values than in Zone I. The Mn, Fe, P contents and Fe/Ti values all decline to low levels and remain relatively stable. Ca counts increase gradually over the whole Zone II.

In Zone III (34-21.5 cm, ~1960-1977), the sediments are mostly characterized by brown-to-reddish laminations (Mn-Fe rich), with thicker and more distinct laminae contacts than in Zone I. Green-pigment concentrations exhibit much higher values with positive trends, intensified variability, and several maxima (seasonal algal blooms). Fe/Mn ratios first drop in the lower part (34-27 cm) and then continue to increase upward to the top-part of Zone III. Fe, Mn, P, and Fe/Ti values show generally opposing trends to Fe/Mn ratios. Ca contents are elevated during this period relative to Zones I and II.

In Zone IV (21.5-0 cm, ~1977-2017), the sediments exhibit a clear laminated structure with much more pronounced light calcite layers. The laminations are characterized by a regular succession of light calcite layers (Ca-rich) and dark organic-rich layers (Fig. S4.4). Green-pigment concentrations display the highest levels with large fluctuations, and reach distinct local maxima at 18 cm (1981), 15 cm (1985), 13 cm (1987), 12 cm (1988), and 8 cm (1997) depths (Fig. 4.4d). Fe/Mn ratios are at similarly high values as in Zone II, yet with more variability. The Fe, Mn, and P element counts and Fe/Ti all show constantly very low values. The Ca amounts are the highest in the profile and show considerable variability.

Two principle components, PC1 and PC2 were shown to be significant using a broken stick model. They explain ~35 % and ~30 % of the total variance in the dataset, respectively (PCA-biplot; Fig. S4.5). The PC1 has strong positive loadings for the terrigenous elements (K, Ti, Rb etc.; Fig. 4.3 and S4.6) and thus represents mainly erosional processes related to allochthonous inputs. The PC2 has strong positive loadings for redox-sensitive elements (Fe, Mn), P and Fe/Ti, but negative loadings for Ca, Fe/Mn ratios and green-pigments index values. Therefore, PC2 reflects changes in redox conditions of hypolimnetic water and lake primary productivity. The results of additional PCA analyses zone by zone (Fig. S4.7b) show that Mn, Fe and P were mostly independent of terrigenous elements (in Zones I to III), however in Zone IV, Mn, Fe and P become correlated with the terrigenous elements. The vertical profile of XRF-P matches very well with the changes of total P concentrations in sediments (Fig. S4.8). It reveals that XRF-P data can reliably represent qualitative variations of total P concentrations in sediment profiles of Lake Burgäschi.

### Bulk elements and P fractions in sediment profiles

Sediment TIC, TOC, TOC/TN ratio, S and P fractions also show distinctive features along the four stratigraphic zones (Fig. 4.5). From the upper part of Zone I (65.2-61 cm; ~1926) to Zone IV, TIC shows a similar pattern to the XRF-Ca contents (Fig. 4.3 and 4.5) suggesting that TIC is mostly present in the form of $CaCO_3$. Over the whole profile, TOC/TN ratios are within the range of 9-11. TOC and TOC/TN ratios exhibit mostly similar patterns from Zone I to Zone III. By contrast, total sulfur (S) contents display a different pattern, showing very low values in Zone I and II (mean ~0.5%), and a substantial increase in Zone III and IV.
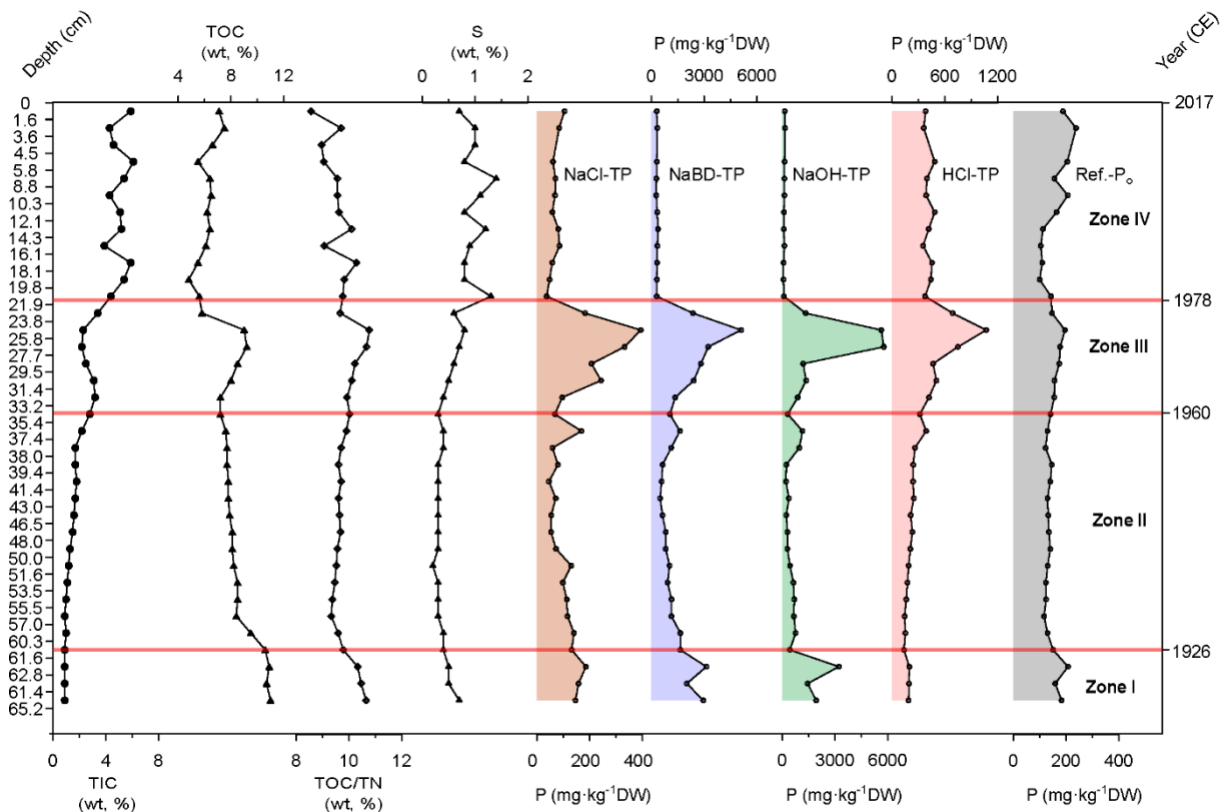


**Figure 4.5**: Time series of Bulk elements and P fractions data. The stratigraphy of total inorganic carbon (TIC), total organic carbon (TOC), sulfur (S) contents, TOC/TN ratio and five phosphorus fractions in sediments of Lake Burgäschi. The y-axis (left) refers to the sediment depth of core Burg17-B. The horizontal red lines separate the significant CONISS zones as in Fig. 4.3. The secondary y-axis (right) indicates approximate ages of sediments inferred from the Burg17-B core chronology.

The concentrations of labile P fractions (i.e. NaCl-TP, NaBD-TP and NaOH-TP) and total P have a similar trend over the whole profile (Fig. 4.5 and 4.6a). They all display rather large values within the upper part of Zone I and generally decreased values in Zone II. In Zone III, the values increase to peaks at ~25 cm depth but sharply decrease to the lowest values in the upper boundary of Zone III and throughout Zone IV. HCl-TP and Ref.-$P_o$ fractions vary differently compared with the other fractions. Low contents of HCl-TP fraction are observed in

Zone I and II. HCl-TP fraction has a rather similar pattern as labile P fractions in Zone III, but then it remains at high levels in Zone IV. Ref.-$P_o$ fraction contents show relatively stable values from Zone I to Zone II, followed by a gradual rise in Zone III and in the upper part of Zone IV. The net burial rates (NBR) of P-fraction since 1934 (Fig. S4.9) show similar trends to the P-fraction concentrations (Fig. 4.5) (because sedimentation rates MAR are rather constant in core Burg17-C; Fig S4.9), except for the Ca-P and Ref.-$P_o$ fractions with decreasing NBR throughout the Zone IV.
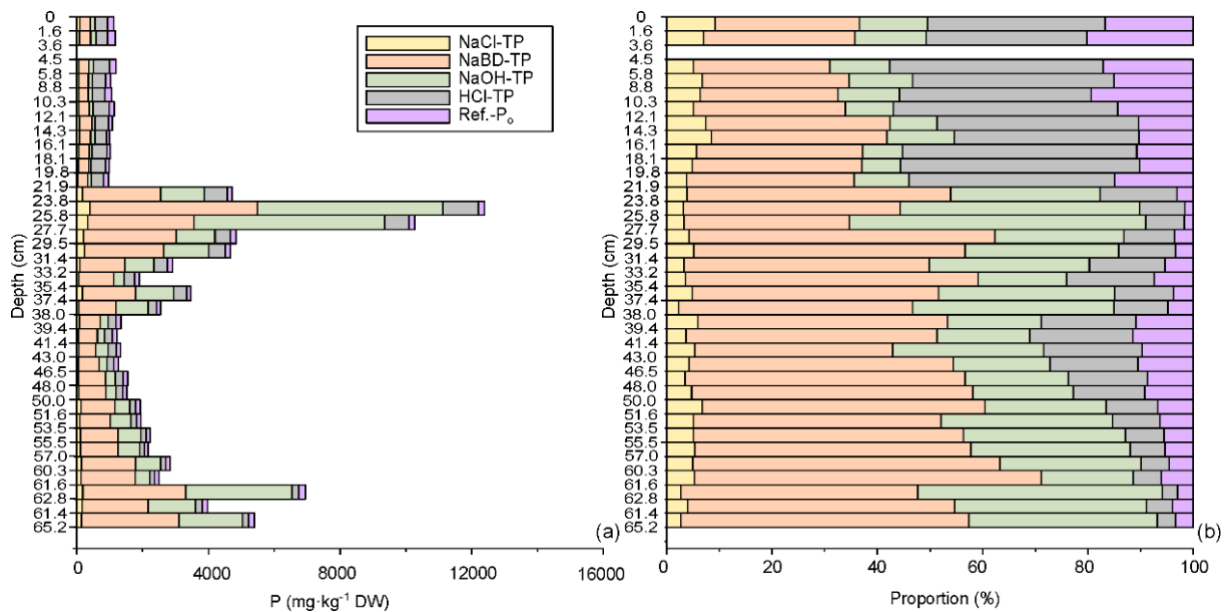


**Figure 4.6:** Vertical profile of P fractions in sediments. (a) P fractions concentrations and (b) their proportions of total P in sediments. The y-axis (left) refers to the sediment depth of Core Burg17-B. Note that the sample between 3.6-4.5 cm depth was removed from dataset because the values were extremely higher than any sample data (data not shown), which is abnormal according to XRF-P counts at the corresponding depth (Fig. S4.8b). We attributed this to the result of contamination during the sample measurements.

Regarding the P composition in sediment profiles (Fig. 4.6, absolute and relative amounts), from Zone I to Zone III (65.2-21.5 cm) NaBD-TP fraction is the most important P-form representing ~50% of total P followed by NaOH-TP fraction. However, in Zone IV (depth above ~ 21.5 cm), HCl-TP becomes the main P fraction (~39% of total P) over NaBD-TP (~30% of total P).

The relationships between response variables and explanatory variables are visible on the redundancy analysis (RDA) biplot (Fig. 4.7), which, in most cases, correspond well to the results of Spearman rank correlation test (Fig. S4.10). The relatively labile P fractions (NaCl-TP, NaBD-TP and NaOH-TP) and total P in sediments are strongly positively correlated with

redox-sensitive elements (Fe and Mn) and autochthonous Fe (Fe/Ti). However, these P fractions are negatively related to hypolimnetic oxygenation proxy (Fe/Mn ratios) and, to some extent, to lake productivity indicators (green-pigments, XRF-Ca and TIC). HCl-TP and Ref.-P$_o$ fractions are positively correlated. However, only HCl-TP fraction has close positive relationships with lake productivity indicators.
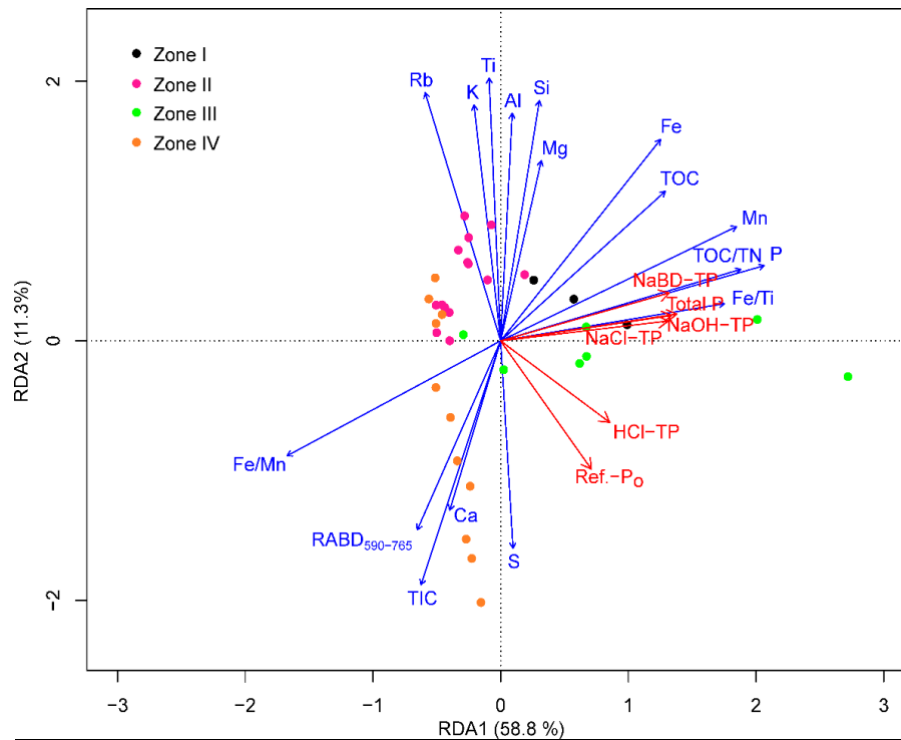


**Figure 4.7:** RDA biplot displaying correlation between response variables (P fraction dataset; red arrows) and explanatory variables (green-pigments and other geochemical records; blue arrows). The colored points represent data points of individual cluster zones in Fig. 4.3, 4.5 and S4.6.

### 4.1.7 Discussion

***Trophic state evolution of Lake Burgäschi***

Four main phases of different lake trophic levels (based on RABD$_{590-765}$ index values) were distinguished since the early 1900s, as summarized in Fig. 4.8 and Fig. S4.11. During the period prior to ~1926 in Zone I, the lowest green-pigments index values reflect low lake primary productivity. In the early 1900s, agricultural impacts around the catchment area of Lake Burgäschi were not prominent (Guthruf et al., 1999). It can be expected that the lake received low nutrient loads from the catchment drainage during this period. Lake Burgäschi is classified as naturally oligotrophic based on morphometric parameters (LAWA, 1998) and as naturally mesotrophic according to Binderheim-Bankay (1998). Therefore, at the times of Zone I, Lake Burgäschi was likely oligo- to mesotrophic.
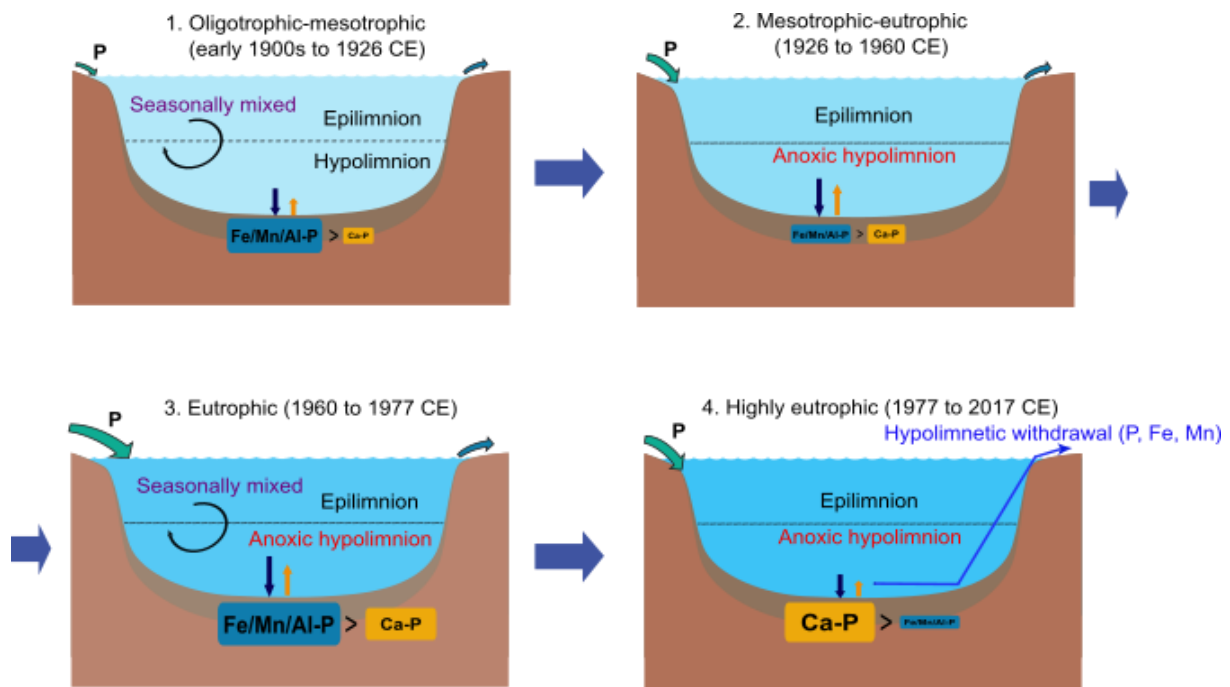
**Figure 4.8**: Conceptual diagram, summarising the inputs/outputs of phosphorus (P), hypolimnetic withdrawal restoration, lake trophic levels, mixing regime and phosphorus (P) fractions retention in sediments of Lake Burgäschi during four stages/zones. Note that the illustrated sizes of P fractions (Fe/Mn/Al-P and Ca-P) among different stages overall indicate the relative amounts of P fractions in sediments.

The transition to Zone II (~1926-1960) was marked by generally increased sedimentary green-pigment concentrations and $CaCO_3$ contents (Fig. 4.3, 4.4d and 4.5), respectively, indicating enhanced lake primary productivity. The slightly decreased TOC/TN ratio also suggests a rise in autochthonous organic matter proportion (Meyers and Ishiwatari, 1993). The first two algal blooms (peaks of green-pigments index; Fig. 4.4d) imply a very likely mesotrophic to eutrophic state of the lake. Indeed, the study of Büren (1949) revealed that in 1943-1945, the trophic state of Lake Burgäschi had already shifted between mesotrophic and eutrophic. Interestingly, the water-table lowering during 1943-1945 (Guthruff et al., 1999) with related enhanced drainage of intensive agricultural fields and meadows (Büren, 1949) did not seem to have had an immediate impact on lake primary productivity (Fig. 4.3).

In Zone III (~1960-1977), continuously increasing green-pigment concentrations indicating several algal bloom events and intensified $CaCO_3$ precipitation (TIC) and sulfur (S) contents in sediments (Fig. 4.4a and 4.5) are in agreement with the findings from other eutrophic lakes (Holmer and Storkholm, 2001; Bonk et al., 2016; Schneider et al., 2018).

During Zone IV (1977-2017), we interpret that Lake Burgäschi was in highly eutrophic

conditions, based on constantly high green-pigments index values and multiple prominent algal blooms (Fig. 4.3). Low and decreasing TOC/TN ratio values (< 10) in this zone suggest a dominant source of organic matter in sediments from aquatic primary production, which has been interpreted as a signal of eutrophic waters (Enters et al., 2006). Our interpretation is further supported by high chlorophyll-*a* concentrations in surface waters (>8 ug L$^{-1}$; GSA, 2007) and the dominance of blue-green algae in the phytoplankton biomass during 1977 to 1992, which characterized Lake Burgäschi as highly eutrophic (GBL, 1995; Guthruf et al., 2013).

### *Reconstruction of hypolimnetic oxygenation regimes of Lake Burgäschi*

A large number of studies have used the proxy of Fe/Mn ratios in sediments to reconstruct past water oxygenation and mixing regimes of the lake, such as Mackereth (1966), Frugone-Álvarez et al. (2017), and Żarczyński et al. (2019) etc. However, this proxy and its interpretation are limited to cases in which the annual cycle of Fe and Mn deposition in lakes is mostly driven by redox changes in the hypolimnion and related diagenetic processes in surface sediments instead of driven by terrestrial inputs (Boyle, 2001; Naeher et al., 2013). In Lake Burgäschi, in Zone I to III, Mn and Fe varied mostly independently of erosion indicators as shown in Fig. S4.7b. Furthermore, Van Raden (2012) has revealed that the presence of Mn-rich laminae in sediments of Lake Burgäschi can indicate frequent short-term wind-induced mixing events in the lake. Therefore, we suggest that the deposition of Fe and Mn during these three zones was mainly controlled by in-lake processes. The proxy of XRF-inferred Fe/Mn ratios together with Mn precipitation in sediments reliably tracks past changes of hypolimnetic oxygenation of Lake Burgäschi.

In Zone I (pre ~1926), the sediments feature well-preserved Mn-Fe rich laminations and very low Fe/Mn ratios (Fig. 4.3 and 4.4a), suggesting that the lake hypolimnion was seasonally well-oxygenated. The similar occurrence of visible Mn-and Fe rich laminae in sediments were also reported by Rey et al. (2017) in Lake Burgäschi and from other lakes, for example, Lake of the Clouds in the US (Anthony, 1977), Lake Cadagno in the Swiss Alps (Wirth et al., 2013), and Lake Żabińskie in Poland (Żarczyński et al., 2018). They revealed that the red-orange Mn-rich layers mostly consist of authigenic rhodochrosite ($MnCO_3$) that was formed when Mn-rich anoxic bottom waters are mixed with oxygenated surface waters for short intervals. The preservation of this Mn-rich layer is only possible when its sedimentation process exceeds the release process under anoxic hypolimnetic conditions (Stevens et al., 2000). Therefore, during this period, short-term mixing events and associated oxygenation may have occurred during overall stratified or anoxic conditions in the hypolimnion.

In Zone II (~1926-1960), the higher Fe/Mn ratios and very low Mn- and autochthonous Fe

(Fe/Ti) amounts are interpreted as the results of stable anoxic hypolimnetic waters. The formation and preservation of Fe-and Mn-oxides in sediments is largely prevented under long-term stratification/reducing conditions (Stevens et al., 2000). The lake most likely developed anoxic hypolimnetic conditions with yearly incomplete or missing circulation in the hypolimnion.

In Zone III (1960-1977), overall decreased Fe/Mn ratios combined with reappearing Mn-and Fe-rich laminations reflect better short-term oxic conditions in hypolimnetic waters than in Zone II. However, during ~1970 to 1977, Fe/Mn ratios gradually increased (Fig. 4.3), which points to less oxic conditions in the hypolimnion. It seems to be related to synchronously progressive lake eutrophication. Higher primary productivity and strengthened anoxia in the hypolimnion are commonly observed in stratified lakes (Giguet-Covex et al., 2010; Mikomägi et al., 2016). Higher lake primary productivity increases high-rate aerobic degradation of organic matter and, consequently, oxygen-depletion in the hypolimnion and sediments (Gächter and Müller, 2003; Nürnberg, 2007).

Finally, in Zone IV (1977- 2017) Fe/Mn ratios proxy is no longer valid to indicate hypolimnetic oxygenation regime, as suggested by predominantly terrestrial sources of sediment Fe and Mn (Fig. S4.7b). Nevertheless, the well-preserved laminated sediments during this period are a clear sign of absent benthic bioturbation and thus represent an indicator of generally strong anoxic conditions in hypolimnetic waters, occurring simultaneously with a highly eutrophic period. According to the limnological monitoring data of Lake Burgäschi between 1978 and 2007 (GSA, 2007), the lake water was anoxic at depths below 20 m during the summer-autumn stratification; even during winter overturn of most years, the lake water was not completely mixed.

***Phosphorus composition and factors controlling long-term P-fraction retention in sediments***

Prior to 1977 (i.e. Zones I-III), NaBD-TP (redox-sensitive Fe- and Mn bound P) and NaOH-TP (partly non-reducible Fe oxides-P) fractions were the primary P forms in sediments of Lake Burgäschi (Fig. 4.6 and 4.8). This seems to compare well with the study of Moosmann et al. (2006), who suggested that sediment Fe contents control P retention in sediments of the Swiss Plateau lakes. However, after ~1977, we observed a change to predominantly Ca-P (apatite-P), occurring concurrently with the operation of hypolimnetic withdrawal restoration. This clear pattern in sedimentary P-fraction change can be largely attributed to this restoration measure. The hypolimnetic withdrawal treatment in Lake Burgäschi removes not only hypolimnetic P but also dissolved metal (Al, Fe and Mn) ions and, thus leads to calcite as the main sorbent for P in upper waters and to an enhanced proportion of Ca-P fraction in sediments.

In spite of the effects of lake restoration on sedimentary P retention in Zone IV, overall, the retention of total P and labile P fractions in the sediment profile was mainly controlled by autochthonous Fe (Fe/Ti), Mn, and hypolimnetic oxygenation proxy-Fe/Mn ratios, as shown by the results of RDA analysis (Fig. 4.7). Our results support the previous suggestion that long-term permanent sediment-P retention is largely limited by the sediment's binding capacity in anoxic conditions (Moosmann et al., 2006; Hupfer and Lewandowski, 2008), which, specifically in our case, is determined by redox-sensitive elements (autochthonous Fe and Mn) preserved in sediments. These findings are discussed in the context of each cluster zone as follows: During Zone I and Zone III, when the hypolimnion had better seasonally oxic conditions (see Fig. 4.8 and Fig. S4.11), the increased retention of Mn and Fe, and labile P fractions occurred simultaneously (Fig. 4.3 and 4.5). This phenomenon might be caused by efficient P-trapping in Mn- and Fe enriched layers. It has been suggested that the formation of laminated Mn- and Fe enriched layers could serve as a protective cap to reduce P release from surface sediment layers to the anoxic hypolimnion (Żarczyński et al., 2018) which, thus, can help improve P retention within these sedimentary layers. In Zone II, small amounts of labile P fractions might result from decreased P-bearing solid phases (Mn and Fe minerals) in sediments under anoxic conditions in the hypolimnion (see higher Fe/Mn ratios in Section *Reconstruction of hypolimnetic oxygenation regimes of Lake Burgäschi*; Fig. S4.11). However, in Zone IV, we observed the lowest retention and NBR of total P and labile P fractions in recent sediments (Fig. 4.5; Fig. S4.9). We interpret this as a combined result of eutrophication-induced hypolimnetic anoxia and hypolimnetic withdrawal since 1977 whereby P-rich hypolimnetic water is discharged out of the lake. On the one hand, under stable anoxic conditions in the hypolimnion caused by strong eutrophication, reduced Mn and Fe preservation (Fig. 4.3) suggests a low capacity of permanent P-trapping within the anoxic sediments. On the other hand, hypolimnetic withdrawal restoration in Lake Burgäschi has substantially reduced hypolimnetic P concentrations by a factor of 5-6 since 1978 (Fig. S4.11; GSA, 2007) and MARs (Fig. 4.2c and Fig. S4.9). This indicates a concomitant decrease in sediment P release to the hypolimnion and P sedimentation to the water-sediment interface (gross sedimentation of P) as well. Consequently, decreased total P concentrations and total P-NBR in sediments were observed (Fig. 4.6a and S4.9). The reduction of total P contents in upper sediments caused by hypolimnetic withdrawal was also reported from Lake Kortowskie of Poland (Dunalska et al., 2007). Moreover, our findings confirm that this restoration is an effective method to reduce sediment P release potentials, as indicated by considerably decreased NBR of labile P fractions in upper sediments (Fig. S4.9).

In the whole sediment profile, HCl-P and Ref.-$P_o$ fractions had mainly autochthonous origins and were mainly controlled by in-lake processes rather than by clastic inputs (e.g. apart from

molasses sandstone), as indicated by absent positive correlations between the two fractions and detrital elements such as Ti, K and Al (Fig. 4.7). HCl-P (i.e. Ca-P) fraction retention, to a large extent, resulted from authigenic $CaCO_3$-P precipitation, and increased with higher eutrophic levels in Zone III and IV (Fig. 4.5). We interpret this as an incidence of biologically driven co-precipitation of Ca and P in highly productive lakes. The phenomenon of Ca-P co-precipitation has been observed and studied in many calcareous lakes (Dittrich and Koschel 2002; Whitehouse, 2010), and is assumed to be responsible for the scavenging of dissolved P from surface waters of eutrophic lakes (Hamilton et al., 2009). In addition, large amounts of Ca-P in surface sediments (top 21 cm) can act as a potential negative feedback to eutrophication in Lake Burgäschi, because Ca-P fraction is relatively stable in sediments and has low potentials of P-release from surface sediments back to lake waters. Interestingly, HCl-P fraction retention and NBR in sediments of Zone IV were generally lower than in Zone III (Fig. 4.5 and Fig. S4.9), although the lake in Zone IV had relatively higher eutrophic levels (see Section *Trophic state evolution of Lake Burgäschi*; Fig. S4.11). The pH in the hypolimnion of Lake Burgäschi varied between 7.0 and 7.5 according to the monitoring data in 1993, 2003, and 2013 (Guthruf et al., 2013). Therefore, the acid dissolution of Ca-P in the hypolimnion and at the water-sediment interface is small and unlikely significant during Zone IV. The generally decreased retention and NBR of Ca-P fraction were seemingly related to hypolimnetic withdrawal, which has caused lower water-P concentrations and MAR of sediments as discussed above. As a result, there are reductions of $CaCO_3$-P co-precipitation in the epilimnion and consequently of Ca-P net sedimentation in surface sediments. Overall, Ref.-$P_o$ fraction retention and NBR in the sedimentary profile show less variability compared with other P fractions (Fig. 4.5 and Fig. S4.9). Nevertheless, the lower NBR of Ref.-$P_o$ fraction in the upper sediments (~ top 10 cm) could be derived from the ongoing early degradation of fresh organic matters.

The interesting observation is that the water-P reductions caused by the hypolimnetic withdrawal in Lake Burgäschi (GSA, 2007; Nürnberg, 2007) have been ineffective in reducing algal blooms and curbing eutrophication. Similar findings were also reported from some lakes in Europe and the US (Kosten et al., 2012; Kolzau et al., 2014; Fastner et al., 2016). These authors have attributed this phenomenon to insufficient external P-load reduction, higher water temperatures under global warming of the last few decades, and the light or nitrogen limitation of surface-water phytoplankton. In Lake Burgäschi, phytoplankton growth in the trophic zone is more likely limited by P during growth season after 1978 rather than by the nitrogen (GSA, 2007) as the algae-available ortho-phosphate is almost completely used up in the epilimnion when the nitrate concentrations stay as high as 0.5-3 mg N / L in the upper 5-m waters (GBL, 1995). Hence, we suggest that these factors mentioned above, except for nitrogen limitation

of lake productivity, may also contribute to promoting persistently high primary productivity in Lake Burgäschi. But the main driver keeping productivity high, is the continuing high external P loads from the lake catchment. During summer stratification, the high lake external P load into the epilimnion primarily supports phytoplankton growth in the photic zone, which is not strongly influenced by the hypolimnetic-P discharge and internal P loadingss. From a management perspective, it is still critically important to focus on lowering external P loads in order to decrease primary production and eutrophication in seasonally-stratified small deep lakes which are more likely to favor stable stratification during phytoplankton growth season.

### 4.1.8 Conclusion

This study shows that in Lake Burgäschi, more than half of sediment P is buried in relatively labile P fractions (Fe/Mn/Al-P), yet with low potentials for P-release from these labile P fractions in deeper layers (below ~21 cm). Our results highlight the importance of hypolimnetic oxygenation/mixing regime in controlling long-term P retention and net burial rates of labile P fractions in sediments of this small deep lake. Irrespective of increasing lake primary productivity during early 1900s to 1977, the two periods of high sedimentary retention of total P and labile P-fraction occurred in Fe- and Mn enriched laminae, which appears to be linked to seasonal mixing of the hypolimnion in the past. Importantly, the positive effects of hypolimnetic withdrawal in Lake Burgäschi were observed primarily in sediment P-fraction data but not in lake trophic state. The 40-year operation of hypolimnetic withdrawal has impoverished sedimentary P, in particular largely decreased net burial rates of labile P fractions (potential internal P loads), and increased the relative proportion of stable Ca-P fraction in top sediment layers (0-21 cm). Nevertheless, the lake is currently still highly eutrophic. We attribute the delay of lake recovery primarily to still high nutrient inputs from the nearby or surrounding agricultural area into the lake trophic zone during stratification seasons. This study calls for consistently more effective measures to minimize external P loadings from the catchment, such as optimizing fertilizer application practices and technical measures in the drainages.

### 4.1.9 Data availability

The data is available at PANGAEA at https://doi.org/10.1594/PANGAEA.908896.

### 4.1.10 Author contributions and Competing interests

L.T. helped with sample collection, analyzed the sediment, conducted data analysis, wrote the manuscript, and acquired most of the funding for the project. P. Z. helped with sediment core subsampling, conducted the hyperspectral imaging (HSI) scanning, helped with XRF-scanning, substantially contributed to the data interpretation. S.S. measured gamma-

spectroscopy radiometric activities, generated the data for chronology and helped with data interpretation. R.L. conducted the XRF-scanning and helped with data interpretation. M.G. designed the study, helped discussing the results, editing the manuscript and supervised the project. All authors commented on the manuscript.

The authors declare that they have no conflict of interest.

### 4.1.11 Acknowledgements

### 4.1.12 References

Anthony, R. S.: Iron-rich rhythmically laminated sediments in Lake of the Clouds, northeastern Minnesota, Limnol. Oceanogr., 22, 45–54, https://doi.org/10.4319/lo.1977.22.1.0045, 1977.

Appleby, P.G.: Chronostratigraphic techniques in recent sediments, In: Tracking Environmental Change Using Lake Sediments. Basin Analysis, Coring, and Chronological Techniques, edited by: Last, W.M., and Smol, J.P., Springer, Dordrecht, Netherlands, 171-203, https://doi.org/10.1007/0-306-47669-X_9, 2002.

Bennett, K. D.: Determination of the number of zones in a biostratigraphical sequence, New Phytol., 132, 155–170, https://doi.org/10.1111/j.1469-8137.1996.tb04521.x, 1996.

Binderheim-Bankay, E. A.: Sanierungsziel für natürlich eutrophe Kleinseen des Schweizer Mittellandes, Ph.D. thesis, ETH Zurich, Switzerland, 149 pp., 1998.

Bonk, A., Kinder, M., Enters, D., Grosjean, M., Meyer-Jacob, C., and Tylmann, W.: Sedimentological and geochemical responses of Lake Żabińskie (north-eastern Poland) to erosion changes during the last millennium, J. Paleolimnol., 56, 239–252, https://doi.org/10.1007/s10933-016-9910-6, 2016.

Boyle, J. F.: Inorganic Geochemical Methods in Palaeolimnology, In: Tracking Environmental Change Using Lake Sediments. Basin Analysis, Coring, and Chronological Techniques, edited by: Last, W.M., and Smol, J.P., Springer, Dordrecht, Netherlands, 83-141,

https://doi.org/10.1007/0-306-47670-3_5, 2002.

Büren, G. von: Der Burgäschisee, Mitteilungen der Naturforschenden Gesellschaft, Bern, 83 pp.,1949.

Burley, K.L., Prepas, E.E., and Chambers, P.A.: Phosphorus release from sediments in hardwater eutrophic lakes: the effects of redox-sensitive and-insensitive chemical treatments, Freshwater Biol., 46, 1061–1074, https://doi.org/10.1046/j.1365-2427.2001.00789.x, 2001.

Butz, C., Grosjean, M., Fischer, D., Wunderle, S., Tylmann, W., and Rein, B.: Hyperspectral imaging spectroscopy: a promising method for the biogeochemical analysis of lake sediments, J. Appl. Remote Sens., 9, 1–20, https://doi.org/10.1117/1.JRS.9.096031, 2015.

Butz, C., Grosjean, M., Goslar, T., and Tylmann, W.: Hyperspectral imaging of sedimentary bacterial pigments: a 1700-year history of meromixis from varved Lake Jaczno, northeast Poland, J. Paleolimnol., 58, 57–72, https://doi.org/10.1007/s10933-017-9955-1, 2017.

Cavalcante, H., Araujo, F. Noyma, N.P., and Becker, V.: Phosphorus fractionation in sediments of tropical semiarid reservoirs. Sci. Total Environ., 619-620, 1022–1029, https://doi.org/10.1016/j.scitotenv.2017.11.204, 2018

Chen, M., Ding, S., Chen, X., Sun, Q., Fan, X., Lin, J., Ren, M., Yang, L., and Zhang, C.: Mechanisms driving phosphorus release during algal blooms based on hourly changes in iron and phosphorus concentrations in sediments, Water res., 133, 153–164. https://doi.org/10.1016/j.watres.2018.01.040, 2018.

Dittrich, M. and Koschel, R.: Interactions between calcite precipitation (natural and artificial) and phosphorus cycle in the hardwater lake, Hydrobiologia, 469, 49–57, https://doi.org/10.1023/A:1015571410442, 2002.

Dunalska, J.A., Wiśniewski, G., and Mientki, C.: Assessment of multi-year (1956-2003) hypolimnetic withdrawal from Lake Kortowskie, Poland, Lake and Reserv. Manage., 23, 377-387, https://doi.org/10.1080/07438140709354025, 2007.

Einsele, W.: Über die Beziehungen des Eisenkreislaufs zum Phosphatkreislauf im eutrophen See, Arch. Hydrobiol., 29, 664–686, 1936.

Einsele, W.: Über chemische und kolloidchemische Vorgänge in Eisen-Phosphat- Systemen unter limnischen und limnogeologischen Gesichtpunkten, Arch. Hydrobiol., 33, 361–387, 1938.

Enters, D., Lücke, A., and Zolitschka, B.: Effects of land-use change on deposition and composition of organic matter in Frickenhauser See, northern Bavaria, Germany, Sci. Total

Environ., 369, 178–187, https://doi.org/10.1016/j.scitotenv.2006.05.020, 2006.

Fastner, J., Abella, S., Litt, A., Morabito, G., Vörös, L., Pálffy, K., Straile, D., Kümmerlin, R., Matthews, D., Phillips, M.G., and Chorus, I.: Combating cyanobacterial proliferation by avoiding or treating inflows with high P load—experiences from eight case studies, Aquat. Ecol., 50, 367–383, https://doi.org/10.1007/s10452-015-9558-8, 2016.

Frugone-Álvarez, M., Latorre, C., Giralt, S., Polanco-Martínez, J., Bernárdez, P., Oliva-Urcia, B., Maldonado, A., Carrevedo, M.L., Moreno, A., Delgado Huertas, A., and Prego, R.: A 7000-year high-resolution lake sediment record from coastal central Chile (Lago Vichuquén, 34° S): implications for past sea level and environmental variability, J. Quaternary Sci., 32, 830–844, https://doi.org/10.1002/jqs.2936, 2017.

Gächter, R.: Die Tiefenwasserableitung, ein Weg zur Sanierung von Seen, Schweizerische Zeitschrift für Hydrologie, 38, 1–28, 1976.

Gächter, R.: Lake restoration. Why oxygenation and artificial mixing cannot substitute for a decrease in the external phosphorus loading, Aquat. Sci., 49, 176–185, https://doi.org/10.1007/BF02538501, 1987.

Gächter, R. and Wehrli, B.: Ten years of artificial mixing and oxygenation: no effect on the internal phosphorus loading of two eutrophic lakes, Environ. Sci. Technol., 32, 3659–3665, https://doi.org/10.1021/es980418, 1998.

Gächter, R. and Müller, B.: Why the phosphorus retention of lakes does not necessarily depend on the oxygen supply to their sediment surface, Limnol. Oceanogr., 48, 929–933, https://doi.org/10.4319/lo.2003.48.2.0929, 2003.

Giguet-Covex, C., Arnaud, F., Poulenard, J., Enters, D., Reyss, J.L., Millet, L., Lazzaroto, J., and Vidal, O.: Sedimentological and geochemical records of past trophic state and hypolimnetic anoxia in large, hard-water Lake Bourget, French Alps, J. Paleolimnol., 43, 171–190, https://doi.org/10.1007/s10933-009-9324-9, 2010.

Gonsiorczyk, T., Casper, P., and Koschel, R.: Phosphorus-binding forms in the sediment of an oligotrophic and an eutrophic hardwater lake of the Baltic Lake District (Germany), Water Sci. Technol., 37, 51–58, https://doi.org/10.1016/S0273-1223(98)00055-9, 1998.

Grimm, E. C.: CONISS: a FORTRAN 77 program for stratigraphically constrained cluster analysis by the method of incremental sum of squares, Comput. Geosci., 13,13–35, https://doi.org/10.1016/0098-3004(87)90022-7, 1987.

Guthruf, J., Zeh, M., and Guthruf-Seiler, K.: Kleinseen im Kanton Bern, Water Protection and Waste Management Office of the Canton of Bern, Bern, 1999.

Guthruf, K., Maurer, V., Ryser, R., Zeh, M., and Zweifel, N.: Zustand der Kleinseen, Construction, Transport and Energy Directorate of the Canton of Bern Office for Water and Waste Water and soil protection laboratory, Bern, 2013.

Håkanson, L. and Jansson, M. (Eds.) : Principles of Lake Sedimentology, The Blackburn Press, New Jersey, USA, 2002.

Hamilton, S.K., Bruesewitz, D.A., Horst, G.P., Weed, D.B., and Sarnelle, O.: Biogenic calcite–phosphorus precipitation as a negative feedback to lake eutrophication, Can. J. Fish. Aquat. Sci., 66, 343–350, https://doi.org/10.1139/F09-003, 2009.

Heiri, O., Lotter, A. F., and Lemcke, G.: Loss on ignition as a method for estimating organic and carbonate content in sediments: reproducibility and comparability of results, J. Paleolimnol., 25, 101–110, https://doi.org/10.1023/A:1008119611481, 2001.

Holmer, M. and Storkholm, P.: Sulphate reduction and sulphur cycling in lake sediments: a review, Freshwater Biol., 46, 431–451, https://doi.org/10.1046/j.1365-2427.2001.00687.x, 2001.

Hupfer, M. and Lewandowski, J.: Oxygen controls the phosphorus release from lake sediments–a long-lasting paradigm in limnology, Int. Rev. Hydrobiol., 93, 415–432, https://doi.org/10.1002/iroh.200711054, 2008.

Juggins, S.: rioja: analysis of quaternary science data, https://cran.r-project.org/web/packages/rioja/index.html, 2017.

Kaiserli, A., Voutsa, D., and Samara, C.: Phosphorus fractionation in lake sediments–lakes Volvi and Koronia, N. Greece, Chemosphere, 46, 1147–1155, https://doi.org/10.1016/S0045-6535(01)00242-9, 2002.

Kolzau, S., Wiedner, C., Rücker, J., Köhler, J., Köhler, A., and Dolman, A. M.: Seasonal patterns of nitrogen and phosphorus limitation in four German lakes and the predictability of limitation status from ambient nutrient concentrations, Plos One, 9, e96065, https://doi.org/10.1371/journal.pone.0096065, 2014.

Kosten, S., Huszar, V.L., Bécares, E., Costa, L.S., van Donk, E., Hansson, L.A., Jeppesen, E., Kruk, C., Lacerot, G., Mazzeo, N., and De Meester, L.: Warmer climates boost cyanobacterial dominance in shallow lakes, Global, Change Biol., 18, 118–126, https://doi.org/10.1111/j.1365-2486.2011.02488.x, 2012.

Kucklentz, V. and Hamm, A. (Eds.): Möglichkeiten und Erfolgsaussichten der Seenrestaurierung, Bayrische Landesanstalt für Wasserforschung, München, Germany, 212 pp., 1988.

LAWA (Länderarbeitsgemeinschaft Wasser): Gewässerbewertung — stehende Gewässer: Richtlinie für die Bewertung nach trophischen Kriterien, Germany, 1998.

Lukkari, K., Hartikainen, H., and Leivuori, M.: Fractionation of sediment phosphorus revisited. I: Fractionation steps and their biogeochemical basis, Limnol. Oceanog- Meth., 5, 433–444, https://doi.org/10.4319/lom.2007.5.433, 2007.

Mackereth, F.J.H.: Some chemical observations on post-glacial lake sediments, Philos. T. Roy. Soc. B., 250, 165–213, https://doi.org/10.1098/rstb.1966.0001, 1966.

GBL. Burgäschisee. Resultate der Wasser- und Planktonuntersuchungen 1977-1995. Office for Water Protection and Waste Management of the Canton of Bern, 1995.

GSA: 30 Jahre Tiefenwasser-Ableitung. Wie geht es dem Burgäschisee heute?, Office for Water Protection and Waste Management of the Canton of Bern, Bern, 2007.

McCulloch, J., Gudimov, A. Arhonditsis,G. Chesnyuk, A., and Dittrich, M.: Dynamics of P-binding forms in sediments of a mesotrophic hard-water lake: Insights from non-steady state reactive-transport modeling, sensitivity and identifiability analysis, Chem. Geol., 354, 216–232, https://doi.org/10.1016/j.chemgeo.2013.06.011, 2013.

Meyers, P. A. and Ishiwatari, R.: Lacustrine organic geochemistry—an overview of indicators of organic matter sources and diagenesis in lake sediments, Org. Geochem., 20, 867–900, http://dx.doi.org/10.1016/0146-6380(93)90100-P, 1993,

Michel, H., Barci-Funel, G., Dalmasso, J., Ardisson, G., Appleby, P., Haworth, E., and El-Daoushy, F.: Plutonium, americium and cesium records in sediment cores from Blelham Tarn, Cumbria (UK), J. Radioanal. Nucl. Ch., 247, 107–110, https://doi.org/10.1023/A:1006719215833, 2001.

Moosmann, L., Gächter, R. Müller, B., and Wüest, A.: Is phosphorus retention in autochthonous lake sediments controlled by oxygen or phosphorus?, Limnol. Oceanogr., 51, 763–771, https://doi.org/10.4319/lo.2006.51.1_part_2.0763, 2006.

Mikomägi, A., Koff, T., Martma, T., and Marzecová, A.: Biological and geochemical records of human-induced eutrophication in a small hard-water lake, Boreal Env. Res., 21, 513–527, 2016.

Naeher, S., Gilli, A., North, R.P., Hamann, Y., and Schubert, C.J.: Tracing bottom water oxygenation with sedimentary Mn/Fe ratios in Lake Zurich, Switzerland, Chem. Geol., 352, 125–133, https://doi.org/10.1016/j.chemgeo.2013.06.006, 2013.

Nikolai, S.J. and Dzialowski, A.R.: Effects of internal phosphorus loading on nutrient limitation in a eutrophic reservoir, Limnologica, 49, 33–41, https://doi.org/10.1016/j.limno.2014.08.005, 2014.

Nürnberg, G.K.: Lake responses to long-term hypolimnetic withdrawal treatments, Lake Reserv. Manage., 23, 388–409, https://doi.org/10.1080/07438140709354026, 2007.

Ogdahl, M. E., Steinman, A. D., and Weinert, M. E.: Laboratory-determined phosphorus flux from lake sediments as a measure of internal phosphorus loading, Jove-J. Vis. Exp., 85, e51617, https://dx.doi.org/10.3791%2F51617, 2014.

Oksanen, J., Blanchet, F.G., Kindt, R., Legendre, P., Minchin, P.R., O'hara, R., Simpson, G.L., Solymos, P., Stevens, M.H.H., and Wagner, H.: Package 'vegan'. Community ecology package, version 2, http://cran.r-project.org/web/packages/vegan/index.html, 2013.

Pennington, W., Tutin, T.G., Cambray, R.S., and Fisher, E.M.: Observations on lake sediments using fallout ^{137}Cs as a tracer, Nature, 242, 324–326, https://doi.org/10.1038/242324a0, 1973.

R Development Core Team: R: A Language and Environment for Statistical Computing, R Foundation for Statistical Computing, Vienna, Austria, 2017.

Rentz, J., Turner, I.P., and Ullman, J.L.: Removal of phosphorus from solution using biogenic iron oxides, Water Res., 43, 20292035, https://doi.org/10.1016/j.watres.2009.02.021, 2009.

Reuss, N., Conley, D.J., and Bianchi, T.S.: Preservation conditions and the use of sediment pigments as a tool for recent ecological reconstruction in four Northern European estuaries, Mar. Chem., 95, 283–302, https://doi.org/10.1016/j.marchem.2004.10.002, 2005.

Rey, F., Gobet, E., van Leeuwen, J.F.N., Gilli, A., van Raden, U.J., Hafner, A., Wey, O., Rhiner, J., Schmocker, D., Zünd, J., and Tinner, W.: Vegetational and agricultural dynamics at Burgäschisee (Swiss Plateau) recorded for 18,700 years by multi-proxy evidence from partly varved sediments, Veg. Hist. Archaeobot., 26, 571–586. https://doi.org/10.1007/s00334-017-0635-x, 2017.

Ribeiro, D., Martins, G., Nogueira, R., Cruz, J.V., and Brito, A.: Phosphorus fractionation in volcanic lake sediments (Azores–Portugal), Chemosphere, 70, 1256–1263, https://doi.org/10.1016/j.chemosphere.2007.07.064, 2008.

Richter, T.O., Van der Gaast, S., Koster, B., Vaars, A., Gieles, R., de Stigter, H.C., De Haas, H., and van Weering, T.C.: The Avaatech XRF Core Scanner: technical description and applications to NE Atlantic sediments, Geol. Soc. London Spec. Publ., 267, 39–50, https://doi.org/10.1144/GSL.SP.2006.267.01.03, 2006.

Rydin, E.: Potentially mobile phosphorus in Lake Erken sediment. Water Res., 34, 2037–2042, https://doi.org/10.1016/S0043-1354(99)00375-9, 2000.

Schmid, S.M., Fügenschuh, B., Kissling, E., and Schuster, R.: Tectonic map and overall architecture of the Alpine orogen, Eclogae Geol. Helv., 97, 93–117, https://doi.org/10.1007/s00015-004-1113-x, 2004.

Schneider, T., Rimer, D., Butz, C., and Grosjean, M.: A high-resolution pigment and productivity record from the varved Ponte Tresa basin (Lake Lugano, Switzerland) since 1919: insight from an approach that combines hyperspectral imaging and highperformance liquid chromatography, J. Paleolimnol., 60, 381–398, https://doi.org/10.1007/s10933-018-0028-x, 2018.

Schnurrenberger, D., Russell, J., and Kelts, K.: Classification of lacustrine sediments based on sedimentary components, J. Paleolimnol., 29,141–154, https://doi.org/10.1023/A:1023270324800, 2003.

Smith, L., . Watzin, M. C., and Druschel, G.: Relating sediment phosphorus mobility to seasonal and diel redox fluctuations at the sediment-water interface in a eutrophic freshwater lake, Limnol. and Oceanogr., 56, 2251–2264, https://doi.org/10.4319/lo.2011.56.6.2251, 2011.

Søndergaard, M., Jensen, P.J., and Jeppesen, E.: Retention and internal loading of phosphorus in shallow, eutrophic lakes, Sci. World J., 1, 427–442, https://doi.org/10.1100/tsw.2001.72, 2001

Stevens, L., Ito, E., and Olson, D.: Relationship of Mn-carbonates in varved lake-sediments to catchment vegetation in Big Watab Lake, MN, USA. J. Paleolimnol., 24,199–211, https://doi.org/10.1023/A:1008169526577, 2000.

Trolle, D., Hamilton, D.P., and Pilditch, C.A.: Evaluating the influence of lakemorphology, trophic status and diagenesis on geochemical profiles in lake sediments, Appl. Geochem., 25, 621–632, https://doi.org/10.1016/j.apgeochem.2010.01.003, 2010.

Tu, L., Jarosch, K.A., Schneider, T., and Grosjean, M.: Phosphorus fractions in sediments and their relevance for historical lake eutrophication in the Ponte Tresa basin (Lake Lugano, Switzerland) since 1959, Sci. Total Environ., 685, 806–817, https://doi.org/10.1016/j.scitotenv.2019.06.243, 2019.

Tylmann, W., Bonk, A., Goslar, T., Wulf, S., and Grosjean, M.: Calibrating ^{210}Pb dating results with varve chronology and independent chronostratigraphic markers: Problems and implications, Quat. Geochronol. 32, 1–10,    https://doi.org/10.1016/j.quageo.2015.11.004, 2016.

van Raden, U. J.: High-resolution Swiss lake records of climate change. Ph.D. thesis, ETH Zurich, Switzerland, https://doi.org/10.3929/ethz-a-009783578, 2012.

Whitehouse, R.D.: Phosphorus scavenging through calcite co-precipitation: bringing clarity to Clear Lake, B.Sc. thesis, University of British Columbia, Canada, 2010.

Wirth, S.B., Gilli, A., Niemann, H., Dahl, T.W., Ravasi, D., Sax, N., Hamann, Y., Peduzzi, R., Peduzzi, S., Tonolla, M., and Lehmann, M.F.: Combining sedimentological, trace metal (Mn, Mo) and molecular evidence for reconstructing past water-column redox conditions: The example of meromictic Lake Cadagno (Swiss Alps), Geochim. Cosmochim. Ac., 120, 220–238, https://doi.org/10.1016/j.gca.2013.06.017, 2013.

Żarczyński, M., Wacnik, A., and Tylmann, W.: Tracing lake mixing and oxygenation regime using the Fe/Mn ratio in varved sediments: 2000year-long record of human-induced changes from Lake Zabinskie (NE Poland), Sci. Total Environ., 657, 585–596, https://doi.org/10.1016/j.scitotenv.2018.12.078, 2019.

Żarczyński, M., Tylmann, W., and Goslar, T.: Multiple varve chronologies for the last 2000 years from the sediments of Lake Żabińskie (northeastern Poland)–Comparison of strategies for varve counting and uncertainty estimations, Quaternary Geochronology, 47, 107–119, https://doi.org/10.1016/j.quageo.2018.06.001, 2018.

## 4.2 Supplementary materials
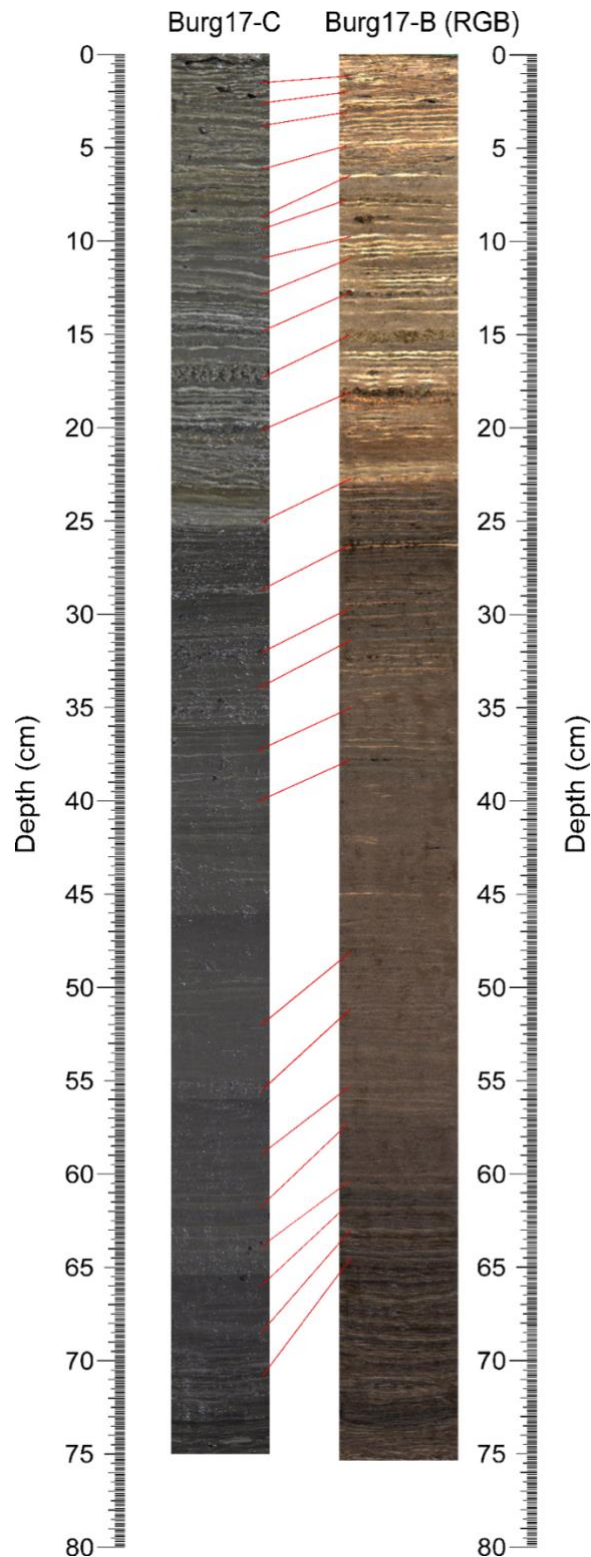


**Figure S4.1**: Core correlation between Core Burg17-C and Core Burg17-B (the dated core) sediment images. The core picture of Burg17-B is a true colour RGB (R: 640 nm, G: 545 nm, B: 460 nm) linear-stretch image. The core picture of Burg17-C was taken with a Nikon D80 digital camera.
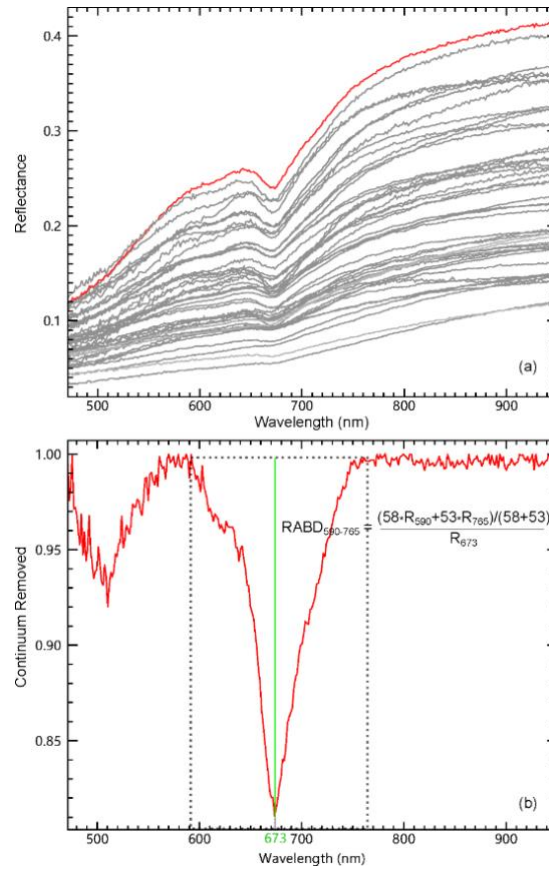
**Figure S4.2**: (a) Spectral endmembers obtained from Spectral Hourglass Wizard. The highlighted red endmember spectrum #19 is used in (b). (b) Continuum removed spectrum of endmember #19, showing the formula for $RABD_{590-765}$ calculation for a trough minimum at $R_{673}$.

**Figure S4.3**: Five-step sequential P extraction protocol. The F1-F4 fractions follow the four-step extraction protocol in Tu et al., (2019), and F5 follows the last extraction step in Lukkari et al. (2007). Sodium dithionite ($Na_2S_2O_4$) dissolved in 0.11 M sodium bicarbonate ($NaHCO_3$) buffer (pH 7.0) henceforth is termed as NaBD.
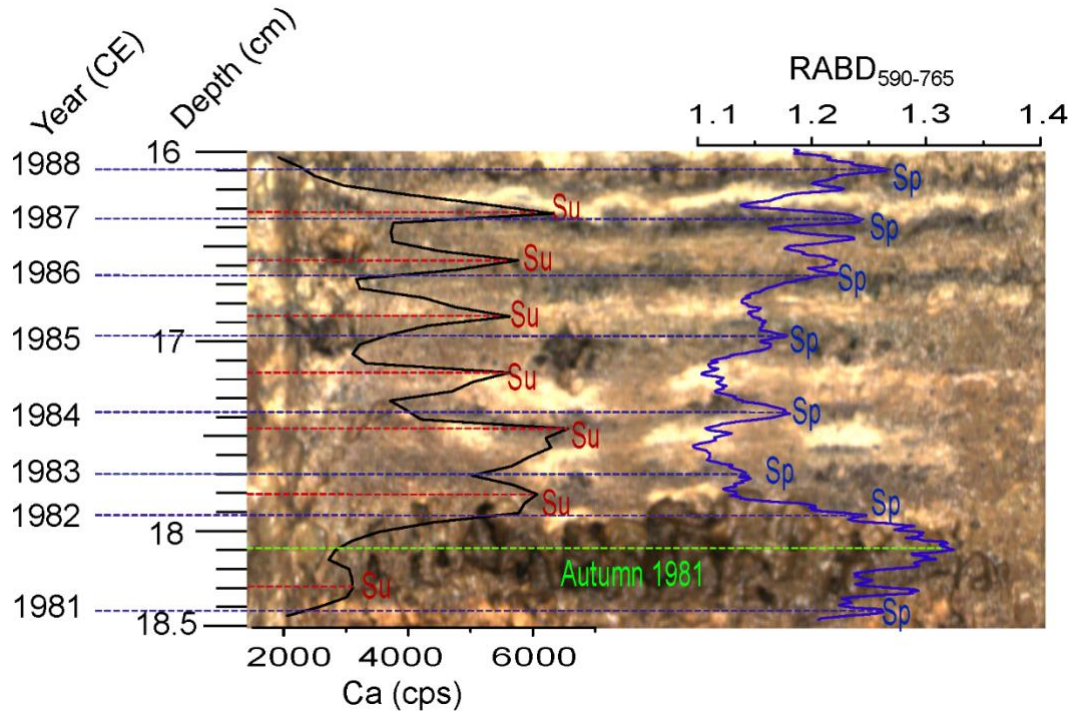
**Figure S4.4**: The laminations from depth 16 cm to 18.5 cm with a regular succession of light calcite layers (Ca-rich) and dark organic-rich ($RABD_{590-765}$ inferred green-pigments) layers indicated by different colored lines (color figure online). The background is the RGB contrast enhanced core picture (Sp: Spring; Su: Summer). The algal bloom in the autumn of 1981 year coincides with the historical record in GSA (2007).
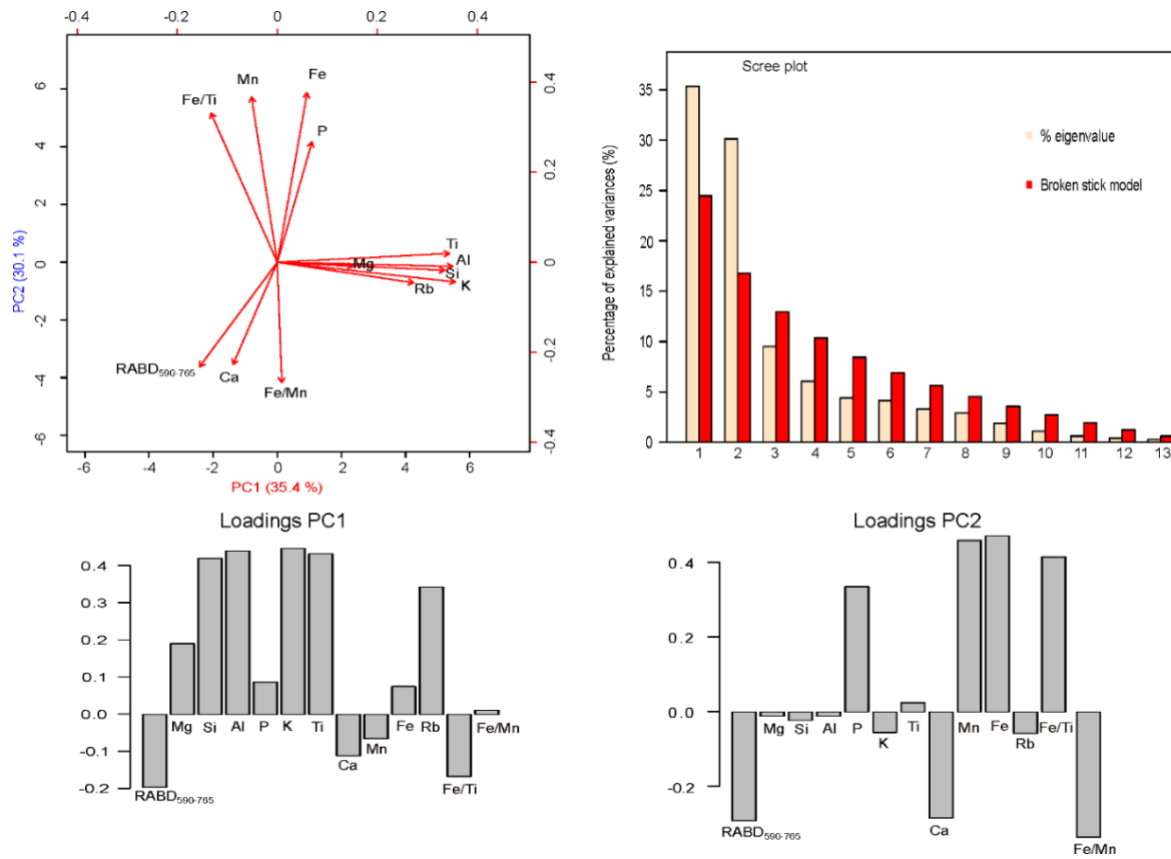
**Figure S4.5**: The biplot on standardized data of variables from Fig. 4.3 and S4.6, the screeplot and the loadings of the PCA.
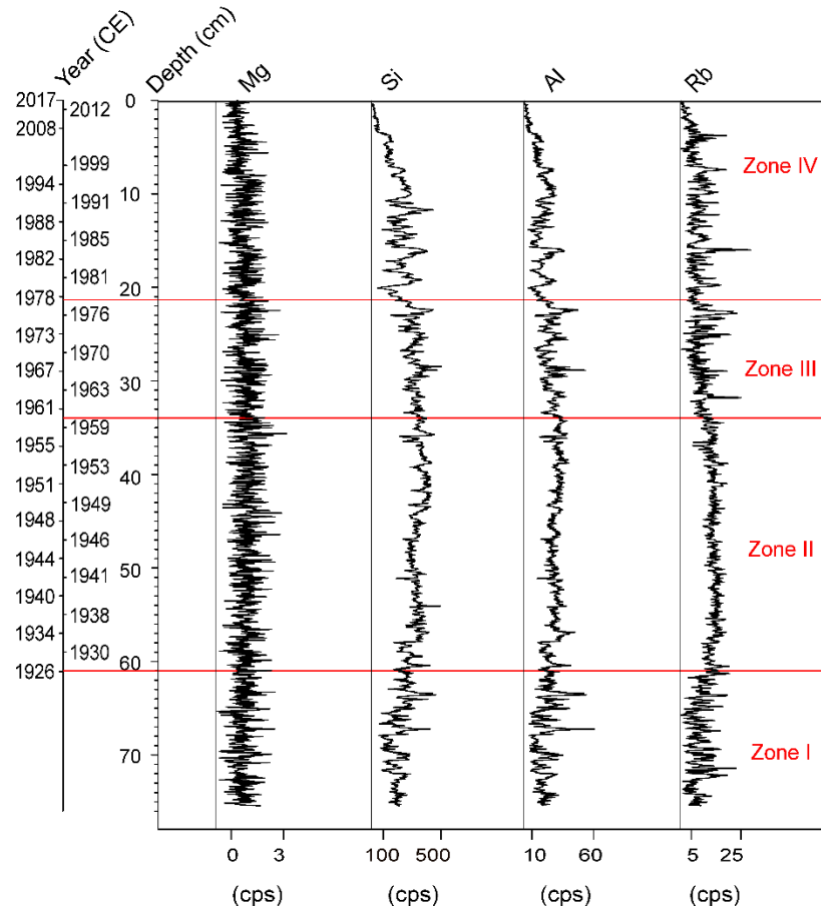
**Figure S4.6**: Stratigraphical records of several XRF-elements in sediments of Core Burg17-B. Elemental counts are represented in cps (counts per second). The red horizontal lines separate the four significant clusters retrieved by the CONISS analysis in Fig. 4.3.

**Figure S4.7**: Multivariate analysis of green-pigments and geochemical dataset from Fig. 4.3 and S4.6. (a) Distribution of four CONISS-zones, and PC1 and PC2 scores along with the sediment Core Burg17-B. (b) Biplots of PC1 and PC2 for individual CONISS-zones in Fig. 4.3.
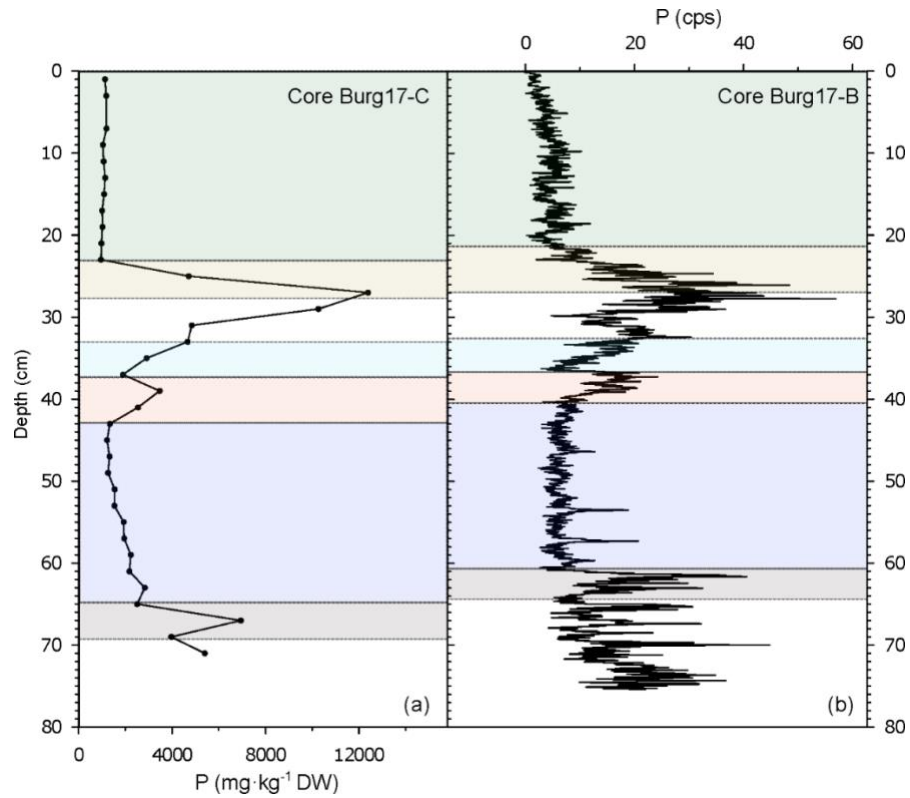
**Figure S4.8**: The profiles of (a) total P concentrations from sequential P extraction (Burg17-B) and (b) semi-quantitative XRF-P (Burg17-C). The colored sections indicate the matching between the two profiles.
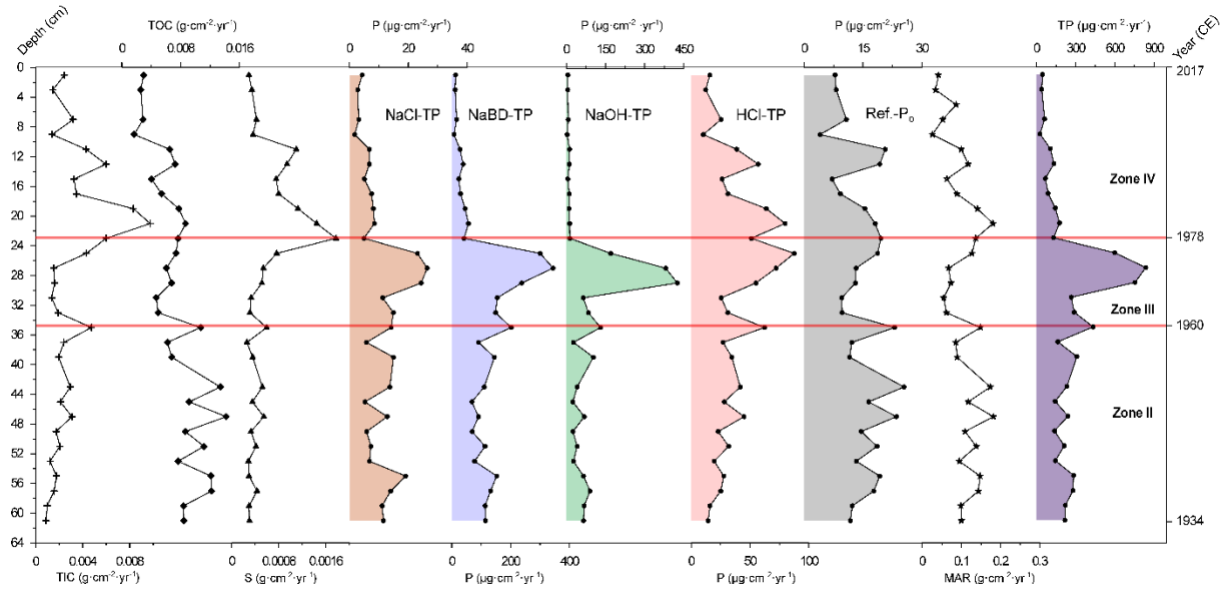
**Figure S4.9**: Net burial rates (NBR) of geochemical records. Total inorganic carbon (TIC), total organic carbon (TOC), sulfur (S) contents, all the five P fractions, total P (TP) and the sediment mass accumulation rates (MAR) in sediments of Lake Burgäschi are between 1934 and 2017 CE. The horizontal red lines separate the significant CONISS zones as in Fig. 4.3 and Fig. 4.5. The y-axis (left) refers to the sediment depth of Core Burg17-C.
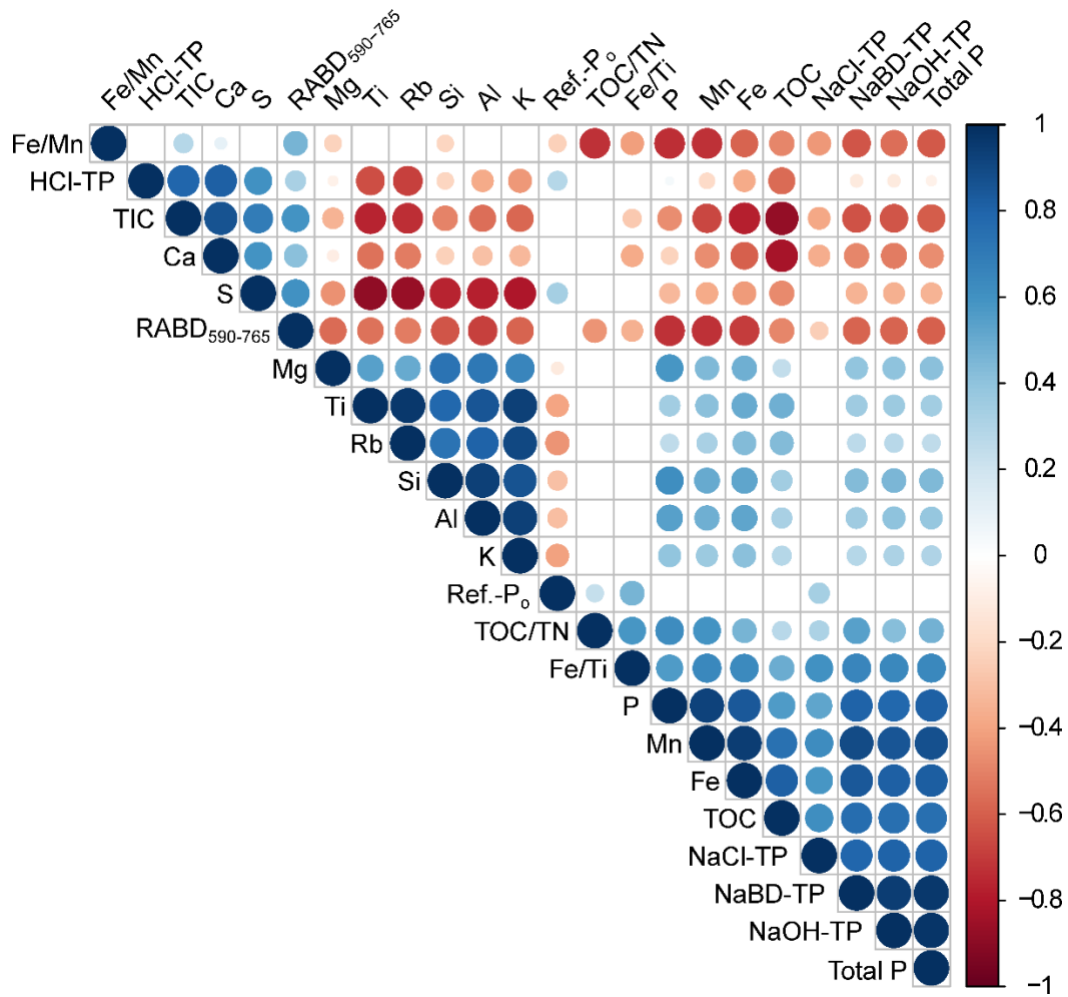
**Figure S4.10**: Spearman's rank correlation matrix of all variables (presented in Fig. 4.7) at the significance level of 0.05. Only the p-value of the correlation < 0.05 is shown. In total 35 samples points are included. The variable-order follows the output of hierarchical clustering.
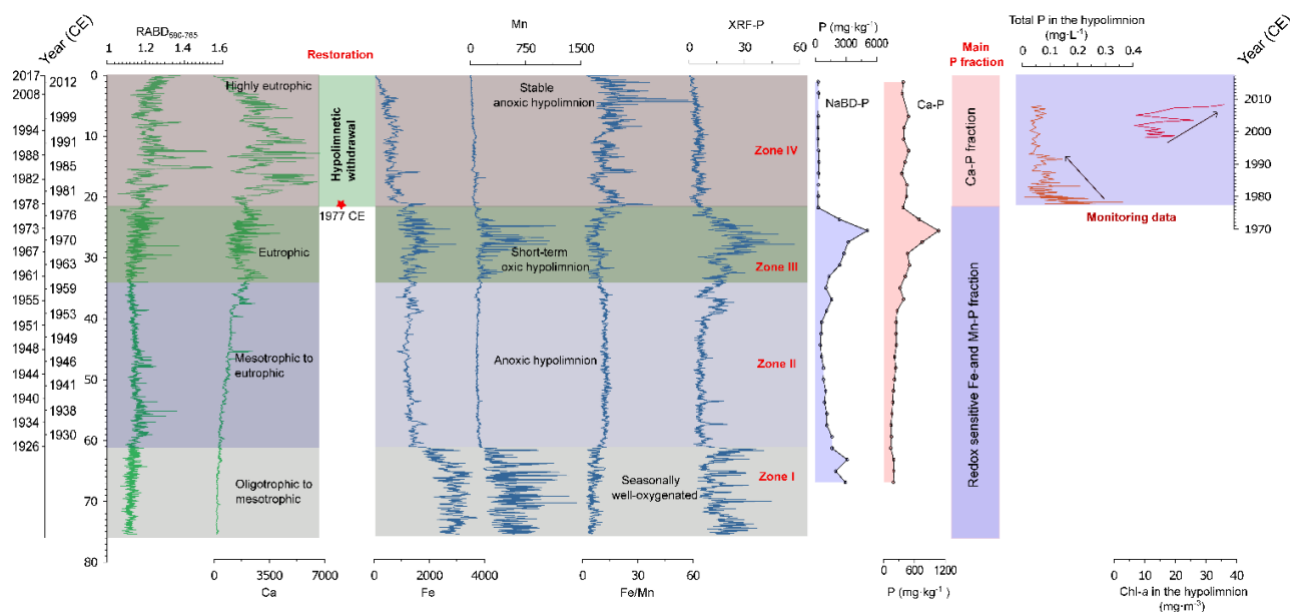
**Figure S4.11**: The synthesis of Lake Burgäschi proxy records. It shows lake trophic levels, hypolimnetic withdrawal restoration, hypolimnetic redox conditions, sedimentary P fractions (e.g. NaBD-P and Ca-P ) retention and lake monitoring data of hypolimnetic total P and Chl-*a* concentrations (GSA, 2007) between early 1900s and 2017.

### References

Lukkari, K., Hartikainen, H. and Leivuori, M.: Fractionation of sediment phosphorus revisited. I: Fractionation steps and their biogeochemical basis, Limnol. Oceanog- Meth., 5,433-444, https://doi.org/10.4319/lom.2007.5.433, 2007.

GSA: 30 Jahre Tiefenwasser-Ableitung. Wie geht es dem Burgäschisee heute?, Office for Water Protection and Waste Management of the Canton of Bern, Bern, 2007.

Tu, L., Jarosch, K.A., Schneider, T. and Grosjean, M.: Phosphorus fractions in sediments and their relevance for historical lake eutrophication in the Ponte Tresa basin (Lake Lugano, Switzerland) since 1959, Sci. Total Environ., 685, 806-817, https://doi.org/10.1016/j.scitotenv.2019.06.243, 2019.

# Chapter 5: The nexus between long-term natural eutrophication, anoxia and phosphorus dynamics in a deep stratified lake: insights from a 15,000-year varved sediment record

## 5.1 The nexus between long-term natural eutrophication, anoxia and phosphorus dynamics in a deep stratified lake: insights from a 15,000-year varved sediment record

Luyao Tu [a], *, Adrian Gilli [b], André F. Lotter [c], Hendrik Vogel [d], Madeleine Moyle [e], John F Boyle [e], Martin Grosjean [a]

[a] *Institute of Geography & Oeschger Centre for Climate Change Research, University of Bern, Hallerstrasse 12, 3012 Bern, Switzerland*

[b] *Geological Institute, ETH Zürich, Sonneggstrasse 5, 8092 Zürich, Switzerland*

[c] *Institute of Plant Sciences & Oeschger Centre for Climate Change Research, University of Bern, Altenbergrain 21, 3013 Bern, Switzerland*

[d] *Institute of Geological Sciences & Oeschger Centre for Climate Change Research, University of Bern, 3012, Bern, Switzerland*

[e] *Department of Geography and Planning, University of Liverpool, Liverpool L69 3BX, United Kingdom*

*Correspondence to: Luyao Tu (luyao.tu@giub.unibe.ch)

**Key words:** Internal phosphorus loadings; natural eutrophication; anoxia; Late-glacial/Holocene; Paleolimnology; Switzerland

### *Highlights*

- First qualitative estimates of internal P loadings in a deep stratified lake during the Holocene

- Evidence of pre-anthropogenic feedbacks between productivity, anoxia and P cycling.

- Microorganisms modulate the Holocene geochemical cycle of P under meromictic conditions.

- Postglacial forest and climate changes affect lake productivity, anoxia and P cycling.

### 5.1.1 Abstract

Increased man-made eutrophication since the 20th century caused by phosphorus (P) enrichment has become a major threat worldwide. In deep, stratified lakes, eutrophication-induced hypolimnetic anoxia often stimulates the release of labile P from the sediment into the water column. This positive feedback, termed internal P loadings, maintains or even accelerates eutrophication. However, most of the studies on internal P loadings concentrate on recent times. Little is known whether such positive feedbacks and labile P recycling from sediments have also played a role under natural conditions with no or little human impact. Here, we investigated a high-resolution 15,000-year sediment record of paleoproduction, anoxia, and five sedimentary P fractions from a small, deep lake, Soppensee, on the Swiss Central Plateau. We estimated long-term qualitative internal P loadings by comparing the Holocene record of diatom-inferred epilimnetic total P (DI-TP) concentrations with labile P fraction (Fe/Al-P) concentrations in sediments under changing trophic, redox, and lake mixing regimes. The results demonstrate that intensified P cycling from sediments into the water column (enhanced internal P loadings) apparently occurred as a positive feedback of natural eutrophication with persisting bottom-water anoxia during the early to mid-Holocene (~9000–6000 cal BP). However, this positive feedback could not be inferred for other eutrophic phases, when Fe-rich layers formed during seasonal mixing of the lake or when magnetite-type minerals produced by magnetotactic bacteria (MTB) appeared to prevent internal P loadings during anoxic phases in the mid- to late Holocene (6000 – 2000 cal BP). This resulted in high concentrations of potentially labile Fe/Al-P in sediments. Our study demonstrates the potential contribution of internal P loadings during long-term natural eutrophication of deep stratified lakes. The example of Soppensee also highlights the importance of the coupled geochemical cycles of P and Fe in the long-term trophic evolution of ferruginous, low sulfate water lakes. Our findings have implications for current lake eutrophication management and restoration.

### 5.1.2 Introduction

Human-induced eutrophication since the 20th century, also known as cultural eutrophication, has become a major environmental threat to freshwater ecosystems worldwide. It can create toxic algae blooms and result in deep-water hypoxia or even anoxia among other adverse effects (Paerl, 1988). In most cases, lake eutrophication is attributed to excessive phosphorus (P) inputs from either external or internal loads because P is often the limiting nutrient for lake primary production (Worsfold et al., 2016). There is increasing recognition that lake internal P loadings (i.e. P released from sediments into the water column) can trigger a positive feedback of eutrophication, delaying lake recovery after reducing external P loadings (Orihel et al., 2017). This holds particularly true for seasonally stratified, deep lakes, where hypolimnetic

anoxia caused by thermal and/or eutrophication-related biochemical stratification is expected to trigger effective P recycling from surface sediments back into the water column (Lepori and Roberts, 2017; Tu et al., 2019). Hypolimnetic anoxia or meromixis-induced sediment-P release in deep eutrophic lakes has received increasing attention (e.g. Cyr et al., 2009; Nurnberg et al., 2018). In stratified eutrophic lakes, the mineralization of organic matter (OM) tends to cause depletion of dissolved oxygen in deep waters, leading to the reductive dissolution of Fe/Mn oxyhydroxides and release of adsorbed P back into bottom waters (Steinsberger et al., 2017). Studies in two seasonally stratified eutrophic lakes in Switzerland (Tu et al., 2019; 2020) have recently demonstrated that enhanced internal P loadings and P-recycling leads to a depletion of the labile P fraction in sediments.

Besides such anthropogenic drivers as residential, industrial, and agriculture discharges, natural drivers can also be responsible for lake eutrophication and hypolimnetic anoxia in deep lakes. For example, higher lake surface temperatures due to climate warming very likely prolong the growing season for phytoplankton and thus strengthen stratification, ultimately leading to an elevated and growing risk of eutrophication and anoxia in deep lakes (Straile et al., 2003). Furthermore, temperate deep lakes in Europe have mostly been found to be naturally nutrient-rich due to their geological or geomorphological settings and ontogenesis (e.g., Kirilova et al., 2009; Makri et al., 2020a; Sanchini et al. 2020).

For decades, many researchers have investigated the potentials of sediment-P release using different P fractions in sediments and their potential bioavailability (e.g. Gao et al., 2005; Kapanen, 2008). Net burial of labile P fractions in sediments, in combination with productivity, redox, and lake mixing proxies, might shed light on P cycling and internal P loads as well as feedbacks in the past under pre-anthropogenic conditions. However, most of the empirical and modeling research dealing with potentials of internal P loadings has focused on timespans of a few decades (Katsev and Dittrich, 2013) and on shallow, polymictic, well-oxygenated lakes (Søndergaard et al., 2001). There is yet a lack of long-term (i.e., Holocene and longer) records of sediment-P fraction retention, eutrophication, and anoxia history, in particular in stratified, deep lakes. This has hampered efforts to reliably test whether past internal P loadings and related positive feedbacks sustaining eutrophication also operated on long time scales under natural or early-anthropogenic impact conditions.

Soppensee is an ideal site to study this question because it is a deep, eutrophic lake offering a sediment record with annual laminations (varves), and its sediments have an exceptionally good chronology. Moreover, a record of diatom-inferred epilimnetic total P (DI-TP) concentrations is available for the entire Holocene (Lotter, 2001), which provides quantitative information about the past lake-water P levels.

In this study, we aim to answer three research questions: 1) How have sedimentary labile and stable P-fraction retention and potentials of internal P loadings changed under pre-anthropogenic, natural conditions in Soppensee? 2) Were there large differences between sedimentary labile P-fraction retention and lake-water P levels or lake primary production? 3) Is there evidence for long-term, pre-anthropogenic positive feedbacks between eutrophication-triggered anoxia and enhanced internal P loadings, which could be detected by depletion of labile P fractions in sediments while DI-TP in the lake water remained elevated? To answer these questions, we combined a Holocene high-resolution paleoproduction and anoxia record with a record of five sedimentary P fractions and DI-TP concentration data. If DI-TP is assumed to be an unbiased estimate of the epilimnetic total P, then this approach allows us to investigate the relationships between epilimnetic total P concentrations and sedimentary labile P fraction concentrations under changing primary production and lake mixing regimes throughout the Holocene. We hypothesize that differences between the DI-TP and sediment labile P records enable qualitative inferences of internal P loadings that indicate a positive feedback of natural eutrophication.

### 5.1.3 Study site

Soppensee is a small, hard-water lake situated on the Swiss Central Plateau at 596 m above sea level (47°05'30"N, 08°05'E). This kettle-hole lake was formed after the retreat of the Reuss glacier around 17–18 ka cal BP (Lotter, 1989). It has a small surface area (0.227 km$^2$) relative to its maximum water depth (27 m). The lake does not have surface inflows and is mainly fed by groundwater and seasonal surface run-off with negligible detrital inputs from a small calcareous sandstone catchment of 1.6 km$^2$. One outflow leaves the lake in the northwest (Fig. 5.1b). The water volume amounts to 2.9 × 10$^6$ m$^3$ with a residence time of ~ 3.1 years (Fischer, 1996).
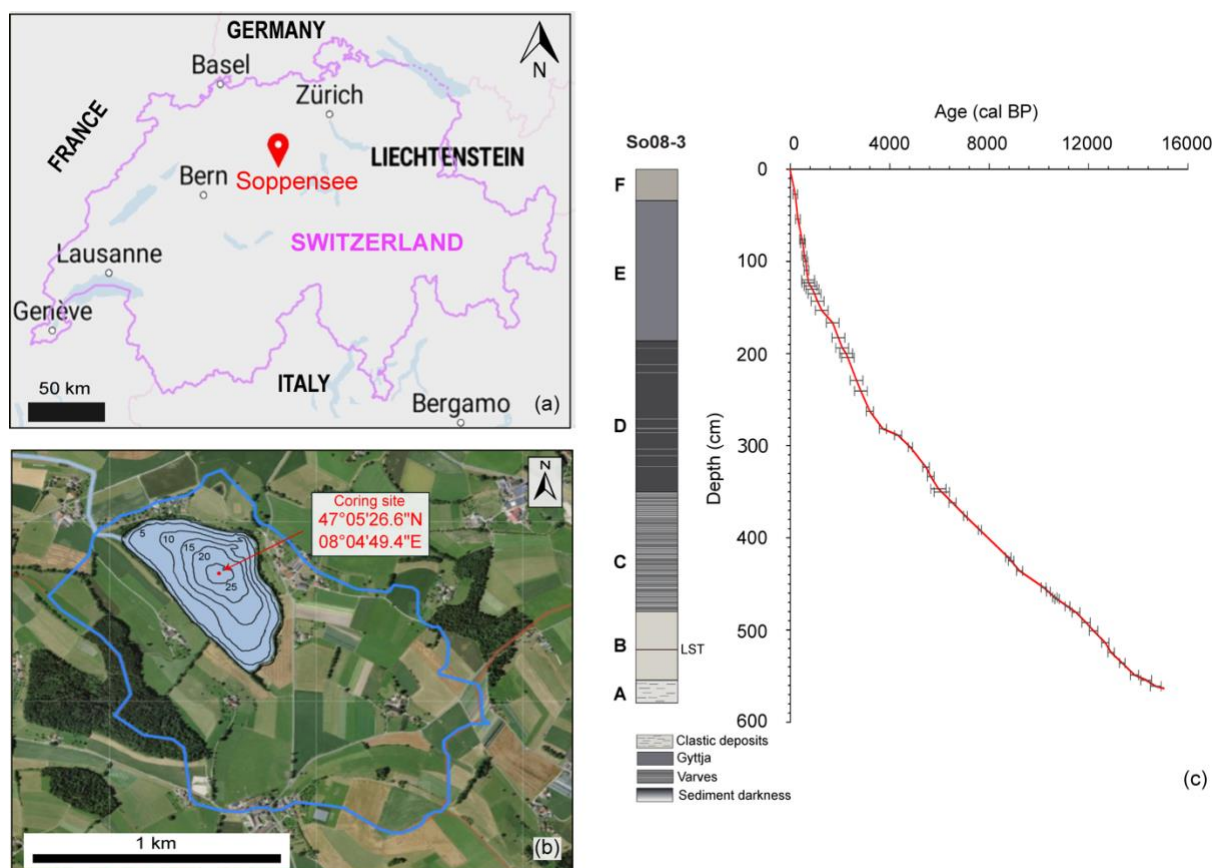
**Figure 5.1**: Study site. (a) Map of Switzerland with the location of Soppensee. (b) Aerial image of the catchment area of Soppensee (inside the blue polygon; background map © swisstopo) and a bathymetric map of the lake with the coring site. (c) Age-depth model and lithology of Core So08-3 and, on the left, the six lithological units A-F according to Gierga et al. (2016). LST marks the Laacher See Tephra at 521–521.5 cm depth.

Soppensee sediments are characterized by well-preserved varves that provide a continuous record of most of the Early-Mid Holocene and part of the Late-glacial (Lotter 1989). The sediments are very well dated with varve counting paired with ^{14}C dates (Hajdas and Michczyński, 2010) and provide an excellent archive for chironomids (Hofmann, 2001), pollen (Lotter, 1999), and diatoms (Lotter, 2001). According to the DI-TP concentrations record, Soppensee remained in meso- to eutrophic conditions throughout the Holocene (Lotter, 2001). Today, the lake is classified as eutrophic to hypertrophic with lake-water total P concentrations in the range of 50–116 µg L$^{-1}$ (Müller et al., 1998). Currently, Soppensee is holomictic with strong thermal and chemical stratification and hypolimnetic anoxia in summer (Gruber et al., 2000). Mixing mostly occurs in fall and winter.

The catchment area of Soppensee is intensively farmed, with arable and pastoral uses accounting for 82% of the catchment area and wooded areas representing 12% (Langenegger et al., 2019). The wooded areas are composed of mixed forest dominated by *Picea abies*

(spruce; planted) and *Fagus sylvatica* (beech). A temperate and oceanic climate prevails in the region, with July (~17.6 °C) the warmest month and January (~ -0.3 °C) the coldest.

### 5.1.4 Materials and methods

*Sediment sampling and chronology*

In August 2008, several UWITEC piston cores with overlapping sequences were retrieved from the deepest part of the lake at a water depth of 27 m (47°05'26.6"N, 08°04'49.4"E; Fig. 5.1a, b). After core collection, the cores were tightly sealed and stored in a cold room at 4°C before opening. In 2019, the cores were split lengthwise in two halves, A and B, and the oxidized surfaces were described according to Schnurrenberger et al. (2003). The A-half cores were used for visual correlation and non-destructive scanning techniques including x-ray fluorescence (XRF) and hyperspectral imaging (HSI). The B-half cores were subsampled for destructive geochemical analysis such as pigment analysis and P extraction. The composite core So08-3 examined in this study was assembled from three overlapping cores based on stratigraphic marker layers and XRF data correlation. The composite sequence has a total length of 571 cm, covering the past ~15,000 years (Fig. 5.1c). The chronology of core So08-3 is based on the correlation of XRF data and sedimentary marker layers to core So08-01/2 dated by Hajdas and Michczyński (2010) and van Raden (2012) using 42 tie points (see Table S1 and Fig. S5.1 in supplementary material).

*Sediment lithology*

Previous research (Hajdas and Michczyński, 2010; Kind et al., 2012; Gierga et al., 2016) has shown that the uppermost ~6 m sediments of Soppensee are organic-rich lacustrine deposits that are divided into six sedimentary units (A to F) based on lithological parameters.

Unit A (571–548 cm in Core So08-3; Fig. 5.1c) contains detrital deposits with light-grey silty clays deposited between ~15,115 and 13,800 cal BP during the deglaciation of the Swiss Plateau (see Gierga et al. 2016). In unit B (548–474 cm), sediments are dark-brownish and rich in organic matter and carbonates. As Fischer (1996) described, unit B is partly laminated with Fe-rich layers formed in the Late-glacial period. According to Gierga et al. (2016), unit B can be attributed to the Allerød interstadial (~13,800–12,700 cal BP) and the Younger Dryas (YD, ~12,700–11,500 cal BP). The Laacher See tephra (LST), dated to ~12,800 cal BP (Hajdas and Michczyński, 2010), is found within this unit prior to the onset of the YD. Unit C (474–350 cm) consists of continuous biogenic calcite varves formed during the early to mid-Holocene until ~6000 cal BP. In unit D (350–187 cm; ~6000–2000 cal BP), sediments are rich in organic matter with an overall very dark color. Vivid blue crystals (vivianite) are visible at some spots from parts of the oxidized core surface in unit D. Unit E (187–35 cm), representing

the period ~2000–200 cal BP, consists of very faint laminations and organic-rich sediments with lighter color than unit D. The uppermost unit, F, (above 35 cm) consists of light brown sediments of the most recent 200 years.

*Geochemical methods*

The semi-quantitative elemental composition was measured on the fresh sediment surface of core So08-3 using an ITRAX XRF Core Scanner (Cox Ltd.) equipped with a Cr-Anode-Tube set to 30 kV and 50 mA at the Institute of Geological Sciences, University of Bern. Measurements were made at 5-mm contiguous intervals and an integration time of 30 s. Prior to scanning, the sediment surface was carefully cleaned and smoothed. All XRF data are given as total counts per area (cts). For the interpretation of selected XRF elements, Ti was used as indicator of lithogenic content; Ca of endogenic calcite content; and Mn of water column redox conditions (van Raden, 2012).

The HSI scans were made with a Specim Ltd. single core scanner equipped with a hyperspectral linescan camera (Specim PFD-CL-65-V10E) in the visual to near-infrared range (VNIR, 400–1000 nm) following the methodology in Butz et al. (2015). Parameters were set to a spatial resolution of ~75 µm per pixel and a spectral sampling of 1.57 nm (binning of 2). Relative absorption band depth (RABD) indices were calculated to quantify the absorbance troughs caused by sedimentary chloropigments and bacteriopheophytins. The $RABD_{567-769}$ spectral index was retrieved from a local minimum of the absorption feature between wavelengths of 567 nm and 769 nm after the method in Schneider et al. (2018), as described in Fig. S2 of supplementary material. The $RABD_{567-769}$ spectral index indicates total chlorophylls and diagenetic products in sediments, from which lake primary production can be inferred (Schneider et al., 2018; Makri et al., 2020a). The $RABD_{845}$ spectral index represents bacteriopheophytins *a* and *b*, a specific biomarker diagnostic for purple sulfur bacteria (PSB). PSB are anoxygenic phototrophic bacteria that live at the chemoclines of stratified lakes with oxic–anoxic interfaces; thus the presence of PSB indicates seasonal hypolimnetic anoxia or meromixis in the lake with light penetration to the chemocline (Butz et al., 2016; Zander et al., 2021).

The pigment extraction of 32 sediment samples (1 cm slices) followed the method in Amann et al. (2014), which was applied to ~0.1–0.5 g freeze-dried homogenized sediments using 100% acetone (HPLC grade) solution. The pigments concentrations in extracts were determined with a Shimadzu UV-1800 spectrometer. We used the molar extinction coefficients for chlorophyll-*a* and chlorophyll-*a* derivatives (here green pigments) from Jeffrey and Humphrey (1975) and for bacteriopheopigments-*a* (Bphe-*a*) from Fiedor et al. (2002). $RABD_{567-769}$ and $RABD_{845}$ values were calibrated to spectrophotometrically determined

concentrations (µg g$^{-1}$ dry sediments) of green pigments and Bphe-*a*, respectively, using linear regression models following Butz et al. (2015). The calibration models were validated by $R^2$ and the root mean squared errors of prediction (RMSEP) (see Fig. S5.3 in supplementary material). Residual analyses of the linear calibration models (Fig. S5.4 and S5.5 in supplementary material) revealed that three samples cause a slight tailing in the normal QQ-plot (Fig. S5.4b and S5.5b) and higher leverage (Fig. S5.4d and S5.5d); a weak heteroscedastic pattern is visible in Fig. S5.4c and S5.5c. However, the Shapiro-Wilk and the Kolmogorov-Smirnov tests both indicate most likely normal distributions of the residuals for the two linear regression models; thus, the inferences from the two calibration models are valid.

The sediment P fractionation procedure in this study principally followed the harmonized protocol developed by the standards, measurements and testing (SMT) of the European Commission as modified in Ruban et al. (1999) and Ruban et al. (2001) based on Williams et al. (1976). The SMT protocol consists of three independent extraction procedures and defines five P fractions: non-apatite inorganic P (mostly P bound to Fe, Al including vivianite, and Mn oxides and hydroxides, hereafter Fe/Al-P), apatite P (calcium bound P, hereafter Ca-P), inorganic P, organic P, and total P. Fe/Al-P in sediments is a labile P source under anoxic conditions and in high pH environments and can be considered potentially bioavailable. Ca-P in sediments is considered non-available, and organic P partly available. In this study, we made slight modifications to the SMT protocol: a) In each extraction step, we used 40 mL (instead of 20 mL) extractant (i.e., NaOH and HCl) for ~0.2 g aliquots of freeze-dried homogenized sediments. The lower dry sediment weight-to-extractant volume ratio (1:200) was to avoid the saturation limit of P released from the solid phase. b) Two 1 M NaCl rinse steps (20 mL) were added after each main extraction step. The P determined in rinsing solutions was added to the corresponding P pools to maximize the extraction efficiency. Following each extraction and rinsing step, supernatant was collected after centrifugation at 4000 rpm for 15 min at room temperature.

Phosphate concentrations in all unfiltered extracts were determined spectrophotometrically with the malachite green method (Ohno and Zibilske, 1991) and the absorbance measured at 610 nm (Shimadzu UV-1800 spectrophotometer). The details of the colorimetrical analyses can be found in Tu et al. (2019). Certified reference sediment material (CRM) BCR-684 was used for quality control of the analytical data and efficiency of the extraction procedure. The analytical results for BCR-684 are in good agreement with the certified contents from the certification report for the SMT procedure (see Table S5.2 in supplementary material).

### 5.1.5 Results

*Time series of geochemical data*

Fig. 5.2 shows that HSI-pigment, P fractions, and XRF data exhibit distinctive features across the six stratigraphic units (A to F in Fig. 5.1c). The long-term phase relationship between Fe/Al-P data and lake paleoproduction history reveals an approximately coherent pattern across the units. Labile P (Fe/Al-P) is the dominant P fraction in most periods (Fig. S5.6a in supplementary material). The labile P fraction exhibits a pattern very similar to total P and inorganic P over time (Fig. 5.2). The Fe- and Mn-rich laminae (Fischer, 1996) and calcite varves (Hajdas and Michczyński, 2010) coincide with relatively high XRF Fe and Mn counts and high Ca counts, respectively (Fig. 5.2). Fig. 5.3 shows four distinct 2-cm example sections with corresponding high-resolution HSI-pigment data from the Late-glacial (Fig. 5.3a and 3b) and Holocene periods (Fig. 5.3c and 3d). Fig. 5.4 primarily compares sedimentary Fe/Al-P data with the DI-TP concentration record (Lotter, 2001) and with centennial-scale records of lake paleoproduction and anoxia. DI-TP data is not available for the Late-glacial period (units A and B) due to diatom dissolution in these sediments. Instead, we compared HSI-pigment-inferred lake primary production with the Fe/Al-P stratigraphy (Fig. 5.4c and 4e).
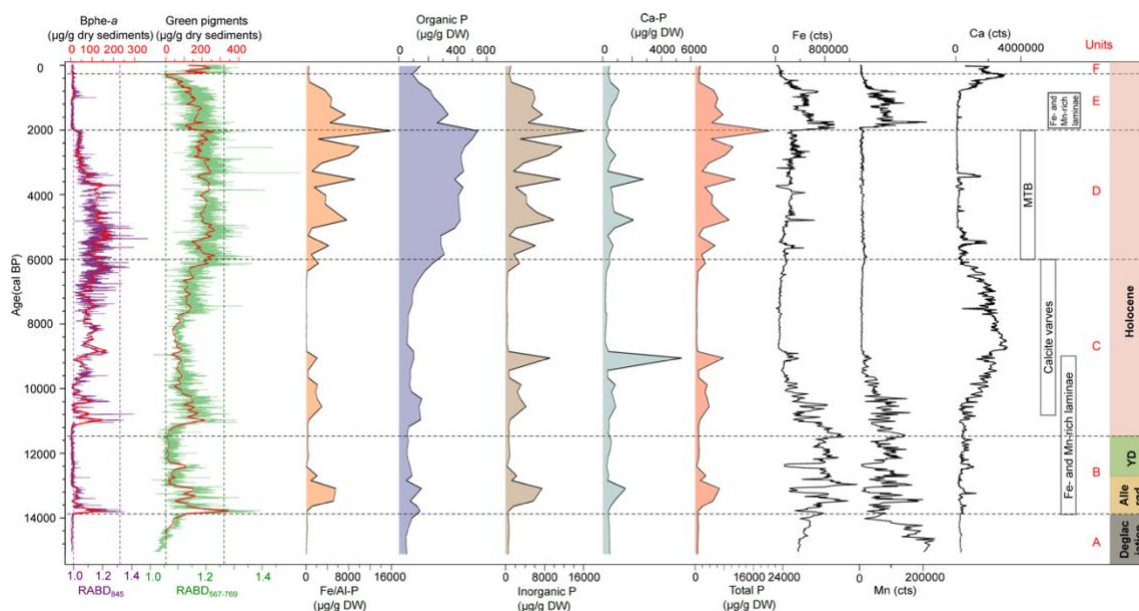


**Figure 5.2**: Time series of HSI-inferred pigment data, P fractions concentrations (µg g$^{-1}$ dry weight; DW and selected XRF data (Fe, Mn and Ca). For the pigment data, purple and green lines show the data at highest resolution (~75 µm) and red lines are 2-cm aggregate averages (267 samples). The vertical dashed lines represent the lower and upper limits of the calibration models (refer to Fig. S5.3 in the supplementary material). The appearance of Fe- and Mn-rich laminae (with siderite) and biogenic calcite varves in sediments was taken from Fischer (1996). MTB: Magnetotactic bacteria, detected by

Kind et al. (2012). The horizontal dashed grey lines separate the different units (A to F; Gierga et al. 2016). Note the different scales of the x-axes. (For interpretation of the references to color in this figure legend, the reader is referred to the web version of this article.)
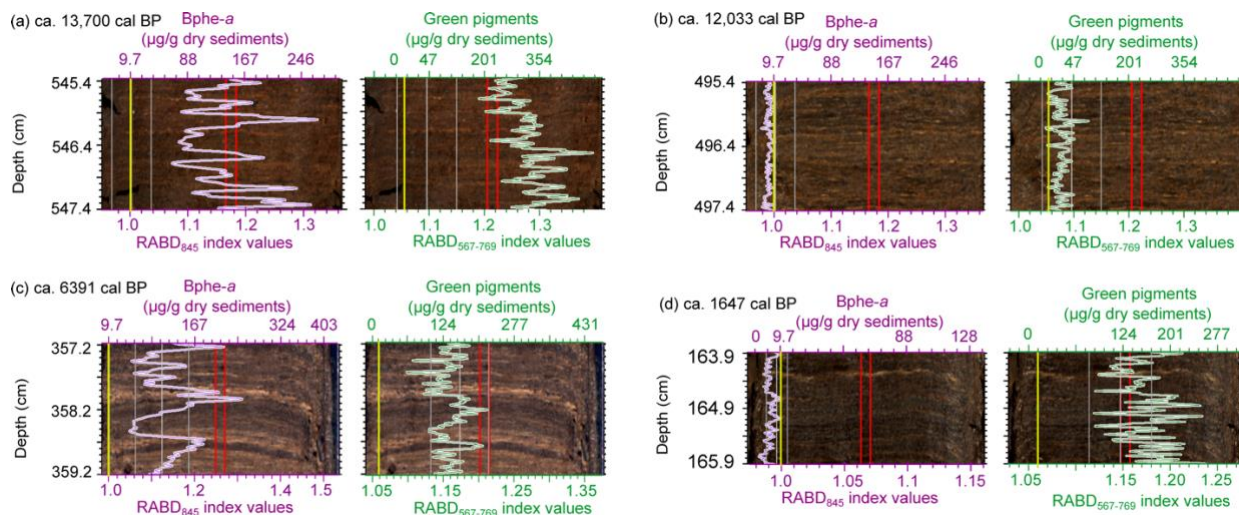


**Figure 5.3**: Example sections from four phases showing 2-cm sediment core sections (sediment depth of the composite core) covering approx. 40 years according to the age-depth model in Fig. 5.1c; variations of Bphe-*a* (in purple) and green pigments (in green) are shown with the spectral indices and the calibrated pigment concentrations at high resolution (~75 µm). For each image, the vertical red lines show the 2-mm wide window used for determining the spectral-index time series for the individual core section; the three grey lines represent the mean value and standard deviations of the two spectral indices for the entire sediment core; and the vertical yellow lines represent the lower limits of the calibration models. a) close-up section from the Allerød interstadial: this is a period with high lake primary production and high Bphe-*a* concentrations, indicating anoxia. b) close-up section from the Younger Dryas (YD), showing decreased lake primary production and almost absent Bphe-*a*, concurrent with Fe- and Mn-rich layers (Fischer, 1996), suggesting a seasonally mixed hypolimnion. c) close-up section from the mid-Holocene: showing high primary production and persistently high Bphe-*a* concentrations, which suggests strongly stratified conditions with anoxia or even meromixis. d) close–up section from the late Holocene, showing high lake production and low Bphe-*a* concentrations in Fe- and Mn-rich sediments, which suggests mostly a well oxygenated water column. The calibration model is valid for green pigments between 13.6 and 321.8 µg g$^{-1}$ dry sediments and for Bphe-*a* between 9.7 and 233.3 µg g$^{-1}$ dry sediments (see Fig. S5.3 in the supplementary material). (For interpretation of the references to color in this figure legend, the reader is referred to the web version of this article.)
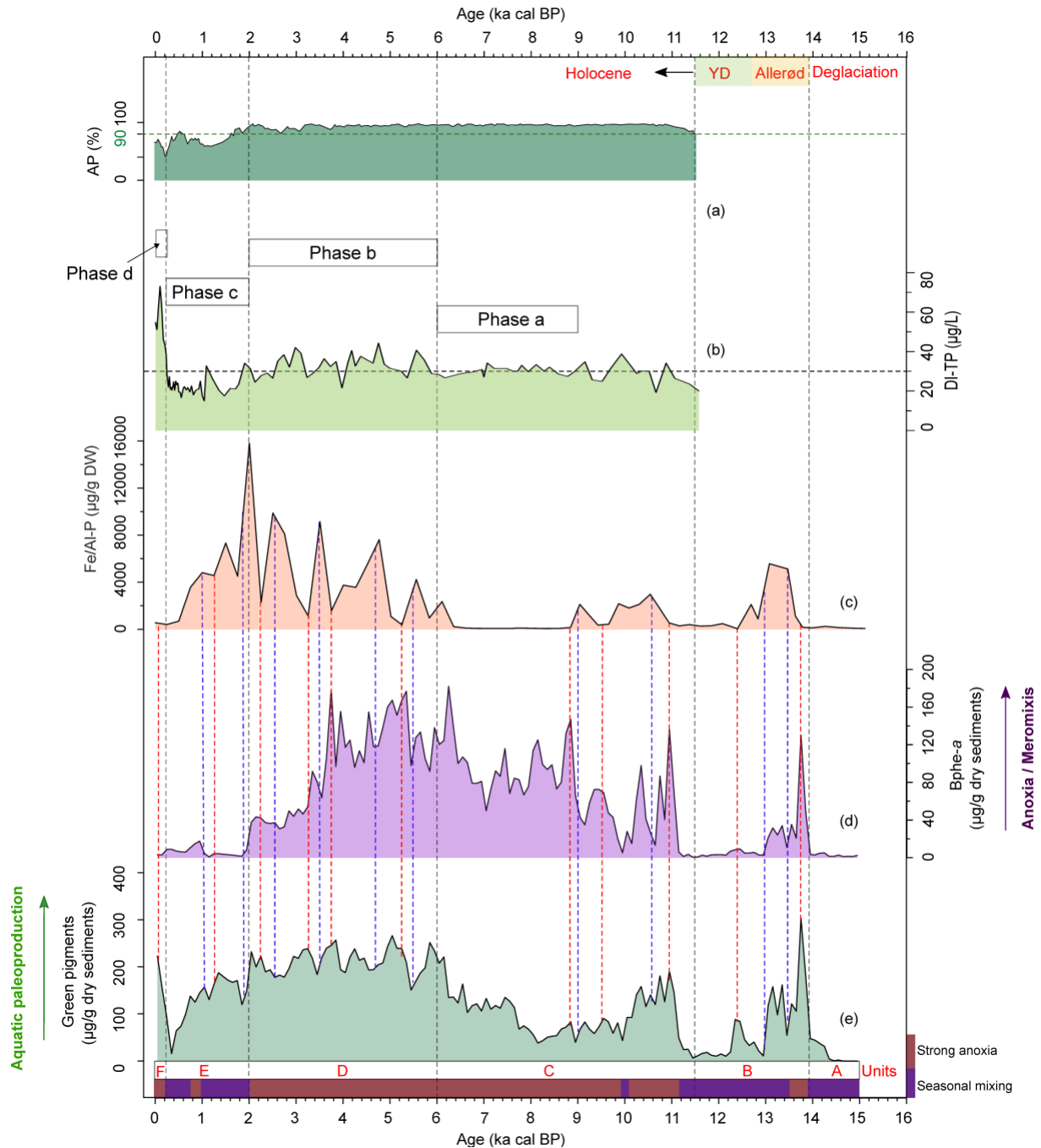
**Figure 5.4**: Comparison of millennial and centennial scale variations of Soppensee trophic status with sediment Fe/Al-P (labile P) data over the Late-glacial and Holocene. (a) Percentage of arboreal pollen (AP) including tree and shrub pollen (Lotter, 2001). (b) The diatom-inferred past epilimnetic total phosphorus (DI-TP) concentrations in Soppensee (Lotter, 2001); the dashed black line represents the mean value of the DI-TP record (30 µg L$^{-1}$). (c) Record of Fe/Al-P concentrations in sediments (µg g$^{-1}_{dry weight}$, DW). (d) The anoxia and (e) aquatic paleoproduction proxies are shown as 100-year running means. The yellow and green vertical bars at the top of the figure highlight the Late-glacial Allerød interstadial and the Younger Dryas (YD) cold period, respectively (according to Gierga et al. 2016). Phase a to Phase d refer to Fig. 5.5. In (c)-(e), dashed red (blue) lines mark relative maxima (minima) in lake paleoproduction/anoxia synchronously with relative minima (maxima) of Fe/Al-P in sediments.

(For interpretation of the references to color in this figure legend, the reader is referred to the web version of this article.)

In unit A, the deglaciation period (~15,115–13,800 cal BP; Gierga et al., 2016), green pigments and Bphe-*a* values remain at minimal levels, indicative of low lake primary production with a poorly stratified water column. High Mn counts (Fig. 5.2) imply a well-mixed water column; high Ti counts (Fig. S5.7) imply high quantities of lithogenic sediments. The values for the Fe/Al-P and all the other P fractions are very low.

In unit B (~13,800–11,500 cal BP), green pigments and Bphe-*a* values generally increase, as do concentrations of Fe/Al-P in sediments. The very beginning of unit B (~13,800–13,600 cal BP, latest part of the Allerød interstadial; Gierga et al. 2016) exhibits the first distinct peaks of green pigments and Bphe-*a* concentrations. This suggests substantially enhanced lake primary production and strongly stratified and anoxic conditions; Bphe-*a* values are well above the limit of quantification (9.7 µg g$^{-1}$ dry sediments) for more than 40 years, which in turn suggests strongly stratified and mostly anoxic, maybe even meromictic conditions (see example image Fig. 5.3a). Concurrently, Fe/Al-P concentrations in sediments remain low during the peak of the green pigments and Bphe-*a*. During the remainder of the Allerød interstadial (~13,600–12,700 cal BP), lake primary production is still relatively high; Bphe-*a* concentrations drop to substantially lower levels, yet counts of Fe and Mn are high, which suggests seasonally oxygenated bottom waters. In the same period, Fe/Al-P and total P concentrations in sediments increase sharply but then decrease to low values at the transition to the YD cold phase at ~12,700 cal BP. During the YD, Bphe-*a* is largely absent or close to the detection limit for several years (see example image Fig. 5.3b), indicating consistently good oxygenation of the hypolimnion. This is also confirmed by high Mn counts (Fig. 5.2). Lake paleoproduction in this phase is relatively low, except for a small peak at ~12,400 cal BP. Concurrently, low values of the Fe/Al-P are found throughout this period.

Unit C is characterized by relatively high Bphe-*a* and aquatic production, as well as overall increased values of all P fractions in the sediments (Fig. 5.2). At the onset of the early Holocene (~11,500–11,000 cal BP), green pigments and Bphe-*a* increase rapidly to a relative maximum between ~11,200 and ~11,000 cal BP, whereas the Fe/Al-P value is still low. Subsequently (11,000–9000 cal BP), lake primary production decreases slightly, yet Fe/Al-P values slightly increase. In the early Holocene (1,500–9000 cal BP), Bphe-*a* values are clearly higher, with multiple local peaks, indicating a strongly stratified water column and sustained anoxia in the hypolimnion for most of this period. This interpretation is supported by constantly declining Mn counts in this phase (Fig. 5.2), suggesting less frequent mixing of the bottom water. Slightly low but increasing DI-TP concentrations from ~11,500 cal BP to 9000 cal BP coincide with moderately low values of Fe/Al-P (Fig. 4b and c). The following early to mid-

Holocene (~9000–6000 cal BP) is characterized by relatively high and increasing lake primary production and constantly elevated Bphe-*a* concentrations. The example section from this period (Fig. 5.3c) shows high concentrations of Bphe-*a* above the detection limit for several years, which is indicative of a strongly stratified water column under mostly meromictic conditions. The persistent anoxia in the bottom water is further supported by very low Mn counts in this period (Fig. 5.2). In contrast to an increasing trend of lake paleoproduction (Fig. 5.4e) and higher DI-TP concentrations (Fig. 5.4b), Fe/Al-P values decline substantially and remain at minimal levels between ~9000 cal BP and 6000 cal BP (Fig. 5.4c).

In unit D, from the mid- to late-Holocene (~6000–2000 cal BP), aquatic production further increases and remains high (Fig. 5.2). High Bphe-*a* well above the detection limit occurs throughout most of this unit (Fig. 5.2), which indicates strongly stratified conditions with anoxia. This interpretation is confirmed by constantly low Mn counts in this period. Both DI-TP and, interestingly, Fe/Al-P records exhibit considerably increased and more variable values (Fig. 5.4b and 4c).

In unit E, from ~2000 to 200 cal BP, lake paleoproduction declines slowly, and Bphe-a remains at very low concentrations overall (Fig. 5.2). The example section from this period (Fig. 5.3d) displays that Bphe-*a* concentrations are close to the detection limit (~9.7 µg g$^{-1}$ dry sediments) for several years. This indicates the absence of a stable chemocline. The Fe- and Mn-rich laminae present in this phase (Fig. 5.2) most likely imply seasonal mixing of the water column with strong anoxia during the summer season. The decreased DI-TP concentrations are synchronous with relatively high but continuously decreasing Fe/Al-P values (Fig. 5.4b and 4c).

In the most recent 200 years (unit F), lake primary production considerably increased; Bphe-*a* concentrations stay at sustained minimal levels (Fig. 5.2), indicating the general absence of a persistent chemocline. However, Mn counts are very low in this period (Fig. 5.2), which still suggests seasonal hypolimnetic anoxia. DI-TP concentrations reach the highest levels, whereas sedimentary Fe/Al-P concentrations decrease to very low values.

### *Centennial-scale relationship between lake primary production and sediment labile-P data*

Over the past ~15,000 years and superposed on the long-term (multi)millennial trends, our results (Fig. 5.4c-4e) reveal, at the shorter-term (centennial) time scale, a commonly occurring inverse relationship between sediment Fe/Al-P concentrations and lake primary production and anoxia: in many, but not all cases, relative minima (maxima) in lake paleoproduction and anoxia tend to correspond to relative maxima (minima) of Fe/Al-P (dashed blue and red lines in Fig. 5.4). For example, during the Late-glacial period represented by unit B, enhanced lake

primary production with stronger anoxia at ~13,700 cal BP and ~12,400 cal BP coincides with relatively low values of Fe/Al-P (see dashed red lines). In contrast, lake primary production and anoxia indicators display decreased values at ~13,500 cal BP and 13,000 cal BP, which corresponds to local peaks of Fe/Al-P (see dashed blue lines). Similar observations can be made in other units during most of the Holocene, pointing to a negative relationship between paleoproduction, anoxia, and sedimentary Fe/Al-P at short (multidecadal to centennial) time scales.

### 5.1.6 Discussion

***Late-glacial and Holocene lake trophic evolution and anoxia history***

Here we present a Late-glacial and Holocene overview of aquatic production and anoxia in Soppensee reconstructed by HSI-inferred sedimentary pigments data. Diatom assemblages and pigment concentrations are two palaeolimnological indicators commonly used to infer past changes of lake trophic status (Davidson and Jeppesen, 2013). In Soppensee, DI-TP concentrations (Lotter, 2001) demonstrated mesotrophic to eutrophic conditions during most of the Holocene, suggesting that Soppensee is a naturally nutrient-rich lake. Our lake primary production record generally exhibits a pattern coherent with the DI-TP record throughout the Holocene (Fig. 5.4b and 4e). For example, both records show moderately high levels from 11,500 to 9,000 cal BP, very high levels from 6000 to 2000 cal BP, and decreased values from ~2000 to 200 cal BP. This coherence confirms that HSI-inferred green pigment data reliably capture epilimnetic aquatic production in Soppensee.

The green pigment record (Fig. 5.2) suggests that the lake primary production was relatively low before ~13,800 cal BP and in the YD cold phase (~12,700–11,500 cal BP), but underwent increasing nutrient enrichment during the Allerød interstadial (~13,800–12,700 cal BP) and for most of the Holocene. From ~8000 to ~3000 cal BP, early human impact was very limited and there is no evidence for strong human disturbance or extensive forest clearance in the catchment (Lotter, 1999; 2001); thus, the long-term eutrophication that Soppensee underwent during this time was mostly natural. Interestingly, the lake evolved into more eutrophic conditions (higher primary production and higher DI-TP) during warm climatic conditions e.g. in the Allerød interstadial and in the mid-Holocene after ~6000 cal BP. During the Allerød interstadial, chironomid-inferred summer temperature increased in Central Europe (Heiri, et al., 2015), and in the mid-Holocene, warm and humid climate conditions prevailed on the Swiss Plateau (Rey et al., 2020). These climate factors likely prolonged the growing season of lake phytoplankton and leached more nutrients from developing catchment soils into the lake, which then promoted natural eutrophication in Soppensee during these long warm phases. Between ~3000 and 200 cal BP, and especially from ~2000 to 200 cal BP, strong

human impact with intense land use occurred in the Soppensee catchment (Lotter, 1999), but less eutrophic conditions prevailed in Soppensee (Fig. 5.4e). Decreased aquatic production during the late Holocene has also been reported from Lake Łazduny and Lake Żabińskie in Poland (Sanchini et al., 2020; Zander et al., 2021). Late-Holocene climate cooling, particularly in summer (Davis et al., 2003), can partly explain this phenomenon. Since the 20th century, lake primary production has increased sharply as a result of cultural eutrophication (see green pigments record; Fig. 5.2). We attribute this observation to anthropogenic nutrient inputs from the catchment into the lake.

Under pre-anthropogenic conditions (here mainly before ~3000 cal BP), strong stratification and anoxic conditions in the hypolimnion (high Bphe-*a*; Fig. 5.2) tended to occur during times of higher lake primary production (high green pigments), for instance ~13, 800–13,600 cal BP and ~8000–4000 cal BP. Similar results (higher lake production causing stronger stratification and anoxia) have also been found in other small lakes in Europe, for example, Moossee in Switzerland (Makri et al., 2020a) and Lake Jaczno (Makri et al., 2020b) and Lake Żabińskie (Zander et al., 2021) in Poland. However, in all these examples closed forest cover around the small lakes was also found to be an important factor favoring long seasonal stratification and stable hypolimnetic anoxia (Makri et al., 2020a; Zander et al., 2021). This was also the case around Soppensee during the early to mid-Holocene (~9000–3000 cal BP), when the lake catchment was covered with dense closed forest (arboreal pollen AP > 90 %; Fig. 5.4a; Lotter, 1999) that reduced wind fetch, thus increasing lake anoxia. From ~2000 cal BP until recent centuries, weaker stratification with periodical oxygen mixing into the hypolimnion is suggested by constantly low Bphe-*a* concentrations (close to the detection limit; Fig. 5.3d) and Fe-and Mn-rich laminae (Fig. 5.2). Indeed, after ~2000 cal BP, better lake mixing can be seen as a result of intense forest clearance during Roman times and the Middle Ages (mostly AP < 80 %; Fig. 5.4a; Lotter, 2001) which increased wind-induced mixing of the water column. A similar process has been well studied in several small deep lakes of Europe e.g. Makri et al. (2020a), Sanchini et al. (2020), and Zander et al. (2021). During Modern Times, Mn counts in sediments of Soppensee are very low (Fig. 5.2), suggesting hypolimnetic anoxia. This confirms Gruber et al.'s (2000) finding that in recent times Soppensee is under holomictic conditions but has strong chemical stratification and persistent anoxia of the deep waters. However, Bphe-*a* values are very low at this time, which is likely explained by poor light conditions at the chemocline due to high algal productivity in the photic zone. Similar observations have been made in Moossee (Makri et al., 2020a; Switzerland) and Lake Żabińskie (Zander et al., 2021; Poland).

### *Estimating internal P loadings in response to lake trophic evolution*

Labile Fe/Al-P was the primary sedimentary P form for most of the Late-glacial and Holocene periods (Fig. S5.6a). In principle, this suggests a high potential of sediment-P release back to the water column in Soppensee's history. Tu et al.'s (2019) conceptual model implies that deep and eutrophic lakes tend to undergo bottom-water anoxia that increases internal recycling of sedimentary labile P forms (mainly Fe/Al-P fraction), referred to as internal P loadings, a positive feedback that sustains or even accelerates epilimnetic eutrophication. As a result, labile-P fraction retention in sediments is depleted because it is recycled back into the water column. We investigate the possibility of such positive feedback during long-term phases of natural eutrophication and evaluate whether Tu et al.'s (2019) conceptual model is valid for Soppensee's long-term Holocene record. For these purposes, the long-term qualitative internal P loadings in Soppensee are inferred by comparing the difference between the record of DI-TP concentrations, as a proxy for lake primary production, and sediment Fe/Al-P data (Fig. 5.4b, 4c and 4e). We hypothesize that higher DI-TP but depleted sediment Fe/Al-P demonstrates that internal P loadings operated as a positive feedback to sustain eutrophication. Fig. 5.5 outlines four distinct phases in a conceptual model that summarizes Fe/Al-P retention in sediments and internal P loadings in response to biogeochemical P cycling coupled with Fe, primary production, and anoxia since the early Holocene.
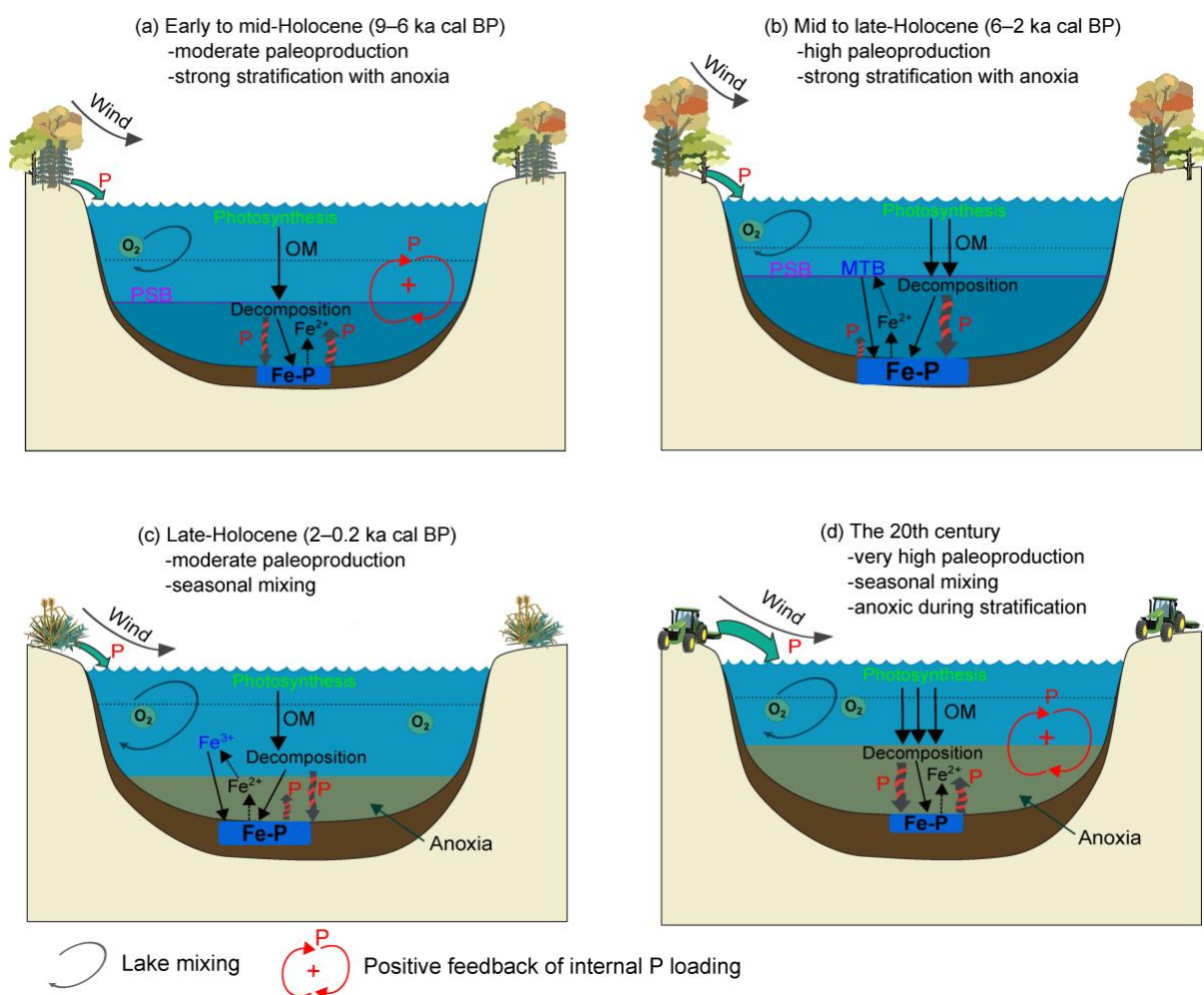
**Figure 5.5**: Conceptual model of four phases (a to d) of lake primary production, mixing regime, P cycling in a small deep eutrophic lake (like Soppensee) during the Holocene (Section 5.1.6). MTB: magnetotactic bacteria; PSB: purple sulfur bacteria; OM: organic matter. Note that, overall, the illustrated sizes of Fe/Al-P among different phases indicate the relative amounts of Fe/Al-P in sediments; the bottom-water (brown-green color) in (c)-(d) represents anoxia during seasonal stratifications. Parts of the symbols for this figure were taken from Symbols courtesy of the Integration and Application Network (ian.umces.edu/symbols/). (For interpretation of the references to color in this figure legend, the reader is referred to the web version of this article.)

We infer largely high internal P loadings to be a positive feedback of eutrophication arising from high lake primary production from the early to mid-Holocene (~9000–6000 cal BP; Phase a in Fig. 5.5). This is the long period in which we observe high DI-TP levels in comparison to notably low values of Fe/Al-P (Fig. 5.4b and 4c). This pattern suggests mobilization of large amounts of internal P loads from labile Fe/Al-P to sustain aquatic production in the photic zone. In Phase a (~9000–6000 cal BP; Fig. 5.5a), the lake had strongly stratified and anoxic conditions, as indicated by persistently high Bphe-*a* (Fig. 5.4d). Bottom-water anoxia during

times of eutrophication is expected to cause large internal P cycling of Fe/Al-P from the sediments (Burley et al., 2001; Tu et al., 2019) and thus depleted the Fe/Al-P in sediments (Fig. 5.5a). This interpretation supports Tu et al.'s (2019) conceptual model.

Interestingly, during the mid- to late Holocene period (~6000–2000 cal BP, Phase b Fig 5.5) both DI-TP levels and sedimentary Fe/Al-P values are very high (Fig. 5.4b and 4c) which does not follow Tu et al.'s (2019) model. Generally, we interpret this period as one of limited sediment-P release into surface waters; thus, internal P loadings might not have operated as the positive feedback of eutrophication (see Phase b in Fig. 5.5), although Soppensee was strongly stratified with anoxia (Fig. 5.4d). During this period, ferromagnetic minerals (e.g., magnetite and hematite, magnetofossils) produced by magnetotactic bacteria (MTB) were found in Soppensee sediments (Kind et al., 2012), which might explain the high burial rates and high amounts of sedimentary Fe/Al-P at this time (Fig. S5.8 in the supplementary material and Fig. 5.2). MTB live around the chemocline, and colonization in the water column is favored by persistent stratification and high epilimnetic P concentrations (Paasche et al., 2004). From ~6000 to 2000 cal BP, high DI-TP levels and stratified, anoxic conditions in Soppensee largely promoted the growth of MTB. These MTB have been shown to be preserved as pure or oxidized magnetite minerals in Soppensee sediments (Kind et al., 2012). Paasche and Larsen (2010) and Rivas-Lamelo et al. (2017) revealed that MTB-produced Fe oxyhydroxides in lake sediments can escape from sulfidization and progressive reductive dissolution and, ultimately, be better preserved together with P accumulation in reductive sediments. This mechanism, in the long term, reduced internal P loadings by lowering P release from sedimentary Fe/Al-P (Phase b in Fig. 5.5), which is different from Phase a (Fig. 5.5). As a result, very high amounts of Fe/Al-P were preserved in sediments during this period. However, throughout this time, the short-term (centennial-scale; dashed red and blue lines in Fig. 4.4c and 4e) inverse relationship between lake paleoproduction and sediment Fe/Al-P records still held true overall. Apparently, the positive feedback between paleoproduction, anoxia, and internal P cycling, and sustained eutrophication still played a subordinate role in shorter terms, but the long-term Fe/Al-P trends in the sediment were largely controlled by MTB between 6000–2000 cal BP. Thus, Tu et al.'s (2019) model needs to be expanded and modified to account for the presence of MTB (Phase b; Fig. 5.5).

The phase of the late Holocene (~2000–200 cal BP; Phase c in Fig. 5.5) is noticeable for generally decreased DI-TP concentrations but relatively high Fe/Al-P values (Fig. 5.4b and 4c), suggesting decreased internal P loadings. Sediments of this phase are marked by the occurrence of Fe- and Mn-rich laminae (Fig. 5.2; Fischer, 1996). The pale-brown Fe- and Mn-rich laminae are commonly formed in holomictic temperate lakes with seasonal anoxia (Zolitschka et al., 2015), where bottom waters are seasonally oxygenated (van Raden, 2012).

This notion agrees well with the better mixed and less stratified water column in Soppensee at this time. Previous research has demonstrated that Fe-oxide layers can reduce internal P loadings by hindering P release from anoxic surface sediments and favor permanent P trapping and P sequestration in sediments (Zarczynski et al., 2019). Such a process very likely led to lower internal P loadings between ~2000 and 200 cal BP, resulting in high amounts of Fe/Al-P preserved in sediments (Phase c in Fig. 5.5). In addition, the inverse relationship between lake primary production and sediment Fe/Al-P record on centennial time scales is not clearly observable between ~2000 and 200 cal BP (Fig. 5.4c and 4e). Therefore, on both long and short time scales, internal P loadings may not have operated as the positive feedback in this phase.

In the most recent 200 years (Phase d in Fig. 5.5), we infer high internal P loadings to be the positive feedback that sustains cultural eutrophication in Soppensee, which can be seen from high water P levels (Fig. 5.4b) and severe hypolimnetic anoxia (indicated by very low Mn counts; Fig. 5.2) in comparison with depleted Fe/Al-P in sediments (Fig. 5.4c). Given this, the pattern of Phase d is very similar to that of Phase a (Fig. 5.5) discussed above, and thus also supports Tu et al.'s (2019) conceptual model.

Due to the lack of preserved diatoms, DI-TP values are not available for the Late-glacial period (Allerød and YD). However, the frequent inverse correlation between paleoproduction and anoxia with Fe/Al-P during the Allerød and the beginning of the YD (Fig. 5.4c-4e) suggests that a mechanism of strong internal P cycling, depleted Fe/Al-P in sediments, and sustained primary production (with related anoxia) also operated in the Allerød interstadial. By contrast, for most of the YD cold phase, better oxygenation of bottom waters, together with low aquatic production and Fe/Al-P (Fig. 5.4c-4e), demonstrates low amounts of internal P cycling into surface waters to promote aquatic production. After the transition of the YD to the Holocene (~11,500–9000 cal BP), DI-TP concentrations were comparatively low while Fe/Al-P values were moderately low but increased slightly compared with the YD (Fig. 5.4b and 4c). This period is characterized by Fe- and Mn-enriched layers in sediments (Fig. 5.2; Fischer, 1996), suggesting a seasonal mixing of the water column and very likely lower internal P loadings in the long term, a pattern similar to Phase c (~2000–200 cal BP; Fig. 5.5) discussed above. Nonetheless, Fe/Al-P values in this period were lower than in Phase c (Fig. 5.4c), which may have resulted from more intense internal P cycling from Fe/Al-P in response to the strongly stratified water column during most of the period from 11,500 cal BP to 9000 cal BP (higher Bphe-*a* values; Fig. 5.4d). Between ~11,500 and 9000 cal BP, on centennial time scales, the inverse relationship of paleoproduction and anoxia with Fe/Al-P (Fig. 5.4c-4e) mostly demonstrates internal P loadings operating as the positive feedback.

We note that our core was taken from the deepest part of the lake, where the sediment P records might not comprehensively reflect the overall P dynamics, burial rates, and releases in the lake. Horizontal variations and geochemical focusing (Schaller and Wehrli, 1996) in the sedimentary P concentrations must be considered. Because of vertical variations of the redox front and horizontal mixing, P sedimentation, net burial rates, and cycling are likely quite different in shallower and in deeper parts of the lake. Sediments from shallower parts of the lake tend to have better oxygen conditions than those in the deepest parts (at least seasonally; Schaller and Wehrli, 1996), potentially causing less sediment P release into the photic zone and better P trapping. It is possible that in Soppensee, internal P loadings as we infer from the core at the deepest part of the lake are overall overestimated and could have been balanced to some extent by higher P sedimentation and net burials in the shallower parts of the lake. Thus, these changes overall would not substantially influence P levels in the epilimnion, where planktonic diatoms live. Therefore, inferences of sedimentary P records from cores at the deepest parts of the lake should be interpreted with caution; they might not show the full picture of the lake. Further work on horizontal distribution patterns (geochemical focusing) of sedimentary P fractions from short cores across a water-depth gradient may provide important insights into whole-lake P dynamics and mass-balance modeling in deep lakes.

### 5.1.7 Conclusion

We propose that internal P loadings have played an important role in the long-term natural eutrophication of stratified deep lakes such as Soppensee during the Late-glacial and Holocene periods. The increased internal P loadings as a positive feedback of eutrophication and related anoxia were inferred in Soppensee from the early to mid-Holocene (~9000–6000 cal BP) under natural conditions and during the most recent 200 years of cultural eutrophication. However, strong recycling and depletion of labile P fractions in the sediment was not observed in other long phases of high aquatic production and anoxia. Fe-rich minerals (magnetofossils) produced by magnetotactic bacteria (MTB) and Fe-rich laminae preserved in anoxic sediments potentially reduced internal P loadings despite high eutrophication between 6000 and 200 cal BP. Our study implies that the presence of (bacterially-mediated) endogenous Fe-minerals restricting P recycling and bioavailability should be considered in conceptual models of biogeochemical P cycling on long-term (multi)millennial timescales in deep stratified eutrophic lakes. This presence helps potentially enhance P removal from the water and decrease internal P loadings in lakes, an implication for the present-day eutrophication management. In future studies, it will be important to assess further related microbially mediated processes that contribute to the P cycle in similar environments.

### 5.1.8 Data availability

The data will be available at Mendeley Data Repository.

### 5.1.9 Credit author statement

### 5.1.10 Declaration of competing interest

None.

### 5.1.11 Acknowledgements

### 5.1.12 Reference

Amann, B., Lobsiger, S., Fischer, D., Tylmann, W., Bonk, A., Filipiak, J., Grosjean, M., 2014. Spring temperature variability and eutrophication history inferred from sedimentary pigments in the varved sediments of Lake Żabińskie, north-eastern Poland, AD 1907–2008. Global and Planetary Change 123, 86–96. https://doi.org/10.1016/j.gloplacha.2014.10.008

Burley, K.L., Prepas, E.E., Chambers, P.A., 2001. Phosphorus release from sediments in hardwater eutrophic lakes: the effects of redox-sensitive and-insensitive chemical treatments. Freshwater Biology 46, 1061–1074. https://doi.org/10.1046/j.1365-2427.2001.00789.x

Butz, C., Grosjean, M., Fischer, D., Wunderle, S., Tylmann, W., Rein, B., 2015. Hyperspectral imaging spectroscopy: a promising method for the biogeochemical analysis of lake sediments. Journal of Applied Remote Sensing 9, 096031. https://doi.org/10.1007/s10933-017-9955-1

Butz, C., Grosjean, M., Poraj-Górska, A., Enters, D., Tylmann, W., 2016. Sedimentary Bacteriopheophytin a as an indicator of meromixis in varved lake sediments of Lake Jaczno, north-east Poland, CE 1891–2010. Global and Planetary Change 144, 109–118. https://doi.org/10.1016/j.gloplacha.2016.07.012

Cyr, H., McCabe, S.K., Nurnberg, G.K., 2009. Phosphorus sorption experiments and the potential for internal phosphorus loading in littoral areas of a stratified lake. Water Research 43, 1654–1666. https://doi.org/10.1016/j.watres.2008.12.050

Davidson, T.A. and Jeppesen, E., 2013. The role of palaeolimnology in assessing eutrophication and its impact on lakes. Journal of Paleolimnology 49, 391–410. https://doi.org/10.1007/s10933-012-9651-0

Fiedor, J., Fiedor, L., Kammhuber, N., Scherz, A., Scheer, H., 2002. Photodynamics of the Bacteriochlorophyll–Carotenoid System. 2. Influence of Central Metal, Solvent and β-Carotene on Photobleaching of Bacteriochlorophyll Derivatives. Photochemistry and Photobiology 76, 145–152. https://doi.org/10.1562/0031-8655(2002)076<0145:POTBCS>2.0.CO;2

Fischer, A., 1996. Isotopengeochemische Untersuchungen (δ18O und δ13C) im Wasser und in den Sedimenten des Soppensees (Kt. Luzern, Schweiz). Ph.D. Thesis, ETH, Zürich, pp.184.

Gao, L., Zhou, J.M., Yang, H., Chen, J., 2005. Phosphorus fractions in sediment profiles and their potential contributions to eutrophication in Dianchi Lake. Environmental Geology 48, 835–844. https://doi.org/10.1007/s00254-005-0005-3

Gierga, M., Hajdas, I., van Raden, U.J., Gilli, A., Wacker, L., Sturm, M., Bernasconi, S.M., Smittenberg, R.H., 2016. Long-stored soil carbon released by prehistoric land use: evidence from compound-specific radiocarbon analysis on Soppensee lake sediments. Quaternary Science Reviews 144, 123–131. https://doi.org/10.1016/j.quascirev.2016.05.011

Gruber, N., Wehrli, B., Wüest, A., 2000. The role of biogeochemical cycling for the formation and preservation of varved sediments in Soppensee (Switzerland). Journal of Paleolimnology 24, 277–291. https://doi.org/10.1023/A:1008195604287

Hajdas, I., Michczyński, A., 2010. Age-depth model of Lake Soppensee (Switzerland) based on the high-resolution 14C chronology compared with varve chronology. Radiocarbon 52, 1027–1040. https://doi.org/10.1017/S0033822200046117

Heiri, O., Ilyashuk, B., Millet, L., Samartin, S., Lotter, A.F., 2015. Stacking of discontinuous regional palaeoclimate records: chironomid-based summer temperatures from the Alpine region. The Holocene 25, 137–149. https://doi.org/10.1177/0959683614556382

Hofmann, W., 2001. Late-Glacial/Holocene succession of the chironomid and cladoceran fauna of the Soppensee (Central Switzerland). Journal of Paleolimnology 25, 411–420. https://doi.org/10.1023/A:1011103820283

Jeffrey, S.t., Humphrey, G., 1975. New spectrophotometric equations for determining chlorophylls a, b, c1 and c2 in higher plants, algae and natural phytoplankton. Biochemie und physiologie der pflanzen 167, 191-–194. https://doi.org/10.1016/S0015-3796(17)30778-3

Kapanen, G., 2008. Phosphorus fractionation in lake sediments. Estonian Journal of Ecology 57, 244–255. doi: 10.3176/eco.2008.4.02

Katsev, S., Dittrich, M., 2013. Modeling of decadal scale phosphorus retention in lake sediment under varying redox conditions. Ecological Modelling 251, 246–259. https://doi.org/10.1016/j.ecolmodel.2012.12.008

Kind, J., Raden, U.J.v., García-Rubio, I., Gehring, A.U., 2012. Rock magnetic techniques complemented by ferromagnetic resonance spectroscopy to analyse a sediment record. Geophysical Journal International 191, 51–63. https://doi.org/10.1111/j.1365-246X.2012.05620.x

Kirilova, E., Heiri, O., Enters, D., Cremer, H., Lotter, A.F., Zolitschka, B., Huebener, T., 2009. Climate-induced changes in the trophic status of a Central European lake. Journal of Limnology 68, 71–82. https://doi.org/10.4081/jlimnol.2009.71

Langenegger, T., Vachon, D., Donis, D., McGinnis, D.F., 2019. What the bubble knows: Lake methane dynamics revealed by sediment gas bubble composition. Limnology and Oceanography 64, 1526–1544. https://doi.org/10.1002/lno.11133

Lepori, F., Roberts, J.J., 2017. Effects of internal phosphorus loadings and food-web structure on the recovery of a deep lake from eutrophication. Journal of Great Lakes Research 43, 255–264. https://doi.org/10.1016/j.jglr.2017.01.008

Lotter, A.F., 1989. Evidence of annual layering in Holocene sediments of Soppensee, Switzerland. Aquatic Sciences 51, 19–30. https://doi.org/10.1007/BF00877778

Lotter, A.F., 1999. Late-glacial and Holocene vegetation history and dynamics as shown by pollen and plant macrofossil analyses in annually laminated sediments from Soppensee, central Switzerland. Vegetation History and Archaeobotany 8, 165–184. https://doi.org/10.1007/BF02342718

Lotter, A.F., 2001. The palaeolimnology of Soppensee (Central Switzerlabnd), as evidenced by diatom, pollen, and fossil-pigment analyses. Journal of Paleolimnology 25, 65–79. https://doi.org/10.1023/A:1008140122230

Makri, S., Rey, F., Gobet, E., Gilli, A., Tinner, W., Grosjean, M., 2020a. Early human impact in a 15,000-year high-resolution hyperspectral imaging record of paleoproduction and anoxia from a varved lake in Switzerland. Quaternary Science Reviews 239, 106335. https://doi.org/10.1016/j.quascirev.2020.106335

Makri, S., Lami, A., Tu, L., Tylmann, W., Vogel, H., Grosjean, M., 2020b. Holocene phototrophic community and anoxia dynamics in meromictic Lake Jaczno (NE Poland) using high-resolution hyperspectral imaging and HPLC data. Biogeosciences Discussions, 1–28. https://doi.org/10.5194/bg-2020-362

Müller, B., Lotter, A.F., Sturm, M., Ammann, A., 1998. Influence of catchment quality and altitude on the water and sediment composition of 68 small lakes in Central Europe. Aquatic Sciences 60, 316–337. https://doi.org/10.1007/s000270050044

Nurnberg, G.K., Fischer, R., Paterson, A.M., 2018. Reduced phosphorus retention by anoxic bottom sediments after the remediation of an industrial acidified lake area: Indications from P, Al, and Fe sediment fractions. Science of the Total Environment 626, 412–422. https://doi.org/10.1016/j.scitotenv.2018.01.103

Ohno, T., Zibilske, L.M., 1991. Determination of low concentrations of phosphorus in soil extracts using malachite green. Soil Science Society of America Journal 55, 892–895. https://doi.org/10.2136/sssaj1991.03615995005500030046x

Orihel, D.M., Baulch, H.M., Casson, N.J., North, R.L., Parsons, C.T., Seckar, D.C., Venkiteswaran, J.J., 2017. Internal phosphorus loading in Canadian fresh waters: a critical review and data analysis. Canadian Journal of Fisheries and Aquatic Sciences 74, 2005–2029. https://doi.org/10.1139/cjfas-2016-0500

Paasche, Ø., Larsen, J., 2010. Changes in lake stratification and oxygen distribution inferred from two contrasting records of magnetotactic bacteria and diatoms. Journal of Geophysical Research: Biogeosciences 115, G02012. https://doi.org/10.1029/2009JG001081

Paasche, Ø., Løvlie, R., Dahl, S.O., Bakke, J., Nesje, A., 2004. Bacterial magnetite in lake sediments: late glacial to Holocene climate and sedimentary changes in northern Norway. Earth and Planetary Science Letters 223, 319–333. https://doi.org/10.1016/j.epsl.2004.05.001

Paerl, H.W., 1988. Nuisance phytoplankton blooms in coastal, estuarine, and inland waters 1. Limnology and Oceanography 33, 823–843. https://doi.org/10.4319/lo.1988.33.4part2.0823

Rey, F., Gobet, E., Schwörer, C., Hafner, A., Szidat, S.,Tinner, W., 2020. Climate impacts on vegetation and fire dynamics since the last deglaciation at Moossee (Switzerland), Climate of the Past 16, 1347–1367. https://doi.org/10.5194/cp-16-1347-2020

Rivas-Lamelo, S., Benzerara, K., Lefèvre, C.T., Monteil, C.L., Jézéquel, D., Menguy, N., Viollier, E., Guyot, F., Férard, C., Poinsot, M., Skouri-Panet, F., Trcera, N., Miot, J., Duprat, E., 2017. Magnetotactic bacteria as a new model for P sequestration in the ferruginous Lake Pavin. Geochemical Perspectives Letters 5, 35–41. doi: 10.7185/geochemlet.1743

Ruban, V., Brigault, S., Demare, D., Philippe, A.-M., 1999. An investigation of the origin and mobility of phosphorus in freshwater sediments from Bort-Les-Orgues Reservoir, France. Journal of Environmental Monitoring 1, 403–407. https://doi.org/10.1039/A902269D

Ruban, V., Lopez-Sanchez, J.F., Pardo, P., Rauret, G., Muntau, H., Quevauviller, P., 2001. Development of a harmonised phosphorus extraction procedure and certification of a sediment reference material. Journal of Environmental Monitoring 3, 121–125. https://doi.org/10.1039/B005672N

Schaller, T. and Wehrli, B., 1996. Geochemical-focusing of manganese in lake sediments—an indicator of deep-water oxygen conditions. Aquatic Geochemistry 2, 359–378. https://doi.org/10.1007/BF00115977

Schneider, T., Rimer, D., Butz, C., Grosjean, M., 2018. A high-resolution pigment and productivity record from the varved Ponte Tresa basin (Lake Lugano, Switzerland) since 1919: insight from an approach that combines hyperspectral imaging and high-performance liquid chromatography. Journal of Paleolimnology 60, 381–398. https://doi.org/10.1007/s10933-018-0028-x

Schnurrenberger, D., Russell, J., Kelts, K., 2003. Core description Classification of lacustrine sediments based on sedimentary components. Journal of Paleolimnology 29, 141–154. https://doi.org/10.1023/A:1023270324800

Søndergaard, M., Jensen, P.J., Jeppesen, E., 2001. Retention and internal loading of phosphorus in shallow, eutrophic lakes. The Scientific World Journal 1, 427–442. https://doi.org/10.1100/tsw.2001.72

Steinsberger, T., Schmid, M., Wüest, A., Schwefel, R., Wehrli, B., Müller, B., 2017. Organic carbon mass accumulation rate regulates the flux of reduced substances from the sediments of deep lakes. Biogeosciences 14, 3275–3285. https://doi.org/10.5194/bg-14-3275-2017

Straile, D., Jöhnk, K., Henno, R., 2003. Complex effects of winter warming on the physicochemical characteristics of a deep lake. Limnology and oceanography 48, 1432-1438. https://doi.org/10.4319/lo.2003.48.4.1432

Tu, L., Jarosch, K.A., Schneider, T., Grosjean, M., 2019. Phosphorus fractions in sediments and their relevance for historical lake eutrophication in the Ponte Tresa basin (Lake Lugano, Switzerland) since 1959. Science of the Total Environment 685, 806–817. https://doi.org/10.1016/j.scitotenv.2019.06.243

Tu, L., Zander, P., Szidat, S., Lloren, R., Grosjean, M., 2020. The influences of historic lake trophy and mixing regime changes on long-term phosphorus fraction retention in sediments of deep eutrophic lakes: a case study from Lake Burgäschi, Switzerland. Biogeosciences 17, 2715–2729. https://doi.org/10.5194/bg-17-2715-2020

van Raden, U.J., 2012. High-resolution swiss lake records of climate change. Ph.D. Thesis, ETH, Zürich, Nr 20596, https://doi.org/10.3929/ethz-a-009783578.

Williams, J., Jaquet, J., Thomas, R., 1976. Forms of phosphorus in the surficial sediments of Lake Erie. Journal of the Fisheries Board of Canada 33, 413–429. https://doi.org/10.1139/f76-063

Worsfold, P., McKelvie, I., Monbet, P., 2016. Determination of phosphorus in natural waters: A historical review. Analytica Chimica Acta 918, 8–20. https://doi.org/10.1016/j.aca.2016.02.047

Zander, P.D., Żarczyński, M., Vogel, H., Tylmann, W., Wacnik, A., Sanchini, A., Grosjean, M., 2021. A high-resolution record of Holocene primary productivity and water-column mixing from the varved sediments of Lake Żabińskie, Poland. Science of the Total Environment 755, 143713. https://doi.org/10.1016/j.scitotenv.2020.143713

Zarczynski, M., Wacnik, A., Tylmann, W., 2019. Tracing lake mixing and oxygenation regime using the Fe/Mn ratio in varved sediments: 2000year-long record of human-induced changes from Lake Zabinskie (NE Poland). Science of The Total Environment 657, 585–596. https://doi.org/10.1016/j.scitotenv.2018.12.078

## 5.2 Supplementary materials

**Table S5.1**: List of the stratigraphic correlation depths between the So08-3 core (this study) and the So08-01/2 core from van Raden (2012) and the ages of the correlation depths. The numbers in the first column correspond to numbers of Figure S5.1.

| Correlation points No. in Figure S2 | So08-3 sediment depth (cm) | So08-01/2 sediment depth (cm) | Mean age at depth (cal. BP) |
|---|---|---|---|
| 1 | 27.3 | 30.2 | 197 |
| 2 | 54.3 | 45.3 | 303 |
| 3 | 76.1 | 69.2 | 467 |
| 4 | 80.1 | 74.9 | 505 |
| 5 | 100.1 | 92.1 | 617 |
| 6 | 109.6 | 97.3 | 652 |
| 7 | 120.1 | 106.7 | 713 |
| 8 | 123.1 | 108.2 | 723 |
| 9 | 126.6 | 114.5 | 808 |
| 10 | 130.1 | 119.1 | 886 |
| 11 | 135.1 | 124.3 | 972 |
| 12 | 153.1 | 142.0 | 1264 |
| 13 | 166.6 | 168.5 | 1702 |
| 14 | 182.8 | 182.6 | 1933 |
| 15 | 193.8 | 191.9 | 2088 |
| 16 | 199.8 | 201.3 | 2242 |
| 17 | 204.3 | 205.5 | 2311 |
| 18 | 229.2 | 226.8 | 2663 |
| 19 | 240.7 | 237.2 | 2835 |

| | | | |
|---|---|---|---|
| 20 | 262.7 | 256.4 | 3199 |
| 21 | 281.7 | 277.2 | 3719 |
| 22 | 288.7 | 301.7 | 4331 |
| 23 | 301.7 | 320.9 | 4828 |
| 24 | 323.3 | 337.0 | 5459 |
| 25 | 333.3 | 346.4 | 5647 |
| 26 | 346.7 | 362.0 | 5959 |
| 27 | 361.8 | 379.6 | 6525 |
| 28 | 376.3 | 394.3 | 7044 |
| 29 | 421.2 | 454.5 | 8771 |
| 30 | 435.7 | 466.5 | 9220 |
| 31 | 453.8 | 486.8 | 10,188 |
| 32 | 464.7 | 496.1 | 10,644 |
| 33 | 480.9 | 514.3 | 11,494 |
| 34 | 491.9 | 521.6 | 11,898 |
| 35 | 500.9 | 526.8 | 12,201 |
| 36 | 513.9 | 537.7 | 12,673 |
| 37 | 524.4 | 542.4 | 12,907 |
| 38 | 535.9 | 554.9 | 13,355 |
| 39 | 548.9 | 564.3 | 13,849 |
| 40 | 554.4 | 570.0 | 14,318 |
| 41 | 560.9 | 574.7 | 14,701 |
| 42 | 563.4 | 578.8 | 15,043 |

**Table S5.2**: Analytical results obtained from the certified reference material BCR-684 using the SMT extraction protocol.

|  | Certified values (mg/kg)[a] | Measured values (mg/kg)[b] | Recovery (%) |
|---|---|---|---|
| Total P | 1373 ±35 | 1344±73 | 97.9 |
| Inorganic P | 1113 ± 24 | 1038±12 | 93.3 |
| Organic P | 209 ± 9 | 169±4 | 80.8 |
| Non-apatite inorganic P | 550 ± 21 | 551±9 | 100.1 |
| Apatite P | 536 ± 28 | 482±12 | 90 |

[a] Certified values are expressed as mean value ± confidence interval (P=0.05)

[b] Experimental results are expressed as mean value of three replicates ± one standard deviation

*Quality control of the applied extraction procedure*

Table S5.2 shows that the analytical results are in good agreement with the certified contents, giving recovery percentages ranging from 93% to 100% for total P, inorganic P, and Fe/Al-P fractions. The recovery rates are ~81% and 90 % for organic P and Ca-P, respectively. The underestimates of these two P fractions might have three causes: i) P may be lost from solid samples when the residue is rinsed, and the supernatant is transferred. ii) A small part of organic P may be lost after calcination, although the crucible is rinsed carefully. iii) It is possible that not all organic P and apatite-P is extracted when 1 M HCl is added. Despite these limitations, the results indicate that large proportions of sediment organic P and Ca-P fractions were extracted with the procedure applied. Total P, potentially bioavailable P (Fe/Al-P), and inorganic P fractions in the sediment samples can be accurately determined with this procedure.
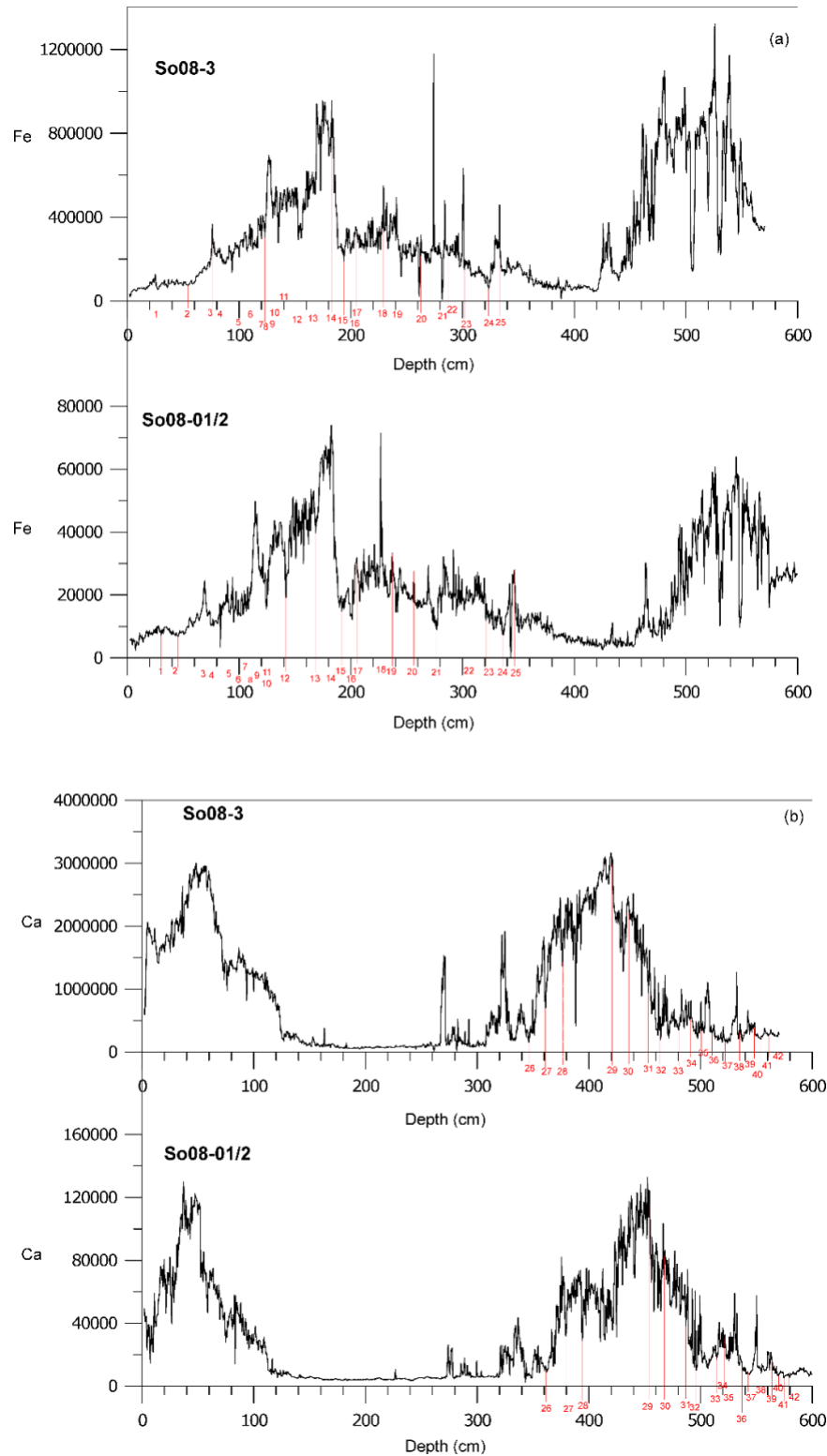
**Figure S5.1**: Chronostratigraphic correlation of the So08-3 core (this study) with the well-dated core So08-1/2 of van Raden (2012). We use, besides diagnostic marker layers, color and texture also XRF-Fe counts in the upper part (Fig. S5.1a) and XRF-Ca counts in the lower part of the core (Fig. S5.1b). The 42 identified tie points (red-color numbers) enable the dating of So08-3 core using the chronology of So08-01/2 core. The corresponding depths of tie points are shown in Table S1. Ages between the tie points were linearly interpolated.
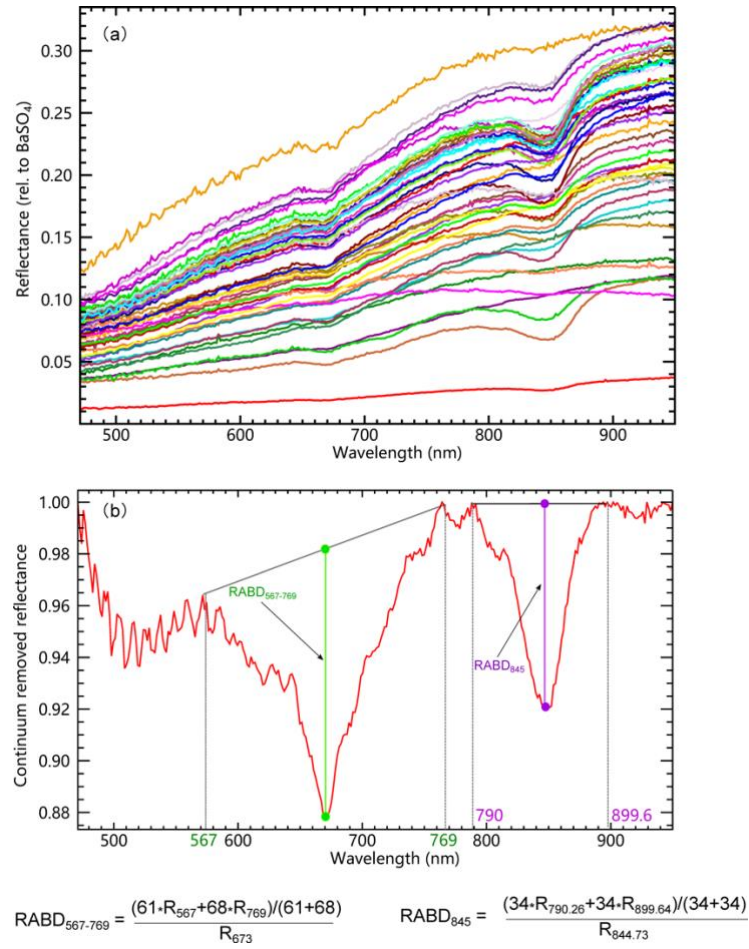
$$RABD_{567\text{-}769} = \frac{(61 \cdot R_{567} + 68 \cdot R_{769})/(61+68)}{R_{673}} \qquad RABD_{845} = \frac{(34 \cdot R_{790.26} + 34 \cdot R_{899.64})/(34+34)}{R_{844.73}}$$

**Figure S5.2**: (a) Spectral endmembers derived from the ENVI Spectral Hourglass Wizard; (b) Continuum removed mean spectrum of these spectral endmembers, indicating the relative absorption band depth (RABD) for the absorption band minima (here for a local trough minimum at 673 nm) between 567 and 769 nm, and at 845 nm. The calculation formulas of the spectral indices $RABD_{567\text{-}769}$ (e.g. for a trough minimum at R673, according to Schneider et al., 2018) and $RABD_{845}$ (according to Butz et al., 2016) are shown.

### Hyperspectral indices: proxy-proxy calibration

Fig. S5.3a shows the calibration model for 27 $RABD_{567-769}$ values compared with absolute green pigments concentrations as measured with a Shimadzu UV-1800 spectrometer. The model has a strong linear correlation ($R_{Pearson}$ = 0.92, $R^2$ = 0.84). The root mean squared error of prediction (RMSEP) calculated using tenfold, leave-one-out and bootstrap methods is around 40.99 µg/g, corresponding to an uncertainty of 13.3 %. The calibration model covers a broad range from minimum values ($RABD_{567-769}$ = 1.03; green pigments = 13.6 µg/g) to maximum values ($RABD_{567-769}$ = 1.25; green pigments = 321.8 µg/g) (see the vertical dashed lines in Fig. 5.2). For $RABD_{567-769}$ values smaller than 1.069, this calibration model calculates negative concentrations of green pigments. This offset is attributed to a matrix effect in the hyperspectral data (Makri et al., 2020). All negative values of green pigments were set to 0.

Fig. S5.3b shows the calibration model for 29 $RABD_{845}$ values with absolute Bphe-*a* concentrations (spectrophotometer) with a strong linear correlation ($R_{Pearson}$ = 0.98, $R^2$ = 0.96) and a mean RMSEP of 16.18 µg/g (~6.9 %). The calibration model covers the lower and upper limits from $RABD_{845}$ value of 1.0 (Bphe-a= 9.7 µg/g) to 1.26 (Bphe-a= 233.3 µg/g) (see the vertical dashed lines in Fig. 5.2).

Different residual plots of the two linear calibration models are shown in Fig. S5.4 and S5.5. The Shapiro-Wilk and the Kolmogorov- Smirnov tests both indicate most likely normal distributions of the residuals for the two linear regression models, thus the inferences from the two calibration models are valid.
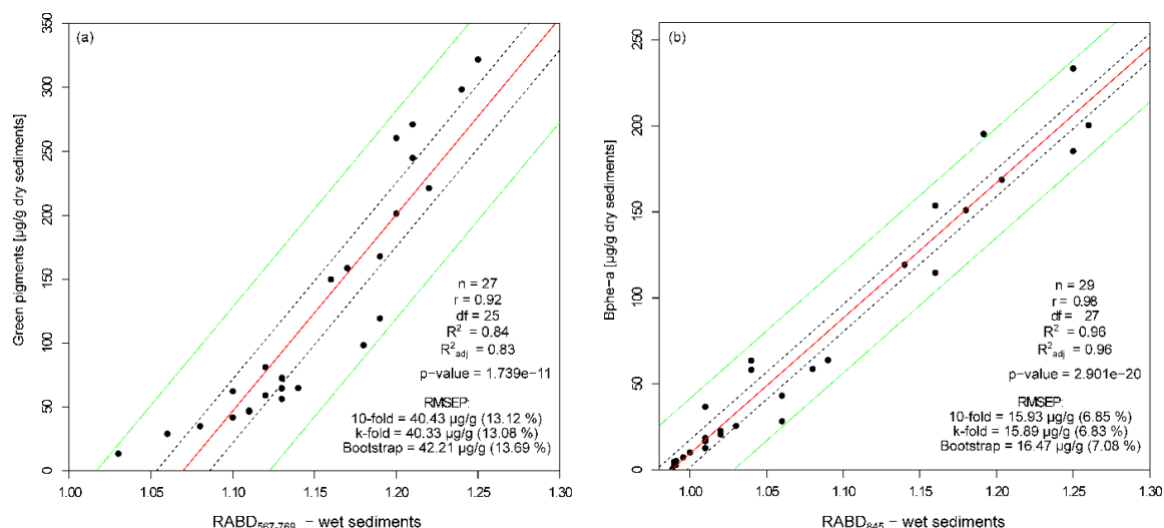
**Figure S5.3**: Pigments calibration. (a) Calibration of $RABD_{567-769}$ with UV/VIS-derived green pigments concentrations (chlorophyll-*a* and chlorophyll-*a* derivatives); (b) calibration of $RABD_{845}$ with UV/VIS-derived bacteriopheophytin-*a* (Bphe-*a*) concentrations. The linear regression models are shown in red; the black dots indicate the sample measurements from dry sediments. The dashed lines are the 95% confidence intervals for the regression function (black) and the predicted values (green).
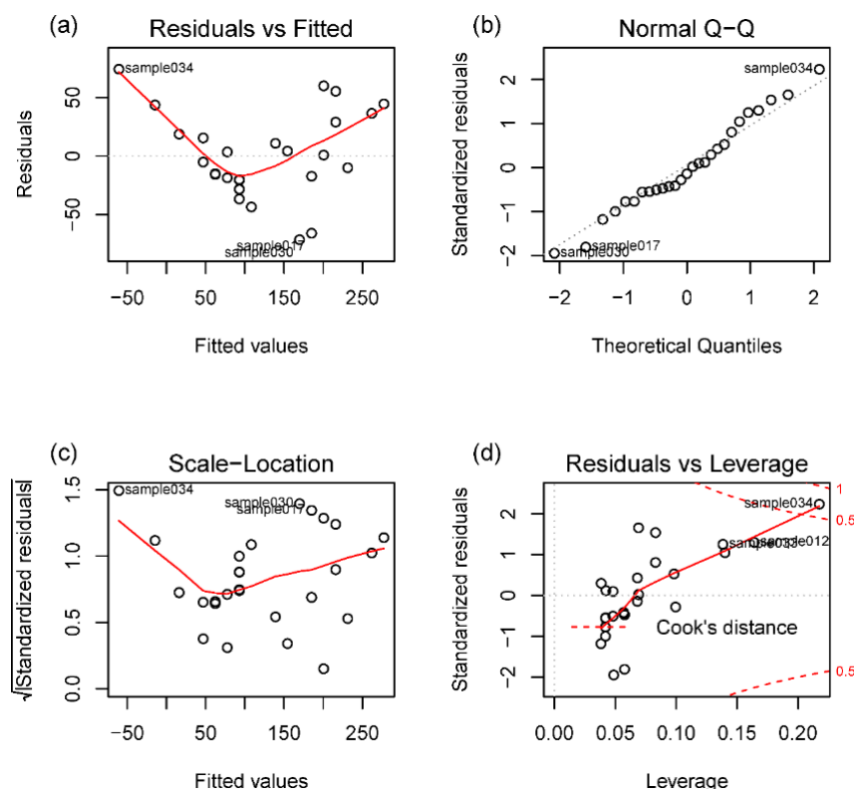


**Figure S5.4**: Different residual plots of the linear calibration model of $RABD_{567-769}$ with absolute green pigments concentrations (a) residuals versus fitted values, (b) standardized residuals versus theoretical quantiles, (c) scale-location plot, and (d) standardized residuals versus leverage plot.
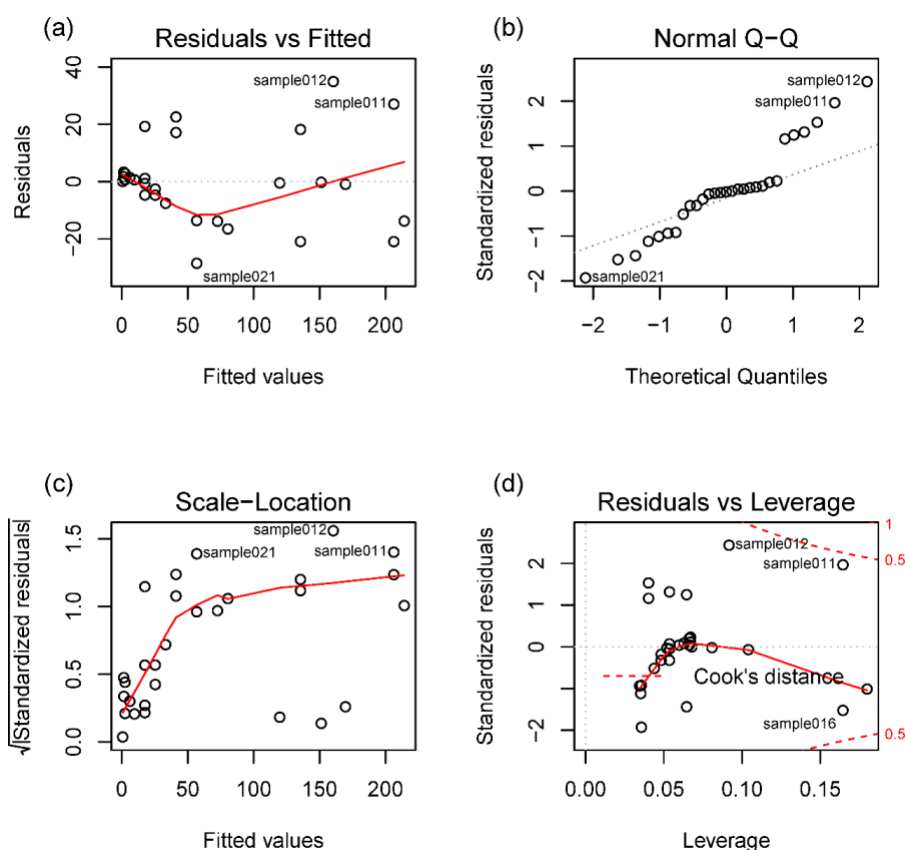
**Figure S5.5**: Different residual plots of the linear calibration model of RABD$_{845}$ with absolute Bphe-*a* concentrations: (a) residuals versus fitted values, (b) standardized residuals versus theoretical quantiles, (c) scale-location plot, and (d) standardized residuals versus leverage plot.

### Sediment P composition and different P fractions

The total P concentrations throughout the sediment core range from 399 µg/g (at ~8300 cal BP) to 20,396 µg/g (at ~2000 cal BP). Sedimentary P is primarily present in inorganic form (i.e. mainly Fe-P and Ca-P), with organic P fraction constituting mostly less than 20% of the sum of Fe-P, Ca-P and organic P (Fig. S5.6b). The Ca-P is the dominant P fraction during the three intervals of ~15,100-13,800 cal BP, ~12,700-11,200 cal BP, and ~9000-6350 cal BP, contributing to ~30-70% of the sum of the abovementioned three P fractions. Correspondingly, Fe-P represents the primary P fraction for the remainder of the sediment record. For example, in the last 6000 years (Zones VI and VII), the Fe-P fraction accounts for 40% up to >60% of the sum of the three P fractions (Fig. S5.6b).
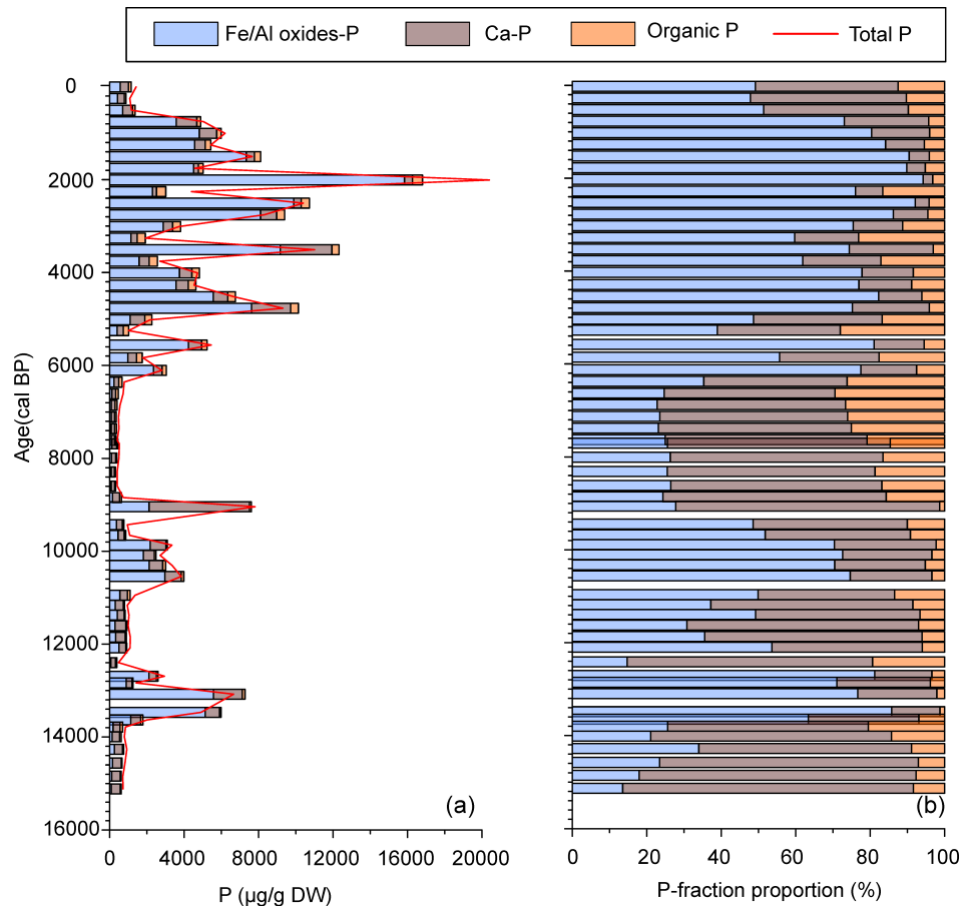
**Figure S5.6**: Time series of (a) concentrations of P fractions and (b) their relative proportions compared to sum of the three P fractions in (a). The concentrations refer to dry weight of sediments (DW).
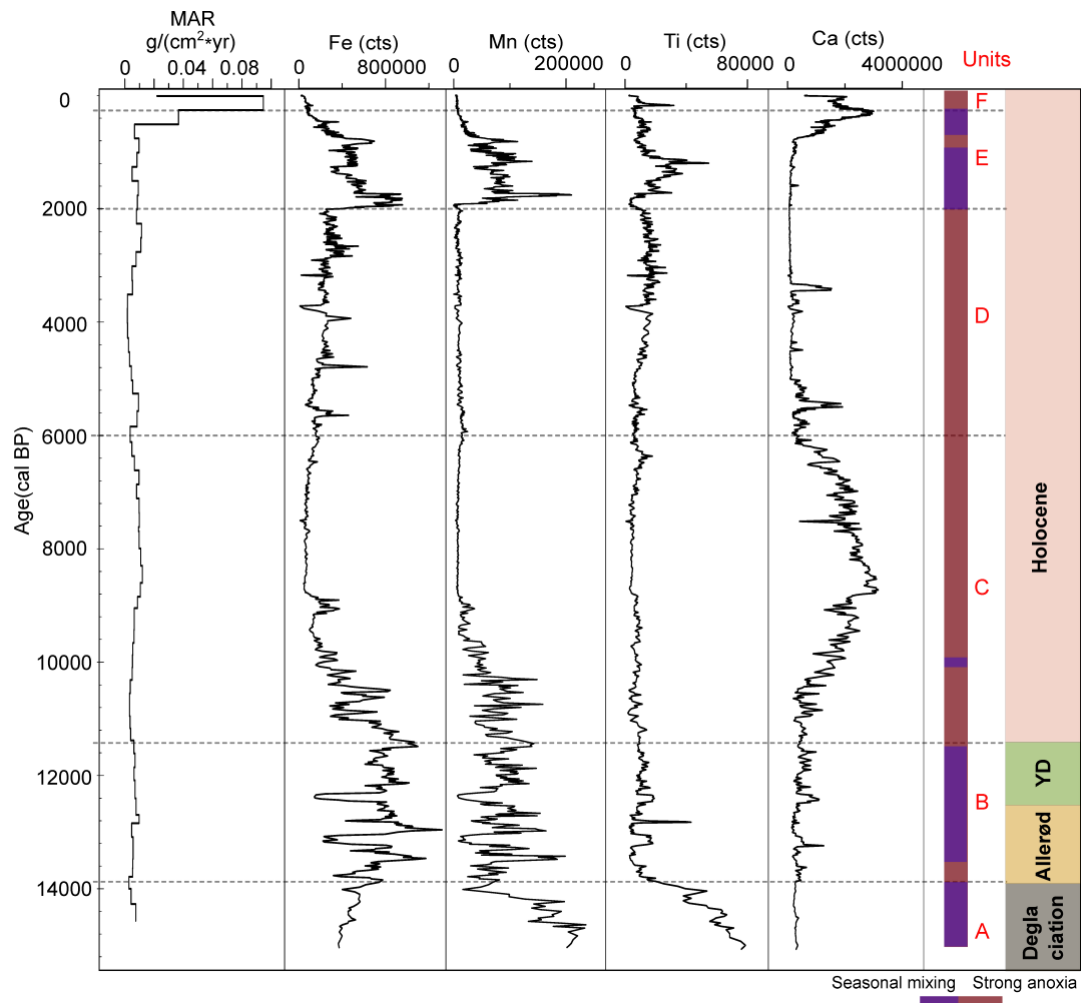
**Figure S5.7**: Time series of key geochemical proxies of Soppensee additional to those shown in Fig 5.2 (main text) including sediment mass accumulation rate (MAR) and XRF data (Fe, Mn, P, Ti and Ca). The grey dotted lines separate different lithological units (A to F in Fig. 5.1c; Gierga et al., 2016).
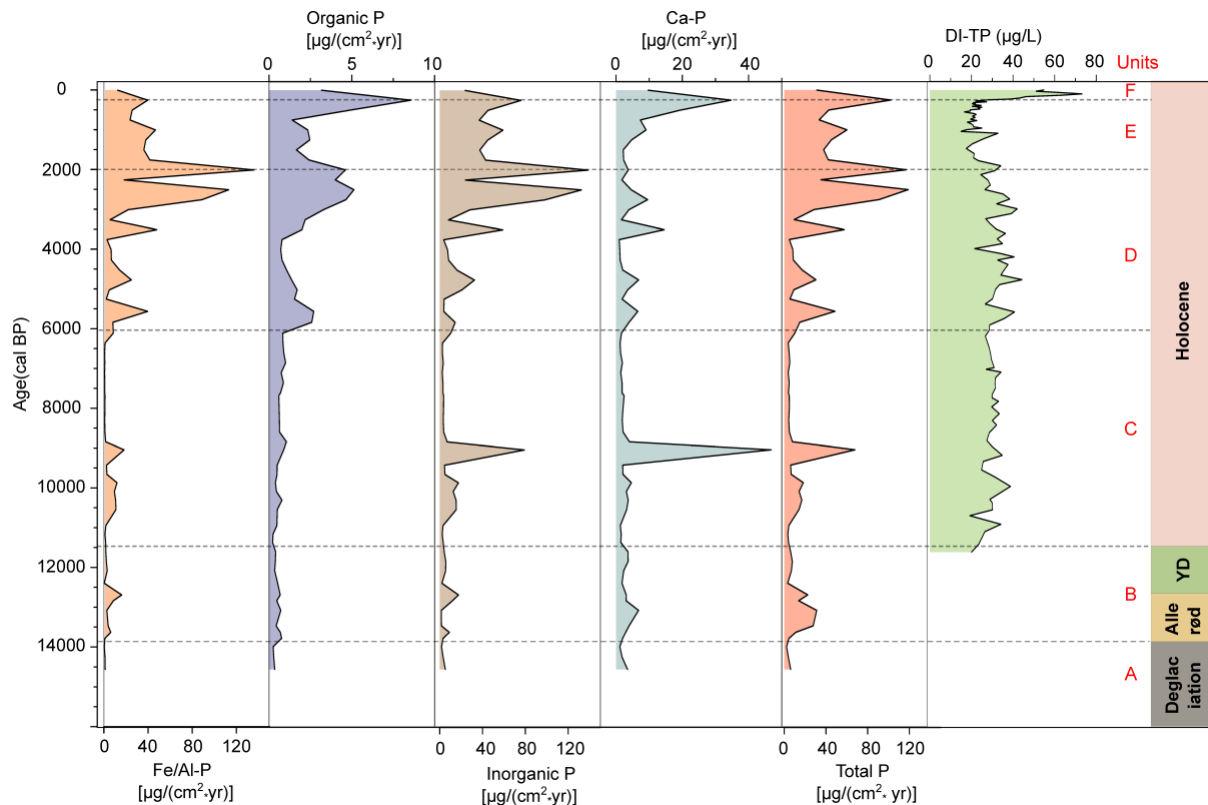
**Figure S5.8**: Vertical distribution of fluxes (net burial rates μg/(cm²·yr)) of different P fractions in the sediments of Soppensee and diatom-inferred past epilimnetic total phosphorus (Diatom-TP) concentrations according to Lotter (2001). The grey dotted lines separate different lithological units (A to F in Fig. 5.1c; Gierga et al., 2016).

### *References*

Butz, C., Grosjean, M., Poraj-Górska, A., Enters, D., Tylmann, W., 2016. Sedimentary Bacteriopheophytin a as an indicator of meromixis in varved lake sediments of Lake Jaczno, north-east Poland, CE 1891–2010. Global and Planetary Change 144, 109-118.

Gierga, M., Hajdas, I., van Raden, U.J., Gilli, A., Wacker, L., Sturm, M., Bernasconi, S.M., Smittenberg, R.H., 2016. Long-stored soil carbon released by prehistoric land use: evidence from compound-specific radiocarbon analysis on Soppensee lake sediments. Quaternary Science Reviews 144, 123-131.

Kind, J., van Raden, U.J., García-Rubio, I., Gehring, A.U., 2012. Rock magnetic techniques complemented by ferromagnetic resonance spectroscopy to analyse a sediment record. Geophysical Journal International 191, 51-63.

Lotter, A.F., 2001. The palaeolimnology of Soppensee (Central Switzerlabnd), as evidenced by diatom, pollen, and fossil-pigment analyses. Journal of Paleolimnology 25, 65-79.

North Greenland Ice-Core Project members, 2004. High-resolution record of the Northern Hemisphere climate extending into the last interglacial period. Nature 431, 147-151.

Schneider, T., Rimer, D., Butz, C., Grosjean, M., 2018. A high-resolution pigment and productivity record from the varved Ponte Tresa basin (Lake Lugano, Switzerland) since 1919: insight from an approach that combines hyperspectral imaging and high-performance liquid chromatography. Journal of Paleolimnology 60, 381–398.

Svensson, A., Andersen, K.K., Bigler, M., Clausen, H.B., Dahl-Jensen, D., Davies, S., Johnsen, S.J., Muscheler, R., Parrenin, F., Rasmussen, S.O., 2008. A 60000 year Greenland stratigraphic ice core chronology. Climate of the Past 4, 47–57.

van Raden, U.J., 2012. High-resolution swiss lake records of climate change. Ph.D. Thesis, ETH, Zürich, pp.140-141.

# Chapter 6: Conclusions and outlook

## 6.1 Conclusions

The main objective of this thesis was to investigate the vertical profiles of P fractions in sediments and potentials of internal P loadings in response to lake trophic status and anoxia over time spans from the past decades to the Late-glacial and Holocene periods. Three Swiss lakes, the Ponte Tresa basin of Lake Lugano, Lake Burgäschi, and Soppensee, were selected because they are seasonally stratified deep lakes. The records obtained from these lakes cover a wide range of possible lake conditions from oligotrophic to hypertrophic states and from well-oxygenated to anoxic conditions. These lakes have been very well studied for paleoenvironmental information under pre-anthropogenic and anthropogenic conditions. Importantly, all of the lake sediments are organic-rich, anoxic, and favorable for good preservation of organic substances (biomarkers) e.g. sedimentary pigments.

Major conclusions can be drawn from this thesis as follows:

i. In the Ponte Tresa basin, net burial rates of total P and the labile P fraction in sediments show significantly decreasing trends under more eutrophic and anoxic conditions since the 1960s. We conclude that, in seasonally stratified deep lakes with hypolimnetic anoxia, of which the Ponte Tresa basin is an example, eutrophication-induced hypolimnetic anoxia can increase sediment P release (mainly from the redox sensitive Fe-P fraction) into surface waters and, thus, reduce net burial rates of P in sediments. Consequently, the intense internal P cycling from surface sediments will work against the restoration actions to decrease eutrophication.

ii. In Lake Burgäschi, before the restoration of hypolimnetic water withdrawal, long-term retention of total P and labile P fractions in sediments was predominately controlled by past hypolimnetic redox conditions. When the hypolimnetic water was seasonally oxygenated, the retention of total P and labile P fractions in anoxic sediments increased, even during eutrophic phases. Moreover, the operation of hypolimnetic water withdrawal in Lake Burgäschi has largely decreased net burial rates of labile P fractions in sediments and potentials of internal P loadings. Nevertheless, the positive effects of hypolimnetic water withdrawal were not observed in the lake trophic state because the lake is currently still highly eutrophic. These findings can inform the management of deep eutrophic lakes in temperate zones.

iii. In Soppensee, enhanced internal P loadings triggered by bottom-water anoxia were inferred under pre-anthropologic conditions. These internal P loadings served as a positive feedback to promote natural eutrophication. However, this inference does not always hold true for other long phases of high aquatic production and anoxia. In the presence of magnetite-type minerals produced by magnetotactic bacteria and Fe-and

     Mn rich laminae, internal P loadings were potentially decreased, resulting in high net burial rates of Fe/Al-P in anoxic sediments. These iron minerals may be considered as new models playing a potentially important role in internal P loadings, geochemical cycles of Fe and P, and long-term trophic evolution of ferruginous lakes with low sulfate contents.

iv.    All studied lake records illustrate that labile P fractions are the primary P form in sediments, which suggests high potentials for internal P loadings. Thus, the labile-P data support the geochemical restoration approaches to limit P release from sediments by applying aluminum and iron as "capping" materials. On short (decadal to centennial) time spans, hypolimnetic anoxia that is caused by human-induced eutrophication tends to trigger higher internal P loadings, which serve as a positive feedback to sustain or accelerate eutrophication. However, on long-term millennial scales, this process is strongly modulated by the Fe-cycle and the presence of magnetotactic bacteria. Our findings suggest that the general interpretation model of internal P loadings needs to be extended to account for the role of Fe-minerals binding labile P in sediments.

## 6.2 Outlook

The present thesis underlines that, in ferruginous deep lakes, hypolimnetic redox conditions and elements of Fe and Mn play an important role in the biogeochemical cycling of P and sedimentary P fractions. In future studies, it will be important to assess microbially mediated processes or specific processes that are related to Fe- and Mn-rich laminae and ferromagnetic minerals endogenously formed in lakes. Also, the combination of P fractionation with the analysis of Fe and Mn speciation will help to better understand the effects of lake environmental conditions and specific processes on P cycling on short-term and long-term timescales.

The studies that use sediment profiles of P fractions to reconstruct past P dynamics of lakes need further attention. The records of total P and P fractions in sediment cores retrieved from the deepest sites might not reflect overall external P loadings and P burial rates in sediments, particularly in stratified deep lakes. For better understanding of the whole-lake P cycling under various environmental conditions, determining the lateral distributions of P fractions in sediments in different lake systems may be of great help. This approach may also provide important insights into P mass-balance modeling in different lakes.

# Acknowledgements

My PhD time at the Paleolimnology group of the University of Bern is coming to an end. It was a great and unforgettable time in my life thanks to the great support of many people.

Most of all, I would like to thank Prof. Dr. Martin Grosjean who made it possible for me to be part of this wonderful group and has been a great supervisor throughout the project. The beginning time of my PhD was a little tough because I had to learn how to work and live in a totally new environment abroad. Luckily, Martin, you are always supportive for my work and my life in Switzerland. Your encouragement and support strengthened my confidence. You also provided me with access to unique expertise, opportunity to attend conferences and meetings, and state-of-the-art facilities in the laboratory. Martin, I really appreciated the timely and helpful feedbacks you gave me. I did greatly benefit from our inspiring discussions at any stage of my work and, of course, those constructive criticisms. Thank you very much for your patience, your guidance, and your encouragement over these four years.

Special thanks go to Prof. Dr. Blas Lorenzo Valero-Garcés for being the co-examiner of my thesis. I also thank Dr. Simon Milligan for the useful instructions about the scientific writing for my thesis and English language editing for Soppensee manuscript.

Many thanks also go to Dr. Klaus A. Jarosch from the Soil Science group of the Institute of Geography and to Dr. Tobias Schneider. Dr. Klaus A. Jarosch introduced me to the skills working in the lab, taught me phosphorus techniques applied in paleolimnology, and supported and inspired me. You are always patient and helpful in answering my questions about lab work and phosphorus. Tobias taught me the skills of field work to the lakes, showed me how to appreciate and work with lake sediments, and also supported and inspired me. The field trip to the Ponte Tresa basin with Klaus and Tobias in Sep., 2017 will not go lost in my memories. It was my first field trip during my PhD time, which excited me with amazing landscapes and beautiful lake views. Despite the all day-long working on the boat with freezing cold temperatures, we had a successful and pleasant trip. Our cooperation in the "Ponte Tresa basin" project was successful. Indeed, both of you contributed significantly to the success of this project.

For field and laboratory support, I would like to first acknowledge Dr. Stamatina Makri and Dr. Andre F. Lotter for supporting me on Lake Burgäschi; further thanks are due to Dr. Daniela Fischer, Dr. Moritz Bigalke, and Patrick Neuhaus for the support during laboratory work. I also want to thank Prof. Dr. Szidat Sönke who measured gamma spectroscopy radiometric activities of samples for us, and Dr. Hendrik Vogel, who helped me with the ITRAX scanner and proceeded the XRF data. A big thank you goes to my office mate Paul Zander, who helped

me a lot with the hyperspectral imaging scanning system (HSI) and helped discuss the data. I really appreciate that Paul helped me with English language editing for my thesis.

I sincerely thank Dr. Adrian Gilli from the ETH for providing the very nice Soppensee cores and for always being open for discussions.

Additionally, I would like to thank all my colleagues in the Paleolimnology group and in the "giub" lab. You have supported me in so many different ways that I really enjoyed my social environment at work. You are all so nice and good work partners and so brilliant people. Paleolimnology people, thanks very much for the great time together and for accepting me the way I am. It was a pleasure to work with you and spend time together during our lunch time and coffee breaks!

At the last, I would like to thank all my friends and family in China and in Switzerland. Without their love and constant support, I would not have stood through the four years of my PhD and been at this stage.

# Appendix
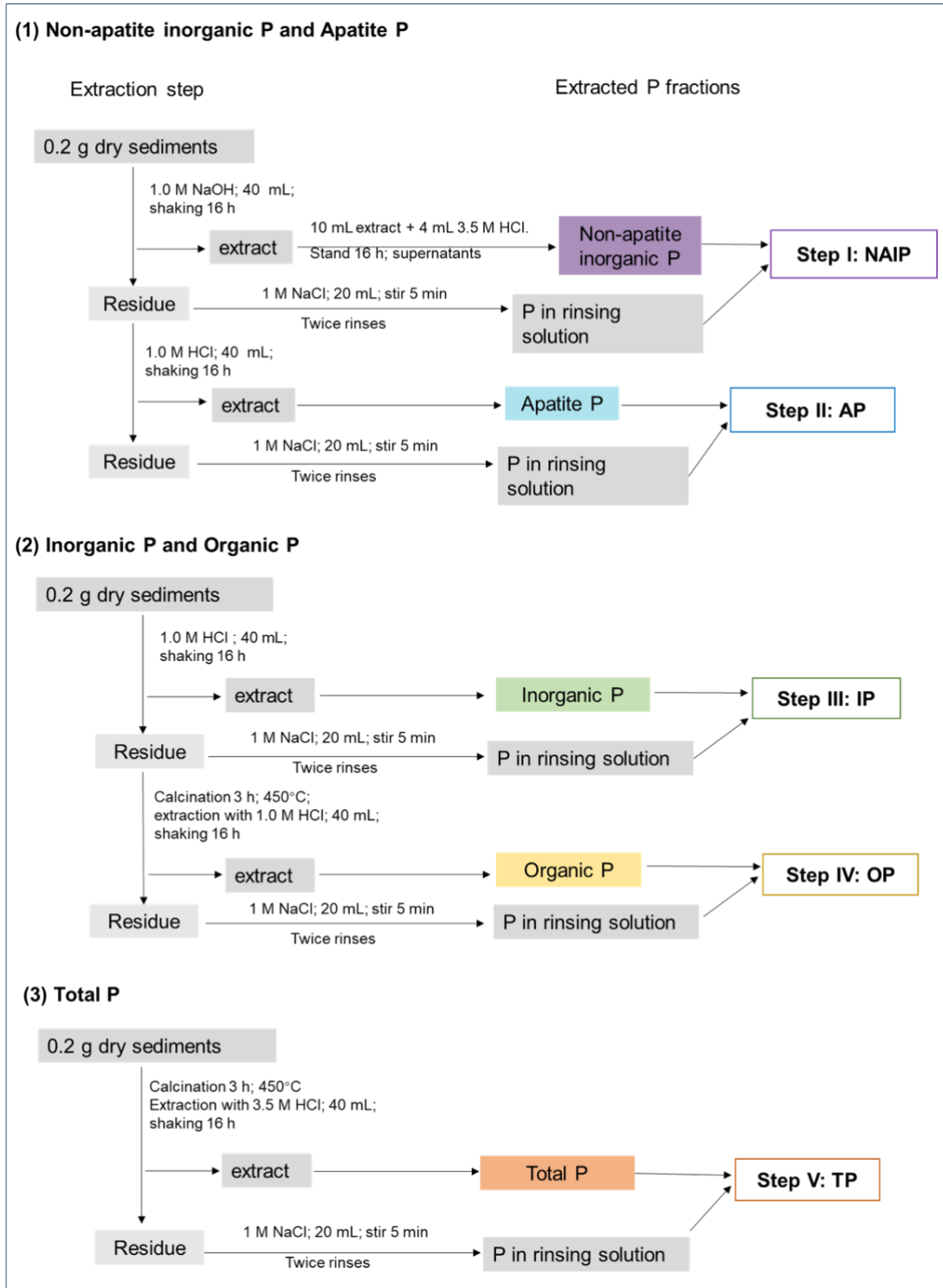
P-fractionation extraction protocol used for Soppensee sediments.

# Erklärung

gemäss Art. 28 Abs. 2 RSL 05

Name, Vorname:    Luyao Tu

Matrikelnummer:    17-123-464

Studiengang:    PhD of Science in Climate Sciences, University of Bern

Bachelor ☐ Master ☐ Dissertation ☑

Titel der Arbeit:    Sedimentary phosphorus dynamics in response to lake trophy and mixing

regime changes during the Late-Glacial, Holocene and the Anthropocene:

three case studies from deep lakes in Switzerland

Leiter der Arbeit:    Prof. Martin Grosjean

Ich erkläre hiermit, dass ich diese Arbeit selbständig verfasst und keine anderen als die

angegebenen Quellen benutzt habe. Alle Stellen, die wörtlich oder sinngemäss aus Quellen

entnommen wurden, habe ich als solche gekennzeichnet. Mir ist bekannt, dass andernfalls

der Senat gemäss Artikel 36 Absatz 1 Buchstabe o des Gesetztes vom 5. September 1996

über die Universität zum Entzug des auf Grund dieser Arbeit verliehenen Titels berechtigt ist.

Bern, den 03. März 2021

Ort, Datum                                                                                    Unterschrift